Research Square

Preprints are preliminary reports that have not undergone peer review.
They should not be considered conclusive, used to inform clinical practice,
or referenced by the media as validated information.

Dietary tryptophan restriction selectively suppresses lipogenesis, lowers cholesterol, and reduces adiposity without altering food consumption

Maralice Conacci-Sorrell

maralice.conaccisorrell@utsouthwestern.edu

UT Southwestern Medical Center https://orcid.org/0000-0002-4371-5087

pedro Augusto silva Nogueira

UT Southwestern Medical Center

Lizbeth Perez-Castro

UT Southwestern Medical Center https://orcid.org/0000-0001-7281-2233

Niranjan Venkateswarran

UT Southwestern Medical Center

Emily Parks

UT Southwestern Medical Center https://orcid.org/0000-0002-7020-8152

Kathleen Mannino

UT Southwestern Medical Center

Yi-Heng Hao

University of Texas Southwestern Medical Center, Dallas

Igor dos Santos

UT Southwestern Medical Center https://orcid.org/0000-0001-9199-9603

Ruth Gordillo

The University of Texas Southwestern Medical Center https://orcid.org/0000-0001-6533-2493

Jessica Kilgore

University of Texas Southwestern

Isabella DePasquale

UT Southwestern Medical Center

Joyane Eriom

UT Southwestern Medical Center

Lei Dong

UT Southwestern Medical Center https://orcid.org/0000-0001-9574-0148

Lin Xu

University of Texas Southwestern Medical Center https://orcid.org/0000-0001-5815-4457

Andrew Lemoff
UT Southwestern Medical Center https://orcid.org/0000-0002-4943-0170
Ralph DeBerardinis
UT Southwestern/HHMI https://orcid.org/0000-0002-2705-7432
Noelle Williams
The University of Texas Southwestern Medical Center at Dallas https://orcid.org/0000-0003-1894-5742
Philipp Scherer
The University of Texas Southwestern Medical Center https://orcid.org/0000-0003-0680-3392

Article

Keywords: ryptophan, obesity, Trp, cholesterol, lipogenesis

Posted Date: October 12th, 2026

DOI: https://doi.org/10.21203/rs.3.rs-10855823/v1

License: This work is licensed under a Creative Commons Attribution 4.0 International License.
Read Full License

Additional Declarations: Yes there is potential Competing Interest. M.C.S. has a pending patent application on Trypt-out. R.J.D. is an adviser for Illumina, General Metabolics, Vida Ventures, Faeth Therapeutics, and Alterris Oncology, and is a founder and adviser at Atavistik Bioscience.

Dietary tryptophan restriction selectively suppresses lipogenesis, lowers cholesterol, and reduces adiposity without altering food consumption

Pedro A. S. Nogueira[1], Lizbeth Perez-Castro[1], Niranjan Venkateswaran[1], Emily Parks[1], Kathleen Mannino[1], Yi-Heng Hao[1], Igor Lopes dos Santos[1], Ruth Gordillo[2], Jessica A. Kilgore[3], Isabella N. DePasquale[1], Joyane Eriom[1], Lei Guo[4], Lin Xu[4], Andrew Lemoff[3], Ralph J. DeBerardinis[5,6,7, 8], Noelle S. Williams[3], Phillipp E. Scherer[2], Maralice Conacci-Sorrell[1,8*]

[1]Department of Cell Biology, University of Texas Southwestern Medical Center, Dallas, TX 75390, USA

[2]Touchstone Center for Diabetes Research, University of Texas Southwestern Medical Center, Dallas, TX 75390, USA

[3]Department of Biochemistry, University of Texas Southwestern Medical Center, Dallas, TX 75390, USA

[4]Quantitative Biomedical Research Center, Peter O'Donnell Jr. School of Public Health, University of Texas Southwestern Medical Center, Dallas, TX, USA

[5] Eugene McDermott Center for Human Growth and Development, University of Texas Southwestern Medical Center, Dallas, TX, USA

[6] Children's Medical Center Research Institute at University of Texas Southwestern Medical Center, Dallas, TX 75390, USA

[7]Howard Hughes Medical Institute, University of Texas Southwestern Medical Center, Dallas, TX 75390, USA

[8]Harold C. Simmons Comprehensive Cancer Center, University of Texas Southwestern Medical Center, Dallas, TX 75390, USA

[*]Corresponding author

Correspondence: Maralice.ConacciSorrell@UTSouthwestern.edu

Keywords: tryptophan, obesity, Trp, cholesterol, lipogenesis

Running title: Dietary tryptophan restriction uncouples adiposity from food consumption

ABSTRACT

We interrogated the consequences of removing individually each of the nine essential amino acids using defined diets in mice. Among the essential amino acids, only tryptophan (Trp) depletion induced rapid and selective fat loss with minimal effects on lean body mass while retaining normal feeding behavior. We named this intervention “Trypt-out.” Trypt-out prevented and reversed obesity, hepatic steatosis, and glucose intolerance in both leptin-deficient and diet-induced obesity. Trypt-out also remained highly effective even with obesogenic high-fat and high-sucrose diets. Mechanistically, short-term Trp depletion did not impair global protein synthesis but selectively resulted in profound inhibition of lipogenic and cholesterol biosynthetic enzymes. This resulted in reduction in cholesterol that exceeded the effects of statin therapy. Trp as a master regulator of systemic lipid homeostasis and establish Trypt-out as a well-tolerated, rapid- acting dietary strategy to selectively eliminate adiposity, normalize metabolic dysfunction, and lower cholesterol without reducing food consumption or lean mass.

INTRODUCTION

Modulation of dietary protein consumption plays a key role in many nutritional interventions. Chemically, dietary protein sources are diverse, yet relatively few studies have investigated the physiological functions of individual amino acids and their specific contributions to systemic metabolism[1]. Elevated circulating levels of essential amino acids, particularly branched-chain amino acids, are consistently associated with obesity in both humans and animal models, whereas low-protein diets promote weight loss[2]. Conversely, leucine deprivation boosts energy expenditure and reduces food consumption and fat mass through GCN2 and mTOR signaling while methionine restriction reduces food consumption, fat mass, and body weight via FGF-21 signaling[3]. Recently, cysteine restriction was shown to promote weight loss by depleting glutathione and coenzyme A. However, this effect is largely driven by reduced food consumption and is particularly pronounced in mice lacking cystathionine γ-lyase[4]. Further studies have also explored the impact of limiting other amino acids such as asparagine, and glycine to prevent growth in various cancer models[5,6]. Because restriction of individual amino acids may alter food consumption, their direct metabolic effects are difficult to distinguish from secondary consequences of caloric restriction.

Among the nine essential amino acids (histidine, isoleucine, leucine, lysine, methionine, phenylalanine, threonine, tryptophan, and valine), tryptophan (Trp) is unique. Although it is the largest amino acid, it is the least abundant amino acid in the proteome as it is preferentially metabolized[1]. Owing to its 11-carbon structure and chemically versatile indole ring, Trp regulates diverse aspects of cellular biology, including cell growth and organismal physiology, through the generation of a wide network of biologically active metabolites[7]. Trp metabolism produces signaling molecules that regulate metabolism, immune function, and tissue homeostasis. This makes Trp both uniquely important for systemic physiology and uniquely accessible to external modulation.

Trp can be metabolized by the gut microbiome into a range of microbe-specific catabolites, which can influence host metabolic and signaling pathways[8]. Moreover, Trp can give rise to numerous

biologically active metabolites through host metabolism using the serotonin, kynurenine (Kyn), and indole-3-pyruvate (I3P) pathways [7,9-11]. In cancer, Trp-derived oncometabolites such as Kyn, I3P, and their downstream products promote tumor growth through both cell-autonomous and non-cell-autonomous mechanisms. Within tumor cells, these metabolites activate transcription factors including the aryl hydrocarbon receptor (AHR) and nuclear factor erythroid 2-related factor 2 (NRF2) to drive pro-tumorigenic gene expression profiles[12-17]. In the tumor microenvironment, Kyn establishes an immunosuppressive niche by inhibiting T-cell activity and preventing cancer cell clearance[18]. Supporting the tumor-promoting effects of Trp, its dietary depletion in mice carrying hepatocellular carcinoma prevents liver cancer progression[11]. Although the role of Trp metabolism in cancer and inflammation has been extensively studied[7], its contribution to body composition and systemic metabolism is poorly understood.

Here, we assessed the physiological consequences of isocaloric diets lacking each of the nine essential amino acids and identified Trp as a unique regulator of body composition. Among all amino acids tested, only dietary Trp depletion (hereafter termed Trypt-out) selectively reduced fat mass while preserving lean mass and food consumption. In male and female wild-type mice, hyperphagic leptin-deficient (ob/ob) mice, and diet-induced obese (DIO) mice, the Trypt-out diet prevented or reversed obesity, improved glucose tolerance, and resolved hepatic steatosis without causing liver injury. Mechanistically, Trp depletion suppressed the synthesis of key lipogenic enzymes required for triglyceride and cholesterol biosynthesis while preserving global protein synthesis. Remarkably, Trypt-out protected against weight gain even during continuous consumption of obesogenic high-fat or sucrose-supplemented diets, demonstrating that Trp depletion can override excess caloric consumption in the regulation of adiposity. Mechanistically, Trp restriction uncoupled dietary lipid uptake from endogenous lipid production by selectively suppressing lipogenic and cholesterol biosynthetic enzymes while preserving intestinal lipid absorption. This metabolic rewiring depleted cholesterol preserved circulating triglycerides, and rapidly reversed obesity through selective loss of adipose tissue

without reducing food consumption or nutrient absorption. Together, our findings identify Trp as a fundamental regulator of lipid homeostasis and establish dietary Trp restriction as a powerful strategy to selectively reduce adiposity without limiting food consumption .

RESULTS

The Trypt-out diet selectively reduces fat mass while maintaining lean mass and food consumption in both wild-type and leptin-deficient (ob/ob) mice.

To identify the effect of single amino acid depletion from the diet on body composition, male wild-type C57BL/6 (B6) mice were fed synthetic, defined isocaloric diets containing either all amino acids (control) or lacking one of the 9 essential amino acids (Fig. 1A). Mice were maintained on these diets for 2 weeks during which food consumption, total body weight, lean mass, and fat mass were measured by MRI in live animals. Overall weight loss occurred in each one of the amino acid-depleted diets. (Fig. 1B; Fig. S1A-B). Specifically, consumption of the isoleucine-free diet resulted in the largest change in weight compared to the control diet; however, this change in weight was accompanied by reduced food consumption, leading to loss of both fat and lean mass. Mice on the phenylalanine-free diet also consumed less food, while mice on either the threonine- or the methionine-free diet experienced weight loss (Fig. S1A) but no change in food consumption. (Fig. S1C). Mice on the Trypt-out diet had the most pronounced fat loss while preserving lean mass (Fig. 1B, Fig. S1D). Circulating levels of Trp and its metabolites decreased by the end of the 3-week feeding period in male B6 mice (Fig. 1E), supporting the depletion of Trp within mice receiving a Trp-lacking diet. To further explore the importance of Trp levels in body composition, the Trypt-out diet was administered to male and female B6 mice beginning at 12 weeks old for 3 weeks and 10 weeks and ob/ob mice for 4 weeks (Fig. 1C). Times of dietary interventions were experimentally determined to allow for 25 % weight loss. Both male and female B6 and ob/ob mice on the Trypt-out diet had a markedly less body weight by

the end of their respective feeding periods (Fig. 1D-F; Fig. S1E) without consuming less food (Fig. 1G-H; Fig. S1F-G). Given the similar phenotypes, male mice were used for further experiments.

Reintroduction of dietary Trp to ob/ob mice after 4 weeks on the Trypt-out diet resulted in delayed body weight gain. Even after 8 weeks of Trp refeeding, body weight remained lower than in mice continuously maintained on the control diet (Fig. 1I). Echo MRI analysis demonstrated that both B6 and ob/ob mice on the Trypt-out diet had a preferentially smaller fat mass relative to lean mass (Fig. 1J-K). In addition, the respiratory exchange ratio (RER) B6 and ob/ob mice fed the Trypt-out diet shifted in energy substrate utilization, indicating increased reliance on fat as an energy source (Fig. 1L). No changes in heat production or locomotor activity were detected in B6 mice fed the Trypt-out diet, as assessed by indirect calorimetry. In contrast, ob/ob mice fed the Trypt-out diet exhibited significant changes in locomotor activity during both the light and dark phases (Fig. S1H-I). B6 and ob/ob mice fed the Trypt-out diet also displayed lower fasting glucose levels (Fig. 1M) and improved glucose tolerance compared with control-fed mice, as demonstrated by both endpoint glucose measurements and area under the curve analysis (Fig. 1N-P). Consistent with these metabolic improvements, circulating insulin and leptin levels were reduced in B6 mice fed the Trypt-out diet relative to controls (Fig. 1Q).

The Trypt-out diet is sufficient to prevent and reverse diet-induced obesity

To determine whether dietary Trp depletion can prevent or reverse obesity, male B6 and FVB mice were fed the HFD containing all essential amino acids to generate diet-induced obese (DIO) mice (Fig. 2A and Fig. S2A). After 12 weeks, the DIO B6 mice were switched to the control or the Trypt-out diet for 4 weeks. The Trypt-out-fed mice weighed less than the control-fed mice but were not different in their food consumption. (Fig. 2B-D). Weight loss in these Trypt-out-fed DIO B6 mice was driven primarily by a loss of percent fat mass (Fig. 2E-F). Similar results were observed in FVB mice (Fig. S2A-G), indicating that the effects of dietary Trp deprivation were not strain-specific; Trypt-out-

fed male DIO FVB mice were lighter than the control-fed mice (Fig. S2B), but were not different in their food consumption (Fig. S2C) lean mass or fat mass (Fig. S2D).

To determine whether the Trypt-out diet could prevent the development of genetic obesity, ob/ob mice were placed on either the control or Trypt-out diet at 6 weeks of age, before the onset of severe obesity. After 4 weeks (Fig. 2G), the Trypt-out-fed mice weighed less than control-fed ob/ob mice (Fig. 2H) with reduced total food consumption (Fig. 2I) but had no detectable changes in food consumption / body weight (Fig. 2J). The Trypt-out-fed mice also had a more pronounced fat mass loss relative to lean mass (Fig. 2K-L). These changes were accompanied by improved glucose tolerance (Fig. S2F). Circulating insulin and leptin levels were lower in the Trypt-out-fed DIO FVB mice (Fig. S2G-H). In contrast, other feeding-related hormones, including ghrelin, glucagon, and GLP-1, were not different (Fig. S2G-H). Heat production and locomotor activity were not altered in the Trypt-out-fed ob/ob pre-obese male mice (Fig. S2L), and continuous monitoring across light and dark cycles revealed no major changes. RER was lower for the Trypt-out–fed ob/ob pre-obese male mice (Fig. S2K), indicating a shift toward fat utilization as a primary energy source.

Dietary protein restriction is sensed by the liver, which induces production of the endocrine hormone FGF21, a key regulator of systemic energy homeostasis [19 20 21,22]. FGF21 acts on adipose tissue and other peripheral organs to promote lipolysis, enhance fatty acid oxidation, suppress de novo lipogenesis, and increase energy expenditure, thereby shifting metabolism away from lipid storage and toward lipid utilization to coordinate the adaptive response to protein restriction [22]. To test whether lack of dietary Trp triggers FGF2 expression, we quantified FGF21in the liver and serum of both B6 and ob/ob mice and found Trypt-out-fed mice had more FGF21 in the liver and a correspondingly more Fgf21 in circulation (Fig. 2M-N).

12-week-old Fgf21 knockout (KO) [25] mice on the Trypt-out diet weigh less than the same mice fed the control diet (Fig. 2O), similar to what occurred with the B6 mice (Fig. S1E). Food consumption was not different between the Trypt-out–fed mice and control-fed mice (Fig. 2P). In addition, 12-week-

old Fgf21 KO mice fed the HF Trypt-out diet weighed significantly less than the HFD-fed mice (Fig. 2Q, Fig. S2M-P) with no difference in their food consumption (Fig. 2R). Although the Trypt-out diet induced Fgf21, its effects on body weight and composition were independent of Fgf21, revealing a distinct pathway linking Trp availability to body homeostasis.

Trypt-out-induced fat loss is not caused by global translation defects of Trp metabolites

To define the molecular mechanisms by which the Trypt-out diet affects fat loss, we first examined the impact of feeding the Trypt-out diet for 3 weeks on global protein synthesis within various mouse tissues. Protein synthesis was assessed by puromycylation [14,23], which relies on the incorporation of puromycin into nascent peptides followed by detection using anti-puromycin immunoblotting (Fig. 3A). First, we assessed the immediate and direct effects of Trp depletion on translation and performed puromycylation assays in cultured hepatocytes and adipocytes with and without Trp. Trp-lacking medium had no detectable effect on H2.35 hepatocyte global translation rates (Fig. 3B). Examining a Trp dose response (0 to 75 μM) in undifferentiated (3T3L1 cells) or differentiated adipocytes, we found only marginal effects on puromycylation in either cell type (Fig. 3C). Next, we tested the impact of the lack of dietary Trp on translation in vivo. B6 mice fed control or Trypt-out diet for 3 weeks received an intraperitoneal injection (IP) of O-propargyl-puromycin (OPP), a puromycin analog[24] 2 hours prior to tissue harvesting. By analyzing translation in the liver, muscle and adipose tissues including brown adipose tissue (BAT), inguinal white adipose tissue (iWAT), and gonadal white adipose tissue (gWAT, Fig. 3D) and we found only a modest increase in the liver.

Because the microbiome generates Trp metabolites, we asked whether microbiome-derived Trp metabolites mimic the effect of Trypt-out–induced fat loss. We first depleted the gut microbiome by providing drinking water with penicillin and streptomycin for 2 weeks on chow diet then switched the B6 mice and the ob/ob mice to either the control or the Trypt-out diet for 3 and 5 weeks with penicillin and streptomycin respectively. Microbiome depletion did not alter the rate or magnitude of weight loss

induced by the Trypt-out diet (Figures 3E-F and Fig. S3A-B), indicating that microbiome-derived metabolites are not primary drivers of this phenotype. The levels of serum Trp metabolites (Fig. 3G) from the ob/ob mice (Fig. 3H) [7,9-11] were significantly less in the mice fed the Trypt-out diet than those fed the control. To test whether restoring Trp-derived metabolites rescues the phenotype, the ob/ob mice received daily IP injections of I3P, Kyn, or 5-hydroxytryptophan (5-HTP), while receiving the Trypt-out diet for 4 weeks (Figures 3I and Fig. S3D-F). None of these interventions affected body weight, liver mass, or fat mass at the end of the feeding period, indicating that Trp-derived metabolites were not sufficient to rescue Trypt-out–induced weight loss (Fig. S3G-O).

Trp, like lysine, is a ketogenic amino acid capable of generating acetyl-CoA (Fig. 3J) through its catabolic breakdown [25]. After conversion to Kyn, Trp is metabolized to acetoacetyl-CoA and alanine. Alanine is further converted to pyruvate, which generates one acetyl-CoA molecule through pyruvate dehydrogenase, while acetoacetyl-CoA is cleaved into two additional acetyl-CoA molecules. Thus, the complete degradation of a single Trp molecule can yield up to three acetyl-CoA units (Fig. 3J) [26] which provides the carbon units required for fatty acid and cholesterol synthesis [26]. Consistent with this, Trypt-out diets caused a trend towards reduction in 2-aminoadipate, the intermediate produced from Trp and lysine during acetyl-CoA and lipid synthesis from amino acids (Fig. S3P-Q). Importantly, lysine levels and its downstream product pipecolate were unchanged in Trypt-out-fed mice, indicating that the reduction in 2-aminoadipate potentially reflects Trp starvation (Fig. S3P-Q). To determine whether alternative sources of acetyl-CoA could compensate for Trp loss, we attempted to rescue Trypt-out–induced weight loss in ob/ob mice by providing drinking water supplemented with sucrose for 4 weeks (Fig. 3K). No differences in weight loss were detected between the mice provided sucrose-containing water and the mice given control water, indicating that sucrose did not compensate for the loss of dietary Trp (Fig. 3L-M). No significant changes in food consumption were observed, likely due to increased caloric consumption from sucrose water (Fig. S3R). In summary, our results demonstrate

that consumption of the Trypt-out diet led to fat loss even in the presence of high fat or high sugar and that this weight loss occurred without changes in food consumption.

The Trypt-out diet reduces adipose tissue mass through lipid depletion rather than adipocyte loss

To define the tissue basis of fat loss induced by Trypt-out, we weighed adipose deposits and livers in B6 male, ob/ob male/female, ob/ob (pre-obese) male and B6 DIO male mice. Mice fed Trypt-out diets consistently displayed reduced weight gWAT, iWAT, BAT, and liver tissue (Fig. 4A-D), accompanied by marked changes in tissue morphology (Fig. 4E and Fig. S4A-D). Histological analysis revealed no changes in muscle of B6 and FVB DIO (Fig. S4E-F) but profoundly less adipocyte lipid content, most prominently in gWAT and to a lesser extent in iWAT, in B6, FVB DIO, ob/ob mice (Fig. 4F-H), B6 HFD and ob/ob pre-obese mice (Fig. S4G-H) and quantified in Fig. S4I-M. The liver displayed a striking clearance of lipid deposits without disruption of tissue architecture (Figures 4F-H, S4H). Metabolomic profiling confirmed the substantial reduction in lipids in both iWAT and gWAT in ob/ob male mice (Fig. 4I).

To determine whether adipose tissue loss resulted from adipocyte death, we cultured undifferentiated 3T3-L1 cells and differentiated adipocytes (Fig. 4J) in control or Trp-free medium. Adipocyte differentiation was confirmed by expression of FABP4, PPARγ, PLIN1, and adiponectin (Fig. 4K). Although Trp deprivation resulted in greater lipid peroxidation in differentiated adipocytes (Fig. 4L), it had only a modest effect on viability in both differentiated and proliferating cells (Fig. 4M-N). Trp deprivation did not alter adipocyte identity, as differentiated cells-maintained expression of canonical adipocyte markers (Fig. 4O). Although Trp deprivation demonstrated modestly increased cleaved caspase-3 and p21 in a dose-dependent manner in adipocytes (Fig. 4O), the limited magnitude of these changes was insufficient to account for the profoundly lighter adipose tissue observed in vivo, suggesting that widespread adipocyte death is unlikely to be the primary mechanism.

Because ferroptosis has been implicated in adipose tissue remodeling with a lower ferroptotic signature in the adipose tissue of individuals and mice with obesity[27], we tested whether Trp deprivation induces ferroptosis. As expected, the ferroptosis inhibitor Ferrostatin-1 effectively rescued RSL3-induced ferroptosis but had little effect on Trp deprivation-induced cell death (Fig. 4M-N, P-Q), indicating that ferroptosis is not the predominant mechanism. Notably, proliferating 3T3-L1 cells were more sensitive to RSL3 than differentiated adipocytes in the control condition (Fig. 4P).

To directly test the contribution of ferroptosis in vivo, we treated ob/ob male mice (10 weeks old) with daily IP injections of the ferroptosis inhibitor liproxstatin-1 (Lip-1) for 3 weeks. Lip-1 failed to rescue the Trypt-out-induced weight loss (Fig. 4R), further demonstrating that ferroptosis is not a major driver of this phenotype. Together, these findings demonstrate that the Trypt-out diet profoundly reduces adipose tissue mass by shifting to depletion of intracellular lipid stores while largely preserving adipocyte viability, revealing a mechanism of adipose remodeling that is driven by metabolic reprogramming rather than adipocyte loss.

The Trypt-out diet reshapes the hepatic transcriptional landscape to prevent lipid biosynthesis

To obtain an unbiased view of molecular adaptations to the Trypt-out diet, we performed RNA-seq on iWAT, liver, and skeletal muscle (quadriceps) from male B6 mice fed either the control or the Trypt-out diet for 3 weeks (Fig. 5A). Using a cutoff of $\log_2FC \geq 1.0$ and $P \leq 0.05$, we identified 521 upregulated and 851 downregulated genes in skeletal muscle, 978 upregulated and 399 downregulated genes in iWAT, and 999 upregulated and 1,446 downregulated genes in the liver (Fig. S5A-C). Pathway analysis revealed striking tissue-specific adaptations. Skeletal muscle exhibited coordinated suppression of protein digestion and amino acid metabolism together with induction of ribosome biogenesis, mTOR-related signaling, and translation-related pathways, which supports the preservation of lean mass in Trypt-out–fed mice (Fig. 5B). Similarly, analysis of iWAT showed suppression of amino acid metabolic pathways accompanied by induction of ribosome biogenesis and a broad reduction in the pathways regulating the tissue microenvironment (Fig. 5C). All three tissues shared a transcriptional signature of

reduced lipogenesis (Fig. 5B-D); however, the liver underwent the most extensive remodeling, with widespread suppression of lipid biosynthetic pathways (Fig. 5D).

The liver exhibited striking transcriptional suppression of genes involved in fatty acid metabolism, including fatty acid biosynthesis, elongation, degradation, and lipid transport, whereas these pathways were only modestly affected in skeletal muscle and iWAT (Fig. 5B-D and Fig. S5D-G). Proteomic analysis of the same liver samples independently validated many of the transcriptional changes identified by RNA-seq (Fig. S5H-I). In addition, proteomics extended these findings by revealing coordinated increases in proteins comprising nearly every component of the protein synthesis machinery, including ribosomal proteins, aminoacyl-tRNA synthetases, and translation initiation and elongation factors, demonstrating a broad activation of the translational apparatus (Fig. S5I-K). These data explain why puromycin incorporation was maintained, and even modestly increased, in the livers of the Trypt-out-fed mice despite the dietary Trp deprivation (Fig. 3D), demonstrating that Trypt-out triggers a compensatory activation of the translational machinery rather than translational collapse.

Importantly, our proteomic analysis revealed that a small subset of proteins was selectively depleted in the liver of Tryp-out-fed mice than the control-fed mice while mRNA abundance is only very modestly altered (Fig. 5E). Among the most strongly affected were key lipogenic enzymes, including fatty acid synthase (FASN, 30 Trp residues), ATP citrate lyase (ACLY; 11 Trp residues), and acetyl-CoA carboxylase alpha (ACACA; 27 Trp residues). These findings suggest that consumption of the Trypt-out diet impairs the expression of proteins with high Trp content, which is a relatively rare feature within the proteome (80% of the proteome contains 0-2% of Trp). We next examined the expression of lipid biosynthetic enzymes that were reduced either at the mRNA level, including stearoyl-CoA desaturase 1 (SCD1), 3-hydroxy-3-methylglutaryl-CoA synthase 1 (HMGCS1), peroxisome proliferator-activated receptor gamma (PPARγ), and peroxisome proliferator-activated receptor alpha (PPARα), or at the protein level, including fatty acid synthase (FASN), acetyl-CoA carboxylase alpha (ACACA), ACLY, mevalonate diphosphate decarboxylase (MVD), and 7-

dehydrocholesterol reductase (DHCR7) (Fig. 5F). The levels of both groups of enzymes were markedly reduced in the livers of B6 mice (Fig. 5G) and ob/ob mice (Fig. 5H) fed the Trypt-out diet, whereas glycolytic enzymes remained unchanged (Fig. 5I). Lipogenic enzyme expression was not altered in the adipose tissue of B6 mice but was reduced in ob/ob mice (Fig. S5L-M). Importantly, we found adipocyte cell death did not increase in Trypt-out–fed B6 mice, as assessed by cleaved caspase-3 (Fig. S5L-M). Because lipogenic enzymes were unchanged in the adipose tissue of B6 mice, we reasoned that the liver is the primary site lessening de novo lipogenesis, thereby limiting lipid deposition in adipose tissue. The expression of the lipid transport apolipoproteins ApoB and ApoE was slightly greater in both the liver and circulation in the Trypt-out-fed mice (Fig. S5N-O). Together, these findings demonstrate that the Trypt-out diet selectively suppresses enzymes required for fatty acid, triglyceride, and cholesterol biosynthesis, providing a mechanistic basis for the profound reduction in adiposity.

To determine whether suppression of these enzymes is a cause or a consequence of fat loss, B6 male mice 12 weeks old were fed the Trypt-out diet for 3 weeks and then fed the Trypt-out diet supplemented with IP injections of Trp for 7 days, which is a period insufficient to restore body weight (Fig. 5K, lower panel). Importantly, hepatic expression of lipogenic enzymes was significantly rescued in the absence of weight gain, demonstrating that suppression of these enzymes is likely a direct consequence of Trp deprivation rather than secondary to weight loss and contributes directly to the metabolic phenotype (Fig. 5K).

The Trypt-out diet overrides the obesogenic effects of a HFD regular binge

B6 mice were fed either a high-fat diet (HFD) or a high-fat Trypt-out (HF Trypt-out) diet for four weeks (Fig. 6A). As expected, HFD-fed mice continued to gain weight, whereas HF Trypt-out-fed mice lost weight (Fig. 6B-C), despite consuming comparable amounts of food (Fig. 6D). HF Trypt-out-fed mice displayed markedly reduced fat mass while preserving lean mass (Fig. 6E-F), with no differences in glucose tolerance (Fig. S6A). To determine whether Trypt-out could reverse established obesity, 10-week-old male ob/ob mice were fed either an HFD or HF Trypt-out diet for four weeks

(Fig. 6G). Despite a marked increase in food consumption (Fig. 6J), HF Trypt-out-fed mice lost weight (Fig. 6H-I), failed to accumulate fat mass (Fig. 6K), and exhibited reduced liver and inguinal white adipose tissue (iWAT) weights (Fig. 6L). Consistent with our findings in lean mice (Fig. 5B), HF Trypt-out also suppressed the expression of enzymes required for triglyceride and cholesterol biosynthesis (Fig. 6M). These results demonstrate that repression of lipogenic enzymes is a direct consequence of Trp deprivation rather than secondary to reduced adiposity or lipid availability.

To better model the irregular eating patterns commonly observed in humans, we designed a long-term dietary intervention incorporating periods of obesity, weight loss, intermittent HFD exposure, and weight regain (Fig. 6N). First, B6 male mice 8 weeks old were fed with HFD for 18 weeks (Fig. 6N) to induce obesity (DIO). These B6 DIO mice were then randomized into two groups: sustained HFD (grey line), which received the HFD for 32 weeks and Binge HFD (purple line). The Binge mice first received 4 weeks of HF Trypt-out ad libitum diet for 5 days and HFD pair-feeding for 2 days to mimic weekend dietary change (4 cycles). Then, at the second phase ("weekend binge ad libitum"), the mice were subsequently fed during 18 weeks in a similar way, however, the 2 days with HFD were given ad libitum to determine whether benefits for a dietary Trp deficiency are maintained under a more realistic dietary pattern with free access to the food. Mice on the intermittent HF Trypt-out diet maintained a substantially lower body weight throughout the study despite repeated weekend exposure to Trp, in the presence of HF demonstrating that a 5-day Tryp-out per week is sufficient to sustain long-term weight control (Fig. 6N). Finally, all mice were then fed with HFD-only diet ad libitum for an additional 10 weeks. Although the Binge mice regained weight, they remained significantly leaner than the mice maintained continuously on the HFD, which contained Trp (Fig. 6N). Histological analysis revealed modest adipocyte changes in the iWAT and gWAT between the Binge and HFD mice after 10 weeks on the HFD with Trp (Fig. 6Q). The hepatic tissue from the Binge mice had markedly fewer lipid droplets (Fig. 6Q) and were largely protected from hepatic steatosis (Fig. 6N-O) with both liver weigh and iWAT weight significantly reduced (Fig. 6P).

We next asked whether the metabolic effects of Trypt-out result from impaired liver function. Despite prolonged HF Trypt-out feeding and continued exposure to obesogenic diets, we found no evidence of hepatocellular injury. Circulating levels of the liver injury markers aspartate aminotransferase (AST) and alanine aminotransferase (ALT) were lower in DIO mice fed HF Trypt-out (Fig. 6P and S6K). ALT levels were not altered in B6 mice fed either the Trypt-out diet or control diet for 3 weeks, however ob/ob and DIO mice had markedly lower ALT levels when fed the Trypt-out diet for 4 weeks (Fig. 6P). These findings demonstrate that the profound reduction in adiposity induced by Trypt-out is not a consequence of hepatotoxicity. Rather, mice lacking dietary Trp preserved liver integrity while providing durable metabolic benefits that persisted despite prolonged exposure to obesogenic diets and partially protected against subsequent weight regain and hepatic steatosis.

Trypt-out outperforms statins in lowering cholesterol while preserving nutrient absorption

Given the downregulation of lipid biosynthetic enzymes in the livers of Trypt-out-fed mice, we directly measured cholesterol and triglyceride levels (Fig. 7A). Cholesterol emerged as the metabolite most consistently affected by lack of dietary Trp; it was significantly lower in B6 mice at 3 days, ob/ob and HFD ob/ob mice at 4 weeks, and the Binge mice after the 10 weeks of HFD feeding (Fig. 7B). In contrast, circulating triglyceride concentrations were not significantly altered (Fig. 7C). This selective reduction in cholesterol is supported by our proteomic and transcriptomic data showing coordinated suppression of cholesterol biosynthetic enzymes in the liver, whereas circulating triglycerides appear to be maintained through mobilization of existing adipose stores.

Cholesterol levels were markedly lower in the liver and iWAT, whereas gWAT levels were largely unaffected in the Trypt-out fed ob/ob mice (Fig. 7D). In contrast, triglyceride levels, free fatty acids and glycerol were not affected in either the liver or adipose tissues in the Trypt-out fed ob/ob mice (Fig. 7E and S7AB). Together, these findings demonstrate that the Trypt-out diet does not broadly deplete lipid stores but instead selectively suppresses cholesterol biosynthesis.

Cholesterol, fatty acids, and triglycerides all derive from cytosolic acetyl-CoA generated by ACLY, one of the enzymes suppressed by the Trypt-out diet. We examined the metabolites linking mitochondrial metabolism to lipogenesis (Fig. 7A). Citrate and malate accumulated in tissues from the Trypt-out-fed mice (Fig. 7F-G), suggesting that carbon was retained within mitochondrial oxidative metabolism rather than being used in the cytosol to fuel de novo lipogenesis.

Because cholesterol supports multiple essential cellular functions, we next investigated which cholesterol-dependent processes are altered by the Trypt-out diet. Cholesterol can be stored as cholesteryl esters in lipid droplets, incorporated into cellular membranes, or converted into bile acids in the liver. Bile acids are then secreted into the intestine, where they emulsify dietary lipids and are required for the absorption of cholesterol, triglycerides, and fat-soluble vitamins. Despite suppression of cholesterol biosynthesis, bile acid components in Trypt-out-fed B6 and ob/ob mice were similar to or higher than those in the control-fed diet (Fig. 7H-J). Cholic acid (CA) was markedly higher in Trypt-out-fed B6 mice (Fig. 7H), ob/ob (Fig. 7I), and HDF-fed ob/ob mice (Fig. 7J). CA is a key determinant of intestinal lipid absorption and cholesterol homeostasis [28] thus, our findings argue against fat malabsorption as the mechanism underlying weight loss. Instead, the marked increase in CA suggests that intestinal lipid uptake was preserved, or even enhanced, while hepatic de novo lipogenesis and cholesterol biosynthesis were selectively suppressed with a lack of dietary Trp. This model is further supported by unchanged fecal caloric content and metabolite levels, indicating that consumption of the Trypt-out diet uncouples dietary lipid absorption from endogenous lipid synthesis and storage.

The caloric content and metabolite levels in the feces were changed only in B6 (Fig. 7K and Fig. S7K). Similarly, urinary ketone levels were unchanged, whereas TCA cycle intermediates were lower (Fig. 7L and Fig. S7G). Together, these findings indicate that the Trypt-out diet does not impair intestinal nutrient absorption but causes the preferential utilization of available lipids to sustain essential physiological processes, including bile acid production and the unexpected induction of ribosome biogenesis and the translation machinery despite the marked inhibition of de novo lipogenesis.

We compared the cholesterol-lowering effects of the current standard-of-care treatment for high cholesterol using atorvastatin (ATO)[29,30], an HMG-CoA reductase inhibitor that blocks a single rate-limiting step in cholesterol biosynthesis to the Trypt-out diet response. We fed ob/ob mice either the Trypt-out diet or the control diet with or without ATO for 3 weeks. ATO causes a drop in intracellular cholesterol, which stimulates increased LDL uptake and recycling, effectively clearing cholesterol from the blood. B6 and ob/ob mice were treated daily with ATO and fed the control diet or fed the Trypt-out diet. As expected, ATO reduced serum cholesterol without affecting body weight or circulating triglycerides (Fig. 7L, N, O). Mice fed the Trypt-out diet had a significantly lower cholesterol level than the ATO-treated, control-fed mice and the untreated, control-fed mice, demonstrating that lacking dietary Trp suppresses cholesterol production more effectively than pharmacological inhibition of HMG-CoA reductase (Fig. 7O). In agreement with previous reports, ATO triggered the well-established compensatory feedback response by activating SREBP-2, which increased the expression of HMG-CoA reductase and other cholesterol biosynthetic enzymes in response to reduced hepatic cholesterol [28] (Fig. 7P). Trypt-out uniformly reduced the expression of enzymes throughout the cholesterol and lipid biosynthetic pathways, ACLY, ACACA, FASN, MVD, DHCR7, HMGCS1, thereby suppressing the pathway at multiple levels (Fig. 8).

DISCUSSION

Short-term removal of dietary Trp is remarkably well tolerated in mice, preserving lean body mass, normal food consumption, and normal liver function. It also provides a useful strategy to alleviate features of human metabolic syndrome, including fatty liver, hypercholesterolemia, and diabetes. One of the most striking findings of our study is the profound reduction in circulating cholesterol despite relatively unchanged triglyceride levels. These observations appear paradoxical, as both lipid classes are synthesized in the liver. However, they reflect fundamental differences in their metabolic origins. Under physiological conditions, approximately 70-90% of cholesterol is produced endogenously through the

mevalonate pathway. In contrast, 80-95% of triglycerides are derived from dietary fatty acids, whereas only 5-20% originate from hepatic *de novo* lipogenesis, depending on nutritional status [31]. Consistent with these observations, Trypt-out depletes key enzymes controlling fatty acid and cholesterol biosynthesis, including ACLY, ACACA, FASN, SCD1, HMGCS1, DHCR7, and MVD, while preserving intestinal lipid absorption, as evidenced by maintaining bile acid production and unchanged caloric and metabolite content in the feces. We interpret these findings to suggest that dietary lipids continue to enter the circulation and sustain circulating triglycerides, whereas endogenous cholesterol synthesis becomes rate-limiting. We therefore propose that tryptophan restriction uncouples dietary lipid uptake from endogenous lipid production, redirecting absorbed lipids away from storage and toward essential physiological functions, including bile acid synthesis, membrane homeostasis, and the unexpected induction of ribosome biogenesis., Thus, Trypt-out causes a global metabolic rewiring leading to preserved nutrient absorption, profound cholesterol depletion, selective adipose tissue loss, and rapid reversal of obesity.

Ribosome biogenesis is one of the most energetically demanding cellular processes. Studies estimate that rapidly proliferating cells devote up to 80% of their energy to ribosome production and protein synthesis [32 33]. Tryp-out induces ribosome biogenesis components, one of the most energetically demanding biosynthetic programs in the cell. In addition, Tryp-out redirects metabolic resources toward essential anabolic processes. Despite profound inhibition of cholesterol biosynthesis, bile acid production is maintained or increased, preserving intestinal lipid absorption. We propose that Trypt-out redirect nutrients away from lipid storage and toward essential physiological functions, creating a metabolically expensive state that preserves nutrient absorption and protein synthesis while driving selective adipose tissue loss and rapid reversal of obesity.

A key finding is that Trp deprivation reduces adiposity primary by reprograming lipid metabolism in the liver causing body weight and adiposity reduction The capacity of adipocytes to proliferate and expand [34], is not disrupted by Trp depletion *in vitro*. This occurs independent of tissue protein synthesis

capacity and Fgf21 signaling which is elevated by Trypt-out, but not essential for the phenotype. This is consistent with studies using cysteine deprivation, where mice exhibited rapid weight loss and an increase in Fgf21, UPR, and Gdf15 markers but the weight loss mechanism reported was independent [35,36].

We established that the Trypt-out diet impairs hepatic lipid biosynthesis and reduces cholesterol levels, which mimics the therapeutic effects of statins [37]. Notably, the Trypt-out diet also reduces adiposity and body weight, lowering blood glucose without affecting eating patterns of mice. At the molecular level, the Trypt-out diet primarily reprograms liver metabolism, disrupting the capacity to sustain lipid biosynthesis and cholesterol production. Furthermore, the low glucose levels increase the capacity of the liver to utilize the lipid to generate energy and produce TCA intermediates contributing to the phenotype. We hypothesize that adipose tissue changes are secondary to changes in the liver. The capacity of adipocytes to proliferate and expand [34], is not disrupted by Trp depletion *in vitro* and *in vivo*. The loss of fat tissue mass is not due to cell death but, may be due to mobilization to sustain triglyceride levels in the tissues and circulation.

In conclusion, our study shows that Trp levels control a powerful non-canonical pathway which regulates lipid biosynthesis and cholesterol levels. In contrast to traditional dietary interventions, the Trypt-out diet causes weight loss that is completely resistant to high fat or sugar consumption . Further, repeated short-term binges of a regular HFD are insufficient to cause full weight to regain. These characteristics make dietary Trp manipulation uniquely interesting. The short term of 3-4 weeks on the diet lacking Trp is enough to produce a significant weight loss in wildtype and obese mice models. Even after returning to a normal diet, Trypt-out fed mice maintained long-term weight loss of approximately 15% their original body weight. Although further research is needed, our findings identify dietary Trp restriction as a potential therapeutic strategy for metabolic syndrome and its associated conditions, including obesity, diabetes, cardiovascular disease, and fatty liver disease.

LIMITATIONS OF THE STUDY

The effects of long-term therapeutic removal of dietary Trp remain to be determined. How much dietary Trp must be reduced to sustain the beneficial effects on adiposity, cholesterol homeostasis, and glucose metabolism while minimizing potential adverse effects remain to be determined. Moreover, Trp is the obligate precursor for serotonin synthesis, thus, sustained lack of dietary Trp could affect mood, sleep and overall well-being [38]. These concerns may be mitigated by supplementation with 5-HTP, which serves as a precursor for serotonin. 5-HTP supplementation does not cause fat gain; therefore, it may be sufficient to safely restore serotonin and preserve the systemic metabolic benefits of Trp restriction while minimizing neurological effects. Defining the long-term safety, tissue-specific adaptations, and therapeutic window of Trp restriction are needed before clinical translation.

Trp is a ketogenic amino acid and similar to lysine it can contribute carbon to acetyl-CoA (lipid precursor). This raises the possibility that the reduced carbon availability caused by the Trypot-out diet contributes to the suppression of lipid synthesis. Because lack of dietary Trp simultaneously decreased the abundance of enzymes required for *de novo* lipogenesis, changes in metabolic flux may be masked by reduced pathway capacity. Stable isotope tracing of Trp, glucose, and fatty acids are necessary to define how the lack of dietary Trp redistributes carbon between oxidation, protein synthesis, and lipid production.

Trp depletion selectively reduces cholesterol while preserving triglycerides, despite coordinated suppression of enzymes required for both cholesterol and fatty acid biosynthesis. It may be that the rapid mobilization of adipose tissue provides sufficient fatty acids and glycerol to buffer triglyceride pools in the liver, masking the reduction in *de novo* triglyceride synthesis. In contrast, cholesterol lacks a comparable storage reservoir and therefore depends more heavily on continuous biosynthesis. Comprehensive lipidomic analyses combined with comprehensive metabolic flux studies are necessary to test this model and determine how lipid pools are maintained during Trp deprivation.

Our RNA-seq and proteomics profiling of the liver strongly suggest that Trp depletion promotes energy expenditure by inducing a futile metabolic cycle in which ribosome biogenesis and protein synthesis

are increased while lipogenesis is simultaneously suppressed. Although this model is supported by transcriptomic and proteomic studies, our work does not establish that activation of this futile cycle is required for increased energy expenditure or fat loss. Future approaches that selectively disrupt ribosome biogenesis or protein synthesis during Trp deprivation may be important to determine whether this response is causal or represents one component of a broader metabolic adaptation.

Methods

Animals

All procedures were approved by the Institutional Animal Care and Use Committee of the University of Texas Southwestern Medical Center (approval number: 2017-101798) and followed the guidelines from National Institutes of Health (NIH). Mice were housed at 22 °C with 30-70 % humidity. Mouse cages were replaced at least every other week, and health checks were performed by the UTSW veterinary team twice a day. Food and water were given ad libitum. Six- to 10-week-old male and female C57BL/6J (B6, Strain #:000664), FVB (Strain #:001800), homozygous obese spontaneous mutation ob/ob (Strain #:000632), and male Fgf21 KO mice (Strain #:033846) obtained from Jackson Laboratories were used.

Diets and feedings studies

Inotiv performed all custom research diets, which were generated to provide consistent kibble weights of. Defined diets lacked one of the following essential amino acids: isoleucine, Trp (hereafter called Trypt-out), valine, threonine, leucine, methionine, histidine, phenylalanine, or lysine. For diet consistency, cellulose was used to replace the amino acid amount. The high fat diet (HFD) contained 60 % kcal from fat, and the high-fat (HF) Trypt-out diet contained 60 % kcal from fat but lacked Trp. Feeding times were established as a that allows for a weight loss ≤ 25%. The following feeding studies were performed, and unless otherwise noted male mice were used for all feeding studies. For the defined diet studies, B6 mice 10-12 weeks old were fed either the control or a diet lacking one of the nine essential amino acid for the specified time points, from 3 days to 5 weeks. For diet-induced obese (DIO) studies using B6 mice and FVB mice, the 10-week-old mice

fed for 12 weeks to generate obese mice. Following verification of DIO, the mice were fed either the control or the Trypt-out diet for 4 weeks. For the pre-obese study using ob/ob mice, 6-week-old mice were fed either the control or the Trypt-out diet for 4 weeks. For the study using Fgf21 KO mice 10-12 weeks old mice were fed either the HFD or the HF Trypt-out diet for 4 weeks. For the microbiome depletion studies, B6 12 weeks old and ob/ob 10 weeks old mice were treated with streptomycin-penicillin G (2 g/L) for 6 weeks and 8 weeks, respectively, while receiving either the control or the Trypt-out diet. For the Trp metabolite supplementation study, ob/ob 10 weeks old mice received by daily intraperitoneal (IP) injections at L-Trp (10 mg/kg), I3P (10 mg/kg), 5-HTP (50 mg/kg), or Kyn (20 mg/kg) for 5 weeks while being fed the Trypt-out diet. For the sucrose supplementation study, ob/ob 10 weeks old mice were fed the Trypt-out diet for 4 weeks with sucrose-containing water (100 g/mL). For the obesity prevention studies, B6 12 weeks, ob/ob 10 weeks old mice were fed either the HFD or the HF-Trypt-out diet for 4 weeks and ob/ob (pre-obese 6 weeks old) were fed either the control or the Trypt-out diet for 4 weeks. For the obesity reversal study, B6 12 weeks old mice were fed for 3 weeks . For the statin (Atovarstatin-ATO) study, ob/ob 10 weeks old mice were fed for 3 weeks either the control diet with or without ATO (80 mg/Kg) supplementation or the Trypt-out diet with vehicle injections .

Microbiome depletion

To deplete the gut microbiota, mice received drinking water containing streptomycin sulfate (2 g/L; #J61299) and penicillin G potassium salt (0.95 g/L; #P8721) ad libitum for at least 1 week before initiation of the experiment. Antibiotic treatment was maintained continuously throughout the duration of the study. This method has previously been verified internally by 16S RNA-seq.

Cell culture

All cultured cells were obtained from ATCC (www.atcc.org). H2.35 hepatocytes (CRL 1995) were derived from a 6-week-old female BALB/c mouse and were cultured in DMEM with 10% fetal bovine serum (FBS), 100 U/mL Penicillin-Streptomycin, and 200 nM Dexamethasone. 3T3-L1 (CL-173) cells were cultured the same way as H2.35 but without dexamethasone. This cell line is a substrain of 3T3 fibroblast cell line derived from an NIH/Swiss embryo and can be differentiated into adipocytes [39]. For

adipocyte differentiation, 3T3-L1 cells were incubated with 5 mg/mL of insulin (1x), 1 mM dexamethasone, and 0.5 mM isobutyl methylxanthine (IBMX). The medium was replaced every 2 days until day 10, at which time it was changed to contain only 5 mg/mL insulin for maintenance. For experiments using Trp-depleted medium, the medium was created from powder according to the manufacturer's instructions (US Biologicals) and supplemented with 10 % dialyzed FBS and 100 U/mL Penicillin-Streptomycin.

Food consumption and body weight measures

Food consumption and body weight were measured once per week during the light cycle phase between 2 pm and 5 pm throughout the experiment course using the electronic balance Bonvoisin Lab Scale (X002FL0N8H). All mice were caged individually during the whole experimental period. Food consumption was calculated by the change in food weight between the previous week and the current week and reported in grams. The body weight was recorded every week by placing the mice on the scale.

Body composition

Whole-body composition was assessed using nuclear magnetic resonance (Bruker Minispec mq10, Bruker Corporation, Billerica, MA, USA) to measure total lean mass and total fat mass, reported in grams and as a percentage of body weight. Measurements were performed during the light cycle between 2 and 5 pm.

Blood glucose and glucose tolerance test

The next EZ blood glucose monitoring system (X002X2KO5F) was used to measure blood glucose and for the glucose tolerance test (GTT). Blood glucose levels were measured after a 4-hour fast. GTTs were conducted by giving intraperitoneal injection of glucose (2.0 g/kg) and collecting blood from the tail vein at 0, 15, 30, 60, 90 and 120 minutes.

Hormone analysis

The Bio-Plex Pro Mouse Diabetes 8-Plex Assay (#171F7001M) was used for hormone analysis. The levels of ghrelin, GIP, GLP-1, glucagon, insulin, leptin, PAI-1 and resistin were measured in the serum obtained from the tail vein.

Morphology and morphometrics

Gonadal white adipose tissue (gWAT), inguinal white adipose tissue (iWAT), and liver from each mouse were harvested and maintained for 48 hours in 10% formalin solution. Then, tissues were dehydrated in ethanol, embedded in paraffin, and sectioned with 5 μm width. Hematoxylin and eosin (H&E) staining was used to visualize morphology. The sections were stained with H&E performed by the UT Southwestern Medical Center (UTSW) Tissue Core as previously described [11]. The H&E sections were scanned using the digital slide scanner Nanozoomer S60v2 C16600-01 (Hamamatsu Photonics K. K., USA). The images were acquired using the software NDPview2 and analyzed using the AdipoQ plugin in ImageJ [40]

Metabolic cages

Metabolic cage studies were performed by the UTSW Mouse Metabolic Phenotyping Core using the CLAMS system (Teppei Fujikawa). Prior to measurements, mice were acclimatized to the metabolic cages for 5 days. Briefly, mice were maintained on a 12 hour dark/light cycle at room temperature. Metabolic parameters were monitored and recorded continuously using the TSE calorimetric system (TSE System, Germany). All mice were single housed in the metabolic chambers and maintained on ad libitum food and water with the respective diets according to the experimental groups. For metabolic rate measurements performed under room temperature then progressing to thermoneutral conditions (~27-30 °C), indirect calorimetry was performed using an open respirometer system (PhenoMaster/LabMaster System; TSE Systems). Prior to experimentation, mice were housed in the calorimeter for 5 days of acclimation at ~28 °C with access to food and water. TSE PhenoMaster environmental chambers were used to measure O_2 consumption, CO_2 production, RER, and heat production by indirect calorimetry. Locomotor activity was recorded using the same equipment, and the data were collected at the same time. The data was acquired at the Metabolic Phenotyping Core of UT Southwestern Medical Center

Urine collection and analysis

Water consumption and urine output were measured using small rodent urine collection cages (Tecniplast Laboratory Animal Equipment, West Chester, PA, USA), which enable accurate quantification

of daily water consumption and 24 hour urine production. Mice were previously acclimated for 3 days in the urine collection cages before the start of collections. Urine analysis was performed using the VITROS XT 3400 system at the UT Southwestern Metabolic Phenotyping Core.

Bomb calorimetry

Stool from 10-week-old obese (ob/ob) male mice fed on the control, Trypt-out, control high-fat, and high-fat Trypt-out diets for 5 weeks were harvested. Stool was dried in a centrifugal evaporator (Centrivap Concentrator, Labconco, Kansas City, MO) for 72 hours. After drying, the pellets were pulverized before analysis. A Parr 6200 Isoperibol Calorimeter (Moline, IL) equipped with a 6510 Parr Water Handling system and a semi-micro vessel was used to conduct the calorific tests. The gross heat of sample combustion (cal/g) is reported.

RNA-sequencing

RNA was prepared from liver, muscle, and iWAT flash-frozen from 12-week-old B6 male mice fed the control and Trypt-out diets for 3 weeks. RNA-seq analysis was performed by Genewiz/Azenta. The data were analyzed using Trim Galore (v0.6.4) with the trimmed reads aligned to the human genome (GRCH38) or mouse genome (mm10) using STAR (2.7.3a). Gene expression was quantified using feature Counts of the Subread (v1.6.3) package. Low-expressed genes (genes with the expression value of 0 in more than 30% of samples) were removed before any subsequent analysis. Gene expression was normalized using the Voom method from the R package limma (v 3.50.3). Differentially expressed genes were identified using the same package. Gene Set Enrichment Analysis for the DEGs was performed using R package clusterProfiler (v4.2.2). The analysis was performed using log2 fold change = 0.585, with a significance threshold of $p \leq 0.05$, and gene enrichment was assessed using Fisher's exact test with a p value threshold of ≤ 0.05.

Western blot

For total protein extraction, RIPA lysis buffer system (sc-24948A) was used containing protease and phosphatase inhibitors. SDS-polyacrylamide gel electrophoresis was used to separate proteins on 4-12%

gradient gels (catalogue number NW04125 and NW04120, Invitrogen, USA) and transferred to nitrocellulose membranes (catalogue number 88018**)** to blot with the specific antibodies (Key Resources Table). Western blots were performed using chemiluminescence (Thermos Fisher-PI34076), and images were acquired using BioRad ChemiDoc Imager system.

Puromycylation

For the in vitro assays, puromycin (20 μg/mL) was added to H2.35 cells and 3T3L1 cells 2 hours prior to harvesting. After incubation, the cells were lysed in RIPA buffer and processed for western blot analysis using an anti-puromycin antibody. For the in vivo assays, OP-Puro (BroadPharm BP-50103, MW 495.54) was diluted in PBS and filtered through a 0.22 μm filter. Mice were weighed and injected intraperitoneally with puromycin (40 nmol/g). Two hours after injection, mice were euthanized, and liver, gWAT, iWAT, and muscle tissues were collected and processed for western blot analysis.

In vitro analyses of metabolic enzymes

When indicated, supplemental Trp was solubilized in 50:50 water:DMSO. All other additional chemical stocks were dissolved in DMSO. In general, when Trp presence was modulated, 75 μM Trp was added or not to Trp-depleted medium to allow for direct comparison.

Trp Metabolite Quantification by LC-MS/MS

Trp metabolites in serum, BAT, gWAT, iWAT and liver were analyzed by LC-MS/MS performed by the UTSW Preclinical Pharmacology Core using a previously established method [41]. Homogenized tissues were resuspended in a 3-fold volume of PBS using a Bead Bug microtube homogenizer prefilled tubes with 3.0 mm Zirconium beads (Sigma Z763802) and run for 2 minutes at 2800 rpm. Each tissue sample (50 μL) was precipitated with 200 μL methanol, incubated at RT for 10 minutes, and spun in a tabletop, chilled centrifuge for 5 minutes at 16,100 x g. Each supernatant was transferred to an Eppendorf tube and dried down using a Speed Vac without heat. The dried sample was resuspended in 0.1 mL ddH_2O containing 10 ng/mL d5-Trp and 100 ng/mL d5-IAA as internal standards. A matrix for preparation of the standard curves was prepared by combining equal amounts of each resuspended sample and then diluting

as needed to accommodate endogenous levels (1:1000 for kynurenine and 5-hydroxytryptophan and 1:5000 for Trp, serotonin, and indole-3-pyruvic acid (I3P) standard curves.) Diluted background matrix (100 µL) was then spiked with 1 µL of the appropriate standard at varying concentrations. Samples were transferred to a low volume 96-well HPLC plate and analyzed by LC-MS/MS.

Metabolomics analyses

Liver, BAT, gWAT, iWAT and stool of ob/ob male mice fed the control and Trypt-out diet for 4 weeks were collected and proceeded for metabolite extraction. Between 20-25 mg of frozen tissues were resuspended in 300 µL of ice-cold methanol/water 80:20 (vol/vol) and homogenized using a manual homogenizer (Sigma Z359947). Lysates were centrifuged at ~20,160g for 15 min in a refrigerated centrifuge and metabolite containing supernatants transferred into a new tube. A volume equivalent to 10 mg of protein was resuspended in 100 mL acetonitrile/water 80:20 (vol/vol) for a final concentration of 0.1 mg/mL] of supernatant protein and then measured by LC-MS/MS at the Metabolomics core at Children's Research Institute at UTSW. The data were plotted using the Metabo Analyst software.

Proteomics

Samples were digested overnight with trypsin (Pierce) following disulfide bond reduction and alkylation. Following solid-phase extraction cleanup with an Oasis HLB µelution plate (Waters), the resulting peptides were reconstituted in 10 µL of 2 % (v/v) acetonitrile (ACN) and 0.1% trifluoroacetic acid in water. Reconstituted peptides (2 µL) were injected onto either an Orbitrap Fusion Lumos or Orbitrap Eclipse mass spectrometer (Thermo) coupled to an Ultimate 3000 RSLC-Nano liquid chromatography systems (Thermo). Samples were injected onto a 75 µm i.d., 75 cm long EasySpray column (Thermo), and eluted with a gradient from 0-28 % buffer B over 90 min. Buffer A contained 2 % (v/v) ACN and 0.1 % formic acid in water, and buffer B contained 80% (v/v) ACN, 10% (v/v) trifluoroethanol, and 0.1 % formic acid in water. The mass spectrometer operated in positive ion mode with a source voltage of 2.5 kV and an ion transfer tube temperature of 30 °C. MS scans were acquired at 120,000 resolutions in the Orbitrap and up to 10 MS/MS spectra were obtained in the Orbitrap for each full spectrum acquired using higher-energy

collisional dissociation for ions with charges 2-7. Dynamic exclusion was set for 25 s after an ion was selected for fragmentation. Raw MS data files were analyzed using Proteome Discoverer v.3.0 (Thermo), with peptide identification performed using Sequest HT searching against the mouse reviewed protein database from UniProt. The false-discovery rate cutoff was 1 % for all peptides. Peaks were detected using the Minora Feature Detector within Proteome Discoverer, and peptide peak intensities were used for peptide quantitation. The sum of peak intensities for all peptides matched to a protein were used as protein abundance values.

Bile acid analysis

Frozen liver samples (approximately 70 mg) were disrupted in 500 µL of chilled methanol on dry ice using a tissue disruption probe. The homogenate was fortified with a cocktail of stable isotopically labeled internal standards, vortex-mixed, and extracted with the addition of 500 µL of chilled acetonitrile. Samples were vortexed thoroughly and incubated at -20 °C for 20 minutes. Following a second vortex-mixing step, samples were incubated for an additional 20 minutes at -20 °C to ensure complete protein precipitation. Samples were then centrifuged at maximum speed in a benchtop microcentrifuge for 10 minutes. The supernatant was transferred to a clean tube and dried under vacuum using a SpeedVac concentrator. The dried extract was reconstituted in 120 µL of methanol, sonicated in a water bath for 5 minutes, diluted with 80 µL of water, and vortex-mixed prior to analysis. Bile acids were quantified by injecting 5 µL of sample with a co-injection of 10 µL of water onto a Nexera X2 UHPLC system coupled to an LCMS-8060 triple quadrupole mass spectrometer (Shimadzu Scientific Instruments). Standard preparation, the stable isotope-labeled internal standard panel, chromatographic conditions, and mass spectrometric parameters followed the LCMS/MS Method Package for Bile Acids (Shimadzu Scientific Instruments). Samples were analyzed at multiple dilution levels to maximize the number of bile acid species that could be accurately quantified.

Cholesterol, triglycerides, AST, and ALT

Serum and tissues were collected from mice, placed into 1.5 mL tubes, let stand for approximately 30 minutes, and then centrifuged at 3,500 rpm for 10 minutes at room temperature. Serum and tissues were

separated and transferred to new tubes, snap frozen and proceeded for analysis of cholesterol, triglycerides, AST, and ALT using the VITROS XT 3400 MicroSlide system.

Free Fatty Acids and glycerol

Serum and tissue samples were prepared as described above for cholesterol. Non-esterified fatty acids (NEFA) and glycerol levels were measured at the UTSW Metabolic Phenotyping Core using an enzymatic colorimetric HR kit (Fujifilm) following the manufacturer's instructions. Glycerol levels were also quantified using an enzymatic colorimetric kit (Millipore-Sigma; Cat # F6428, G7793).

Free amino acid and TCA intermediates quantification

Free amino acids were quantified by LC-MS/MS as previously described, using a Nexera X2 UHPLC system coupled to an LC-MS-8060 triple quadrupole mass spectrometer (Shimadzu Scientific Instruments), according to the referenced method [42]

Lipid peroxidation assay

Differentiated 3T3-L1 cells were incubated with 5 μM C11-BODIPY for 3 days. Cells were then harvested and analyzed by flow cytometry to assess lipid peroxidation. Fluorescence was detected using a bandpass filter (485-565 nm) and acquired on the FL1 channel. Data were analyzed using FlowJo software, with approximately 10,000 live cells per sample.

Cell proliferation

Incucyte ZOOM Live-Cell Analysis System (Sartorius) was used to quantify cell proliferation in 96-well plates which were followed 4-5 days as previously described[36]. Cells were seeded at 1,000 cells per well in 96-well plates and cultured for 5 days. Time points immediately prior to the plateau of the growth curves were selected for presentation. Cell growth was quantified as percent confluence and normalized to control samples at time 0. Six replicates per condition were run concurrently, and the average values were graphed. RSL3 was used at a working concentration of 1 μM, and Ferrostatin1-F1 was used at a working concentration of 2 μM.

Trp mapping

Sequences of each gene were obtained from UniProt database to determine Trp content. The following UniProtKB/SwissProt ID numbers were used for each gene for mapping: Human SCD1: O00767, Mouse SCD1:P13516, Human HMGCS1: Q01581, Mouse HMGCS1: Q8JZK9, Human PPAR-g: P37231, Mouse PPAR-g: P37238, Human PPAR-a: Q07869, Mouse PPAR-a: P23204, Human ACACA: Q13085, Mouse: ACACA: Q5SWU9, Human FASN: P49327, Mouse FASN: P19096, Human DHCR7: Q9UBM7, Mouse DHCR7: O88455, Human ACLY: P53396, Mouse ACLY: Q91V92, Human MVD: P53602, Mouse MVD: Q99JF5.

QUANTIFICATION AND STATISTICAL ANALYSIS

All analyses were performed using the software GraphPad Prism 11 (https://www.graphpad.com). For experiments of 2 groups, Welch's two-tailed unpaired T-tests considering $p \leq 0.05$ as significant were used. For analysis using 3 or more groups, we performed one-way ANOVA with $p \leq 0.05$ designated as significant. All values are reported as mean ± SD in each figure. When noted, n refers to the number of animals per group in each experiment. Further statistical details can be found in Fig. legends. For RNA-seq analysis cutoffs used were p value ≤ 0.05 and log2 fold change ≤ -0.0585 and ≥ 0.0585. Additionally, proteomics analysis was performed using a cutoff of p value ≤ 0.1 and fold change of ≤ 0.5 and ≥ 1.5. During the preparation of this work, the authors used OpenAI to check spelling and grammar, helping improve the readability of a few specific sentences. After using this tool/service, the authors reviewed and edited the content as needed and take full responsibility for the content of the publication.

RESOURCE AVAILABILITY

Lead contact

Requests for further information and resources should be directed to and will be fulfilled by the Lead Contact, Maralice Conacci-Sorrell (maralice.conaccisorrell@utsouthwestern.edu).

ACKNOWLEDGEMENTS

We are grateful to the Sorrell lab members for their valuable feedback on this manuscript. We thank Adriana Ventura for help with analysis and Jan-Bernd Funke for help with tissue lysis and Dr. Shun Fang for help with initial measurement of lipid droplet size in H&E images. We thank the Sorrell lab, Dr. Jerry Shay, Dr. Beatriz Fontoura, Dr. Russell deBoise-Boyd for discussions and feedback.

DECLARATION OF FUNDING

The research was financially supported by Cancer Prevention and Research Institute of Texas (CPRIT) (RP220046 and RP250402), American Cancer Society (724003), Welch Foundation (I-2058-20210327), NCI R01CA245548, and NIGMS GM145744-01 to MCS, U19CA264385 to JWS, Mary Kay and American Heart Association (AHA) 10070838 for postdoctoral fellowships to PN and Mary Kay postdoctoral fellowships to SF, and Mechanisms of Disease and Translational Science T32 (T32CA291654) to AG. MCS is the Virginia Murchison Linthicum Scholar in Medical Research. The authors acknowledge the support of UT Southwestern Metabolomics Core CRI CPRIT RP180778 Proteomics Core, and Histo Pathology Core and the Simmons Comprehensive Cancer Center P30CA142543. The authors thank UT Southwestern Metabolic Phenotyping Core (RRID:SCR_026404) for the analysis and expertise.

AUTHOR CONTRIBUTIONS

MCS and PASN planned the experiments. MCS, PASN, LPC, and EP wrote the manuscript. NV, LPC, PASN, EP, JAK, IND, ILS, YH performed the experiments. LG and LX performed the RNA-seq data analyses. AL performed the proteomics analyses. RG quantified amino acids, lipids, and liver damage. RJD, PS, NSW, and MCS supervised the study.

DECLARATION OF INTERESTS

M.C.S. has a pending patent application on Trypt-out. R.J.D. is an adviser for Illumina, General Metabolics, Vida Ventures, Faeth Therapeutics, and Alterris Oncology, and is a founder and adviser at Atavistik Bioscience.

FIGURE LEGENDS

Fig. 1. Trypt-out drives fat loss with minimal lean mass wasting and preserved food consumption in wild-type and leptin-deficient (ob/ob) mice.

(A) Experimental design comparing nine synthetic diets, each lacking one of the essential amino acids. Male B6 mice were fed either the control or a single amino acid–free diet for 3 weeks.

(B) Summary of the effects of single essential amino acid deprivation diets on body weight (BW), fat mass, and lean mass in C57BL/6J (B6) male mice (n = 3). Values are normalized to the control diet group. Data are presented as mean ± SD and were analyzed using an unpaired Welch's t-test. **Reduced food consumption , $p \leq 0.05$; *reduced food consumption , $p \leq 0.07$.

(C) Experimental design for both male and female B6 and ob/ob mice fed either the control or the Trypt-out diet for 3 or 4 weeks, respectively.

(D) Representative images of male B6 and ob/ob mice fed either the control or the Trypt-out diet for 3 and 4 weeks, respectively.

(E) Serum levels of Trp metabolites in B6 male mice (n =) fed either the control or the Trypt-out diet for 3 weeks. Trp, Tryptophan, Kyn, kynurenine, Serot, serotonin. Data are presented as mean ± SD and were analyzed using an unpaired Welch's t-test.

(F) Percent body weight change in male (n = 3) and female (n = 4) B6 mice and male (n = 4) and female (n = 4) ob/ob mice fed either the control or the Trypt-out diet. Data are presented as mean ± SD and were analyzed using an unpaired Welch's t-test.

(G) Cumulative food consumed by male (n = 3) and female (n = 4) B6 mice and male (n = 4) and female (n = 4) ob/ob mice fed either the control or the Trypt-out diet. Data are presented as mean ± SD and were analyzed using an unpaired Welch's t-test.

(H) Food consumption normalized per body weight in male (n = 3) and female (n = 4) B6 mice and male (n = 4) and female (n = 4) ob/ob mice fed either the control or the Trypt-out diet. Data are presented as mean ± SD and were analyzed using an unpaired Welch's t-test.

(I) Weekly body weights in male ob/ob mice (n = 4) beginning at 10 weeks old and fed either the control or the Trypt-out diet for 4 weeks and then maintained on the control diet for an additional 9 weeks. Data are presented as mean ± SD and were analyzed using an unpaired Welch's t-test.

(J) Percent lean mass and percent fat in male B6 (n = 3) and ob/ob (n = 4) mice fed either the control or Trypt-out diet. Data are presented as mean ± SD and were analyzed using an unpaired Welch's t-test.

(K) Lean and fat mass (g) in male B6 (n = 3) and ob/ob (n = 4) mice fed either the control or the Trypt-out diet. Data are presented as mean ± SD and were analyzed using an unpaired Welch's t-test.

(L) Respiratory exchange ratio (RER), measured by indirect calorimetry over 4 days across light and dark cycles in male B6 (n = 3) and ob/ob (n = 4) mice fed either the control or the Trypt-out diet. Data are presented as mean ± SD and were analyzed using an unpaired Welch's t-test. p values correspond to the area under the curve.

(M) Blood glucose levels after 4 hours of fasting in male B6 (n = 3) or ob/ob (n = 4) mice fed either the control or the Trypt-out diet. Data are presented as mean ± SD and were analyzed using an unpaired Welch's t-test.

(N) Area under the curve (AUC) for glucose tolerance test (GTT) for male B6 (n = 3) and male ob/ob mice (n = 4) fed either the control or Trypt-out diet. Data are presented as mean ± SD and were analyzed using an unpaired Welch's t-test.

(O) GTT curve comparing male B6 mice (n = 3) fed either the control or Trypt-out diet.

(P) GTT curve comparing male ob/ob mice (n = 4) fed either the control or Trypt-out diet.

(Q) Leptin and insulin serum levels in male B6 mice fed either the control (n = 2) or Trypt-out diet (n = 3).

Fig. 2. Trypt-out prevents and reverts obesity in DIO mice.

(A) Experimental design for the diet-induce obesity (DIO) study. Male B6 mice were fed a high-fat diet (HFD) for 12 weeks to induce obesity and then feed either the control (n = 3) or the Trypt-out diet (n = 4) for 4 weeks.

(B) Body weight gain over the 4 weeks of diet intervention and percent body weight change in B6 DIO male mice fed either the control (n = 3) or Trypt-out (n = 4) diet. Data are presented as mean ± SD and were analyzed using an unpaired Welch's t-test.

(C) Cumulative food consumed comparing B6 DIO male mice fed either a control (n = 3) or Trypt-out diet (n = 4). Data are presented as mean ± SD and were analyzed using an unpaired Welch's t-test.

(D) Food consumption normalized per body in male B6 DIO mice fed either a control (n = 3) or Trypt-out diet (n = 4). Data are presented as mean ± SD and were analyzed using an unpaired Welch's t-test.

(E) Percent lean mass and percent fat mass in male B6 DIO mice fed either a control (n = 3) or Trypt-out diet (n = 4). Data are presented as mean ± SD and were analyzed using an unpaired Welch's t-test.

(F) Lean and fat mass in grams (g) comparing male B6 DIO mice fed either a control (n = 3) or Trypt-out diet (n = 4). Data are presented as mean ± SD and were analyzed using an unpaired Welch's t-test.

(G) Experimental design of 6-week-old male ob/ob (pre-obese) mice fed either a control or Trypt-out diet for 4 weeks (n = 4).

(H) Body weight gain over the 4 weeks of diet intervention and percent body weight comparing 6-week-old male ob/ob mice fed either a control or Trypt-out diet (n = 4). Data are presented as mean ± SD and were analyzed using an unpaired Welch's t-test.

(I) Cumulative Food consumed in 6-week-old male ob/ob mice fed either a control or Trypt-out diet (n = 4). Data are presented as mean ± SD and were analyzed using an unpaired Welch's t-test.

(J) Food consumption normalized to body weight in 6-week-old male ob/ob mice fed either a control or Trypt-out diet (n = 4). Data are presented as mean ± SD and were analyzed using an unpaired Welch's t-test.

(K) Percent lean mass and percent fat mass in 6-week-old male ob/ob mice fed either a control or Trypt-out diet (n = 4). Data are presented as mean ± SD and were analyzed using an unpaired Welch's t-test.

(L) Lean and fat mass in grams (g) in 6-week-old male ob/ob mice fed a control or Trypt-out diet (n = 4). Data are presented as mean ± SD and were analyzed using an unpaired Welch's t-test.

(M) Western blot analysis of FGF21 in liver lysates (top) and serum (bottom) from male B6 mice fed control or Trypt-out diets for 3 weeks (n = 3).

(N) Western blot analysis of FGF21 in liver lysates (top) and serum (bottom) from male ob/ob mice fed control or Trypt-out diets for 4 weeks (n = 4)

(O) Body weight of Fgf21 knockout (KO) male mice fed either a control or Trypt-out diet (n = 4) for 4 weeks. Data are presented as mean ± SD and were analyzed using an unpaired Welch's t-test.

(P) Food consumed by Fgf21 KO male mice fed either a control or Trypt-out diet (n = 4) for 4 weeks. Data are presented as mean ± SD and were analyzed using an unpaired Welch's t-test.

(Q) Body weight of Fgf21 KO male mice fed either a HFD or HF Trypt-out diet (n = 4) for 4 weeks. Data are presented as mean ± SD and were analyzed using an unpaired Welch's t-test.

(R) Food consumption of Fgf21 KO male mice fed HFD or HF Trypt-out diet (n = 4) for 4 weeks. Data are presented as mean ± SD and were analyzed using an unpaired Welch's t-test.

Fig. 3. Trypt-out effects on body composition are not mediated by global changes in translation or by Trp-derived metabolites.

(A) Puromycylation method to measure translation.

(B) Puromycin immunoblot in cultured mouse hepatocytes (H2.35) 24 and 48 hours in Trp-sufficient or -depleted media. Puromycin was added to the culture medium 2 hours prior to harvesting.

(C) Immunoblot for puromycylation in lysates of undifferentiated and differentiated 3T3L1 cells cultured in Trp-sufficient or -depleted media. Puromycin was added to the culture medium 2 hours prior to harvesting.

(D) Immunoblot for puromycin in lysates from muscle, BAT, gWAT, iWAT, and liver of B6 mice (n = 3) after 3 weeks on either control or Trypt-out diets. Puromycin was administered 3 hours prior to tissue collection.

(E) Body weight of male B6 mice (n = 3) fed either control or Trypt-out diet following microbiome depletion with penicillin G (0.95 g/L) and streptomycin (2 g/L) in drinking water for 3 weeks prior to diet initiation and maintained throughout the intervention. Data are presented as mean ± SD and were analyzed using an unpaired Welch's t-test.

(F) Body weight of male ob/ob mice (n = 4) fed either a control or Trypt-out diet following microbiome depletion with penicillin G (0.95 g/L) and streptomycin (2 g/L) in drinking water for 3 weeks prior to diet initiation and maintained throughout the intervention. Data are presented as mean ± SD and were analyzed using an unpaired Welch's t-test.

(G) Schematic of Trp metabolism and its main catabolic pathways.

(H) Serum levels of Trp metabolites (Trp, Kyn, I3P and 5-HT) (ng/mL) in ob/ob male mice fed either a control or Trypt-out diet for 4 weeks. Data are presented as mean ± SD and were analyzed using an unpaired Welch's t-test.

(I) Body weight of male ob/ob mice (n = 4) on a Trypt-out diet concomitantly with daily intraperitoneal injections of Trp-derived metabolites (Kyn, I3P, or 5-HTP) for 5 weeks. Data are presented as mean ± SD and were analyzed using an unpaired Welch's t-test.

(J) Metabolic pathway leading to Acetyl-CoA generation from Trp and Lys.

(K) Experimental design for dietary intervention in male ob/ob mice fed a Trypt-out diet with either normal water or sucrose supplementation for 4 weeks.

(L) Representative images of male ob/ob mice fed a Trypt-out diet with either control water or sucrose supplementation for 4 weeks.

(M) Body weight in ob/ob male mice fed Trypt-out diet and supplemented with either normal water (n = 3) or sucrose (n = 4). Data are presented as mean ± SD and were analyzed using an unpaired Welch's t-test.

Fig. 4. Trypt-out decreases adiposity and hepatic lipid droplets in obese mice.

(A) gWAT weight in mice fed either a control or Tryp-out diet. B6 male mice were fed either a control (n = 5) or Trypt-out (n = 4) diet for 3 weeks. Male (n = 4) and female (n = 4) ob/ob mice were fed either a control or Trypt-out diet for 4 weeks. Male pre-obese ob/ob mice (n = 4) were fed either a control or Trypt-out diet for 6 weeks. Male B6 DIO mice (n = 3) were fed either a control or Trypt-out diet for 4 weeks. Data are presented as mean ± SD and were analyzed using an unpaired Welch's t-test.

(B) iWAT weight in male B6 mice fed either a control (n = 5) or Trypt-out (n = 5) diet for 3 weeks; male (n = 4) and female (n = 4) ob/ob mice; male pre-obese ob/ob mice (6 weeks, n = 4); and male B6 DIO mice (n = 3), fed either a control or Trypt-out diet for 4 weeks. Data are presented as mean ± SD and were analyzed using an unpaired Welch's t-test.

(C) BAT weight in male B6 mice fed either a control (n = 5) or Trypt-out (n = 5) diet for 3 weeks; male (n = 4) and female (n = 4) ob/ob mice; male pre-obese ob/ob mice (6 weeks, n = 4); and male B6 DIO mice (n = 3), fed either a control or Trypt-out diet for 4 weeks. Data are presented as mean ± SD and were analyzed using an unpaired Welch's t-test.

(D) Liver tissue weight in male B6 mice fed either a control (n = 5) or Trypt-out (n = 5) diet for 3 weeks, male (n = 4) and female (n = 4) ob/ob mice; male ob/ob (6 weeks, n = 4), and male B6

DIO (n = 3) mice fed either a control or Trypt-out diet for 4 weeks. Data are presented as mean ± SD and were analyzed using an unpaired Welch's t-test.

(E) Representative tissue image (liver, BAT, iWAT and gWAT) of male ob/ob mice fed either a control or Trypt-out diet for 4 weeks.

(F) Images of H&E-stained gWAT, iWAT, BAT and liver of male B6 mice (n = 3). Scale bar: 50 μm.

(G) Images of H&E-stained gWAT, iWAT, BAT and liver of male FVB DIO mice (n = 3). Scale bar: 50 μm.

(H) Images of H&E-stained gWAT, iWAT, BAT and liver of male ob/ob mice (n = 3). Scale bar: 100 μm.

(I) Metabolomics analysis of iWAT and gWAT from male ob/ob mice (n = 3). The raw data are presented in heatmap plotted using MetaboAnalyst with the unpaired Welch's t-test.

(J) Schematic of 3T3-L1 preadipocyte differentiation into adipocytes.

(K) Immunoblot for adipocyte markers in lysates of undifferentiated and differentiated adipocyte lineage cell line (3T3L1).

(L) Flow cytometry analysis for C11-BODIPY in undifferentiated and differentiated 3T3L1 cells cultured in Trp-sufficient or -depleted medium. Data are presented as mean ± SD and were analyzed using an unpaired Welch's t-test.

(M) Growth analysis represented as a relative confluence undifferentiated 3T3L1 cells cultured in Trp-sufficient or -depleted medium and in the presence of the inhibitor (Ferrostatin1-F1, at 2 μM) or activator (RSL3, at 1 μM) of ferroptosis for 116 hours. Data was acquired from Incucyte live-cell analysis system and presented as mean ± SD, analyzed using ordinary one-way ANOVA with Dunnett's multiple comparisons.

(N) Growth analysis represented as a relative confluence differentiated 3T3L1 cells cultured in Trp-sufficient or -depleted medium and in the presence of the inhibitor (Ferrostatin1-F1 at 2 μM)) or

activator (RSL3 at 1 μM) of ferroptosis for 116 hours. Data was acquired from Incucyte live-cell analysis system and presented as mean ± SD, analyzed using ordinary one-way ANOVA with Dunnett's multiple comparisons.

(O) Immunoblot for adipogenesis and cell death markers in lysates of undifferentiated and differentiated 3T3L1 cells cultured in Trp-sufficient or -depleted medium.

(P) Cell death represented by CellTox uptake in undifferentiated or differentiated adipocytes (3T3L1) cells cultured in Trp-sufficient or -depleted medium at 48 hours. Data was acquired from Incucyte live-cell analysis system and presented as mean ± SD, analyzed using ordinary one-way ANOVA with Dunnett's multiple comparisons.

(Q) CellTox assays fluorescent image of undifferentiated and differentiated 3T3L1 cultured in Trp-sufficient or -depleted medium.

(R) Body weight in male ob/ob mice (n = 3) fed the Trypt-out diet and treated with daily intraperitoneal injections of vehicle or liproxstatin-1 (Lip1). Data are presented as mean ± SD and were analyzed using an unpaired Welch's t-test.

Fig. 5. Trypt-out reduces the expression of lipogenic enzymes.

(A) Experimental design showing B6 mice fed either a control (n = 3) or Trypt-out (n = 3) diet for 3 weeks, and the tissues collected for RNA-seq analysis.

(B) KEGG pathways upregulated and downregulated in RNA-seq analysis of muscle from B6 mice (n = 3) fed the Trypt-out diet for 3 weeks. Cutoff used was ≥ 0.585 or ≤ -0.585-fold change; $p \leq 0.05$.

(C) KEGG pathways upregulated and downregulated in RNA-seq analysis of iWAT from B6 mice (n = 3) fed the Trypt-out diet for 3 weeks. Cutoff used was ≥ 0.585 or ≤ -0.585-fold change; $p \leq 0.05$.

(D) KEGG pathways upregulated and downregulated in RNA-seq analysis of liver from B6 mice (n = 3) fed the Trypt-out diet for 3 weeks. Cutoff used was ≥ 0.585 or ≤ -0.585-fold change; $p \leq 0.05$.

(E) List of lipogenic enzymes selectively downregulated at the protein level, with no corresponding changes detected by RNA-seq. Proteomics mass spectrometry of liver protein lysates. Cutoff used was 30% downregulation $p \leq 0.1$.

(F) Schematic of lipogenic and cholesterol biosynthetic enzymes regulated by the Trypt-out diet on transcriptional and protein (green) or only protein (blue) levels.

(G) Immunoblot analysis of lipogenic enzymes in liver lysates from B6 male mice (n = 3) fed either a control or Trypt-out diet for 3 weeks.

(H) Immunoblot analysis of lipogenic enzymes in liver lysates from ob/ob male mice (n = 3) fed either a control or Trypt-out diet for 4 weeks.

(I) Immunoblot analysis of TCA cycle and β-oxidation proteins in liver lysates from ob/ob male mice (n = 4) fed either control or Trypt-out diet for 4 weeks.

(J) Immunoblot analysis of lipogenic enzymes in liver lysates from B6 male mice (n = 3) fed either a control or Trypt-out diet for 3 days.

(K) Immunoblot analysis of lipogenic enzymes in liver lysates from B6 male mice (n = 3) fed for 3 weeks a diet of control, Trypt-out, or Trypt-out with Trp supplementation by intraperitoneal injections for the last 7 days.

Fig. 6. Trypt-out-induced weight loss is resistant to HFD supplementation.

(A) Experimental design for dietary intervention in male B6 mice fed either a high-fat diet (HFD) or HFD Trypt-out diet for 4 weeks.

(B) Percent body weight change in male B6 mice fed either a HFD (n = 5) or HF Trypt-out (n = 5) diet for 4 weeks. Data are presented as mean ± SD and were analyzed using an unpaired Welch's t-test.

(C) Cumulative food consumption in male B6 mice fed either a HFD (n = 5) or HF Trypt-out (n = 5) diet for 4 weeks. Data are presented as mean ± SD and were analyzed using an unpaired Welch's t-test.

(D) Food consumption normalized per body weight in male B6 fed either a HFD (n = 5) or HF Trypt-out (n = 5) diet for 4 weeks. Data are presented as mean ± SD and were analyzed using an unpaired Welch's t-test.

(E) Lean and fat mass percentage (%) in male B6 mice fed either a HFD (n = 5) or HF Trypt-out (n = 5) diet for 4 weeks. Data are presented as mean ± SD and were analyzed using an unpaired Welch's t-test.

(F) Lean and fat mass grams (g) in male B6 mice fed either a HFD (n = 5) or HF Trypt-out (n = 5) diet for 4 weeks. Data are presented as mean ± SD and were analyzed using an unpaired Welch's t-test.

(G) Schematic of the experimental design for dietary intervention in male ob/ob mice fed either a HFD or HFD–Trypt-out diet for 4 weeks.

(H) Representative images of male ob/ob mice fed either a HFD (n = 4) or HF Trypt-out (n = 4) diet for 4 weeks.

(I) Body weight of male ob/ob mice fed either a HFD (n = 4) or HF Trypt-out (n = 4) diet. Data are presented as mean ± SD and were analyzed using an unpaired Welch's t-test.

(J) Food consumption in ob/ob male mice fed either a HFD (n = 4) or HF Trypt-out (n = 4) diet for 4 weeks. Data are presented as mean ± SD and were analyzed using an unpaired Welch's t-test.

(K) GTT in male ob/ob mice fed either a HFD (n = 4) or HF Trypt-out (n = 4) diet for 4 weeks. Data are presented as mean ± SD and were analyzed using an unpaired Welch's t-test.

(L) Tissue weight of male ob/ob mice fed a either HFD (n = 4) or HF Trypt-out (n = 4) diet for 4 weeks. Data are presented as mean ± SD and were analyzed using an unpaired Welch's t-test.

(M) Immunoblot analysis of lipogenic enzymes in liver lysates from male ob/ob mice fed either a HFD (n = 3) or HF Trypt-out (n = 3) diet for 4 weeks.

(N) Body weight gain of male B6 DIO mice fed a HFD (n = 6) for 18 weeks and followed by dietary intervention with HF Trypt-out diet (n = 3) altered with by HFD pair feeding (n = 3, binge diet) for 4 weeks and HF Trypt-out altered with by HFD ad libitum (binge diet) for 18 weeks. After the binge period, both groups were returned to HFD for 10 weeks. Data are presented as mean ± SD and were analyzed using an unpaired Welch's t-test.

(O) Representative image of a male B6 DIO mouse fed the HFD and a male B6 DIO mouse fed the Binge diet.

(P) Serum levels of alanine aminotransferase (ALT) in male B6 mice (n = 3) fed either a control or Trypt-out for 3 weeks. Male ob/ob mice fed either a control (n = 3) or Trypt-out (n = 3) diet for 4 weeks. Male B6 DIO mice fed either a control (n = 3) or Trypt-out (n = 3) diet for 4 weeks. Male B6 DIO fed the Binge diet (n = 3) as described in N. Data are presented as mean ± SD and were analyzed using an unpaired Welch's t-test.

(Q) Images of H&E-stained liver, gWAT and iWAT from a B6 DIO mouse fed the HFD and from a B6 DIO mouse fed Binge diet. Scale bar: 50 μm.

Fig. 7: The Trypt-out diet is a potent inhibitor of hepatic biosynthesis of lipids and cholesterol in obese mice.

(A) Schematic representation of the relationship between the TCA cycle and lipogenic pathways through citrate and acetyl-CoA.

(B) Serum cholesterol levels in mice. Male B6 mice were fed either the control (n = 3) or Trypt-out (n = 3) diet for 3 days or 3 weeks. Male ob/ob mice were fed either the control (n = 3) or Trypt-

out (n = 3) for 4 weeks. Male B6 DIO mice were fed either the HFD (n = 3) or Binge diet (n = 3) as described in Fig. 6N. Data are presented as mean ± SD and were analyzed using an unpaired Welch's t-test.

(C) Serum triglyceride levels in mice. Male B6 mice were fed either the control (n = 3) or Trypt-out (n = 3) diet or 3 weeks. Male ob/ob mice were fed the control (n = 3) or Trypt-out (n = 3) diet for 4 weeks. Male B6 DIO mice were fed either the HFD (n = 3) or Binge diet (n = 3) as described in Fig. 6N. Data are presented as mean ± SD and were analyzed using an unpaired Welch's t-test.

(D) Cholesterol levels in the serum, liver, iWAT and gWAT of male ob/ob mice fed either the control (n = 3) or Trypt-out (n = 3) diet for 4 weeks. Data are presented as mean ± SD and were analyzed using an unpaired Welch's t-test.

(E) Triglyceride levels in the serum, liver, iWAT, and gWAT of male ob/ob mice fed either the control (n = 3) or Trypt-out (n = 3) diet for 4 weeks. Data are presented as mean ± SD and were analyzed using an unpaired Welch's t-test.

(F) Liver citrate levels in mice. Male B6 mice were fed either the control (n = 3) or Trypt-out (n = 3) diet for 3 weeks. Male ob/ob were fed either the control (n = 3) or Trypt-out (n = 3) diet for 4 weeks. Male ob/ob mice were fed either the HFD (n = 3) or HF Trypt-out (n = 3) diet for 4 weeks. Data are presented as mean ± SD and were analyzed using an unpaired Welch's t-test.

(G) Liver malate levels in mice. Male B6 mice were fed either the control (n = 3) or Trypt-out (n = 3) diet for 3 weeks. Male ob/ob mice were fed the control (n = 3) or Trypt-out (n = 3) diet for 4 weeks and ob/ob male mice (n = 4) were fed either HFD (n = 3) or HF Trypt-out (n = 3) diet. Data are presented as mean ± SD and were analyzed using an unpaired Welch's t-test.

(H) Bile acids in the liver of male B6 mice fed either the control (n = 3) or Trypt-out (n = 3) diet for 3 weeks. Data are presented as mean ± SD and were analyzed using an unpaired Welch's t-test.

(I) Bile acids in the liver of male ob/ob mice fed either the control (n = 3) or Trypt-out (n = 3) diet for 4 weeks. Data are presented as mean ± SD and were analyzed using an unpaired Welch's t-test.

(J) Bile acids in the liver male ob/ob mice fed either the HFD (n = 3) or HF Trypt-out (n = 3) diet. Data are presented as mean ± SD and were analyzed using an unpaired Welch's t-test.

(K) Stool calories as measure by using BOMB caloric content assay. Male B6 mice were fed either the control (n = 4) or Trypt-out (n = 4) diet for 3 weeks. Male ob/ob mice were fed either the control (n = 4) or Trypt-out (n = 3) diet for 4 weeks. Male ob/ob were fed either the HFD (n = 4) or HF Trypt-out (n = 4) diet. Data are presented as mean ± SD and were analyzed using an unpaired Welch's t-test.

(L) Body weight of male ob/ob mice either fed the control diet with (n = 3) or without atorvastatin administration (ATO, n = 4) or fed the Trypt-out diet with only vehicle administration (n = 4) for 3 weeks. Data are presented as mean ± SD and were analyzed using one-way ANOVA with Tukey multiple comparison test.

(M) iWAT weight of male ob/ob mice either fed the control diet with (n = 3) or without atorvastatin administration (ATO, n = 4) or fed the Trypt-out diet with only vehicle administration (n = 4) for 3 weeks. Data are presented as mean ± SD and were analyzed using one-way ANOVA with Tukey multiple comparison test.

(N) Serum triglycerides levels of male ob/ob mice either fed the control diet with (n = 3) or without atorvastatin administration (ATO, n = 4) or fed the Trypt-out diet with only vehicle administration (n = 4) for 3 weeks. Data are presented as mean ± SD and were analyzed using one-way ANOVA with Tukey multiple comparison test.

(O) Serum cholesterol levels of male ob/ob mice either fed the control diet with (n = 3) or without atorvastatin administration (ATO, n = 4) or fed the Trypt-out diet with only vehicle

administration (n = 4) for 3 weeks. Data are presented as mean ± SD and were analyzed using one-way ANOVA with Tukey multiple comparison test.

(P) Immunoblot analysis of lipogenic enzymes in liver lysates from male ob/ob mice either fed the control diet with (n = 3) or without atorvastatin administration (ATO, n = 3) or fed the Trypt-out diet with only vehicle administration (n = 3) for 3 weeks.

Fig. 8: Working model for lipogenesis and lipid whole body homeostasis in the presence or absence of dietary Trp.

SUPPLEMENTARY FIGURE LEGENDS

Fig. S1. Body weight, food consumption , and body composition in mice fed diets lacking individual essential amino acids.

(A) Body weight of male B6 mice fed either the control diet (n = 3) or a diet lacking the indicated single essential amino acid (n = 3). Data are presented as mean ± SD and were analyzed using an unpaired Welch's t-test.

(B) Change in body weight of male B6 mice fed either the control diet (n = 3) or a diet lacking the indicated single essential amino acid (n = 3). Data are presented as mean ± SD and were analyzed using ordinary one-way ANOVA with Dunnett's multiple comparisons.

(C) Cumulative food consumption in male B6 mice fed either the control diet (n = 3) or a diet lacking the indicated single essential amino acid (n = 3). Data are presented as mean ± SD and were analyzed using an unpaired Welch's t-test.

(D) Fat mass and lean mass in B6 male mice fed either the control diet (n = 3) or a diet lacking the indicated single essential amino acid (n = 3). Data are presented as mean ± SD and were analyzed using ordinary one-way ANOVA with Dunnett's multiple comparisons.

(E) Body weight of B6 male mice fed either the control (n = 5) or Trypt-out (n = 5) diet for 3 weeks. Data are presented as mean ± SD and were analyzed using an unpaired Welch's t-test.

(F) Food consumption in B6 male mice fed either the control (n = 5) or Trypt-out (n = 5) diet for 3 weeks. Data are presented as mean ± SD and were analyzed using an unpaired Welch's t-test.

(G) Food consumption normalized per body weight of male B6 mice fed either the control (n = 5) or Trypt-out (n = 5) diet for 3 weeks. Data are presented as mean ± SD and were analyzed using an unpaired Welch's t-test.

(H) Respirometry analysis for VO_2, VCO_2, locomotor activity, and heat production during dark and light cycle in male B6 mice fed either the control (n = 3) or Trypt-out (n = 3) diet for 3 weeks. Data are presented as mean ± SD and were analyzed in the area under the curve and using an unpaired Welch's t-test.

(I) Respirometry analysis for VO_2, VCO_2, locomotor activity, and heat production during dark and light cycle in ob/ob male mice fed either the control (n = 4) or Trypt-out (n = 4) diet for 4 weeks. Data are presented as mean ± SD and were analyzed the area under the curve and using an unpaired Welch's t-test.

Fig. S2. Trypt-out prevents and reverts obesity in DIO mice and ob/ob mice

(A) Experimental design of male FVB DIO mice fed either the control or Trypt-out diet for 4 weeks.

(B) Body weight of male FVB DIO mice fed either the control (n = 4) or Trypt-out (n = 4) diet on days 10 and 20 of a 4-week feeding period. Data are presented as mean ± SD and were analyzed using an unpaired Welch's t-test.

(C) Food consumption normalized per body weight of FVB DIO male mice fed either the control (n = 4) or Trypt-out (n = 4) diet on days 10 and 20 of a 4-week feeding period. Data are presented as mean ± SD and were analyzed using an unpaired Welch's t-test.

(D) Lean and fat mass (percentage and grams) of FVB DIO male mice fed either the control (n = 4) or Trypt-out (n = 4) diet for 4 weeks. Data are presented as mean ± SD and were analyzed using an unpaired Welch's t-test.

(E) Intraperitoneal glucose tolerance test (GTT) in FVB DIO male mice fed the control (n = 4) or Trypt-out (n = 4) diet for 4 weeks. Data are presented as mean ± SD and were analyzed using an unpaired Welch's t-test.

(F) Intraperitoneal glucose tolerance test (GTT) in ob/ob (pre-obese) male mice fed either the control (n = 4) or Trypt-out (n = 4) diet for 4 weeks. Data are presented as mean ± SD and were analyzed using an unpaired Welch's t-test.

(G) Serum hormones measurements in FVB DIO male mice fed a control or Trypt-out diet (n = 4). Data are presented as mean ± SD and were analyzed using an unpaired Welch's t-test.

(H) Serum hormone levels in B6 male mice fed either the HFD (n = 5) or HF Trypt-out (n = 5) diet for 4 weeks. Data are presented as mean ± SD and were analyzed using an unpaired Welch's t-test.

(I) Respirometry analysis for VO_2during dark and light cycle in male ob/ob (pre-obese) mice fed either the control (n = 4) or Trypt-out (n = 4) diet for 4 weeks. Data are presented as mean ± SD and were analyzed by calculating the area under the curve and using an unpaired Welch's t-test.

(J) Respirometry analysis for VCO_2 during dark and light cycle in male ob/ob (pre-obese) mice fed either the control (n = 4) or Trypt-out (n = 4) diet for 4 weeks. Data are presented as mean ± SD and were analyzed by calculating the area under the curve and using an unpaired Welch's t-test.

(K) Respirometry analysis for RER, heat production, and locomotor activity during dark and light cycle in male ob/ob (pre-obese) mice fed either the control (n = 4) or Trypt-out (n = 4) diet for 4 weeks. Data are presented as mean ± SD and were analyzed by calculating the area under the curve and using an unpaired Welch's t-test.

(L) Heat production, locomotor activity during dark and light cycle in male ob/ob (pre-obese) mice fed either the control (n = 4) or Trypt-out (n = 4) diet for 4 weeks. Data are presented as mean ± SD and were analyzed by calculating the area under the curve and using an unpaired Welch's t-test.

(M) Locomotor activity during dark and light cycle in male ob/ob (pre-obese) mice fed either the control (n = 4) or Trypt-out (n = 4) diet for 4 weeks. Data are presented as mean ± SD and were analyzed by calculating the area under the curve and using an unpaired Welch's t-test.

(N) Representative images of male Fgf21 KO mice fed either the control or Trypt-out diet for 4 weeks.

(O) Tissue weight of male Fgf21 KO mice fed either the control (n = 3) or Trypt-out (n = 3) diet for 4 weeks. Data are presented as mean ± SD and were analyzed using an unpaired Welch's t-test.

(P) Representative images of male Fgf21 KO mice fed either the HFD or HF Trypt-out diet for 4 weeks.

(Q) Tissue weight of male Fgf21 KO mice fed either the HFD (n = 3) or HF Trypt-out diet (n = 4) for 4 weeks. Data are presented as mean ± SD and were analyzed using an unpaired Welch's t-test.

Fig. S3. Trypt-out diet reduces adipose tissue in obese and non-obese mice.

(A) Food consumption for male B6 mice fed chow (n = 3) for 2 weeks and then fed either the control (n = 3) or Trypt-out (n = 3) diet with antibiotic depletion of the microbiome using 0.95 g/L Penicillin G and 2 g/L Streptomycin provided ad libitum in the drinking water. Data are presented as mean ± SD and were analyzed using an unpaired Welch's t-test.

(B) Food consumption for male ob/ob mice fed chow (n = 3) for 2 weeks and then fed either the control (n = 3) or Trypt-out (n = 3) diet with antibiotic depletion as in (A). Data are presented as mean ± SD and were analyzed using an unpaired Welch's t-test.

(C) Tissue levels of Trp metabolites from male ob/ob mice fed either the control (n = 4) or Trypt-out (n = 4) diet for 4 weeks. Data are presented as mean ± SD and were analyzed using an unpaired Welch's t-test.

(D) Food consumption by male ob/ob mice (n = 4) fed the Trypt-out diet for 4 weeks with daily supplementation via IP injections of listed Trp-derived metabolites. Data are presented as mean ± SD and were analyzed using an unpaired Welch's t-test.

(E) Body weight of male ob/ob mice (n = 4) fed the Trypt-out diet for 7 weeks. Daily supplementation via IP injections of listed Trp-derived metabolites began week 4 and continued until week 7. Data are presented as mean ± SD and were analyzed using an unpaired Welch's t-test.

(F) Food consumption of male ob/ob (n = 4) mice fed the Trypt-out diet for 7 weeks. Daily supplementation via IP injections of listed Trp-derived metabolites began week 4 and continued until week 7. Data are presented as mean ± SD and were analyzed using an unpaired Welch's t-test.

(G) Representative images of a male ob/ob mouse fed the Trypt-out diet with and without daily IP injections of 5-HT for 4 weeks.

(H) Change in body weight of male ob/ob mice fed the Trypt-out diet with (n = 4) or without (n = 4) daily IP injections of 5-HT for 4 weeks. Data are presented as mean ± SD and were analyzed using an unpaired Welch's t-test.

(I) Tissue weight of ob/ob male mice fed the Trypt-out diet with (n = 4) or without (n = 4) daily IP injections of 5-HT for 3 weeks. Data are presented as mean ± SD and were analyzed using an unpaired Welch's t-test.

(J) Representative images of a male ob/ob mouse fed the Trypt-out diet with and without daily IP injections of I3P for 3 weeks.

(K) Change in the body weight of male ob/ob mice fed the Trypt-out diet with (n = 4) or without (n = 4) daily IP injections of I3P for 3 weeks. Data are presented as mean ± SD and were analyzed using an unpaired Welch's t-test.

(L) Tissue weight of male ob/ob mice fed the Trypt-out diet with (n = 3) or without (n = 3) daily IP injections of I3P for 3 weeks. Data are presented as mean ± SD and were analyzed using an unpaired Welch's t-test.

(M) Representative images of a male ob/ob mouse fed the Trypt-out diet with and without daily IP injections of Kyn for 3 weeks

(N) Change in body weight of male ob/ob mice fed the Trypt-out diet with (n = 3) and without (n = 3) daily IP injections of Kyn for 3 weeks. Data are presented as mean ± SD and were analyzed using an unpaired Welch's t-test.

(O) Tissue weight of male ob/ob mice fedt he Trypt-out diet with (n = 3) and without (n = 3) daily IP injections of Kyn for 3 weeks. Data are presented as mean ± SD and were analyzed using an unpaired Welch's t-test.

(P) Levels of Trp, Kyn, 2-aminoadipate (2-AAA), Lys, and pipecolate in the liver of male B6 mice fed either the control (n = 3) or Trypt-out (n = 2) diet for 3 weeks. Data are presented as mean ± SD and were analyzed using an unpaired Welch's t-test.

(Q) Levels of Trp, Kyn, 2-aminoadipate (2-AAA), Lys, and pipecolate metabolites (ng/mL) in liver of male B6 DIO mice fed either the control (n = 3) or Trypt-out (n = 3) diet for 4 weeks . Data are presented as mean ± SD and were analyzed using an unpaired Welch's t-test.

(R) Cumulative food consumption by male ob/ob mice fed the Trypt-out diet and supplemented with normal water (n = 3) or sucrose (n = 4) for 3 weeks. Data are presented as mean ± SD and were analyzed using an unpaired Welch's t-test.

Fig. S4. Trypt-out diet reduces the body composition of obese and non-obese mice.

(A) Representative images of tissues from male B6 mice fed either the control or Trypt-out diet for 3 weeks.

(B) Representative images of tissues from male FVB DIO mice, which were fed for 12 weeks with HFD, and then fed either HFD or HF Trypt-out diet for 4 weeks.

(C) Representative images of tissues from male B6 mice fed either the HFD or HF Trypt-out diet for 3 weeks.

(D) Representative images of tissues from male ob/ob (pre-obese) mice fed either the control or Trypt-out diet for 4 weeks.

(E) H&E-stained muscle tissue from B6 male mice fed either the control or Trypt-out diet for 3 weeks.

(F) H&E-stained muscle tissue of male FVB DIO mice fed either the control or Trypt-out diet for 3 weeks.

(G) H&E-stained gWAT, iWAT, BAT and liver from male B6 HFD mice fed either the control or Trypt-out diet for 3 weeks.

(H) H&E-stained gWAT, iWAT, BAT and liver of male ob/ob mice fed either the control or Trypt-out diet for 3 weeks.

(I) Tissue morphometric quantification of cells in the gWAT, iWAT, BAT and liver by using the AdipoQ plugin in Image J. Images of tissues from male B6 male mice fed either the control (n = 1) or Trypt-out (n = 1) diet for 3 weeks. Data are presented as mean ± SD and were analyzed using an unpaired Welch's t-test.

(J) Tissue morphometric quantification of the cells in gWAT, iWAT, BAT and liver by using the AdipoQ plugin in Image J. Images of tissues from male FVB DIO mice fed either the control (n = 1) or Trypt-out (n = 1) diet for 4 weeks. Data are presented as mean ± SD and were analyzed using an unpaired Welch's t-test.

(K) Tissue morphometric quantification of the cells in gWAT, iWAT, BAT and liver by using the AdipoQ plugin in Image J. Image of male B6 HFD mice tissues fed control or Trypt-out diet for

3 weeks (n = 1). H&E-stained tissues (gWAT, iWAT, BAT and Liver) of B6 HFD male mice (n = 1). Data are presented as mean ± SD and were analyzed using an unpaired Welch's t-test.

(L) Tissue morphometric quantification of the cells (gWAT, iWAT, BAT and liver) by using the AdipoQ plugin in Image J. Image of male ob/ob (pre-obese) male mice tissues fed control (n = 3) or Trypt-out diet for 3 weeks (n = 3). Data are presented as mean ± SD and were analyzed using an unpaired Welch's t-test.

(M) Tissue morphometric quantification of the cells (gWAT, iWAT, BAT and liver) by using the AdipoQ plugin in Image J. Image of male ob/ob male mice tissues fed control (n = 3) or Trypt-out (n = 3) diet for 3 weeks. Data are presented as mean ± SD and were analyzed using an unpaired Welch's t-test.

(N) Glutathione levels in the tissues (BAT, iWAT and gWAT) of male ob/ob mice fed control (n = 3) or Trypt-out (n = 3) diet for 4 weeks. Data are presented as mean ± SD and were analyzed using an unpaired Welch's t-test.

Fig. S5: Gene expression profiles of liver, iWAT, and muscle from mice fed control or Trypt-out diets.

(A) Volcano plot of RNA-seq of liver of mice in control diet or Trypt-out diet.

(B) Volcano plot of RNA-seq of iWAT of mice in control diet or Trypt-out diet.

(C) Volcano plot of RNA-seq of Muscle of mice in control diet or Trypt-out diet.

(D) Heatmaps showing genes involved in lipid biosynthesis in the muscle, liver, and iWAT of mice in control diet or Trypt-out diet.

(E) Heatmaps showing genes involved in lipid transport and lipid processing in the liver of mice in a control diet or Trypt-out diet.

(F) Heatmaps showing genes involved in lipid biosynthesis, lipid transport, and lipid processing in the iWAT of mice in a control diet or Trypt-out diet.

(G) Heatmaps showing genes involved in lipid biosynthesis and lipid transport in the muscle of mice in control diet or Trypt-out diet.

(H) Volcano plot of proteomics of liver of male B6 mice in a control diet or Trypt-out diet for 3 weeks.

(I) Major genes related to lipid breakdown in mitochondria and its transcription and protein levels, and functions.

(J) Pathway analysis of proteins upregulated in the livers of Trypt-out-fed mice.

(K) Schematics showing more than 80 components of the basal protein synthesis machinery, including ribosomal proteins, translation initiation and elongation factors, and aminoacyl-tRNA synthetases, are increased in the livers of Trypt-out-fed mice.

(L) Immunoblot for lipogenesis enzymes in iWAT of B6 mice fed control or Trypt-out diets for 3 weeks.

(M) Immunoblot of lipogenesis enzymes in iWAT of ob/ob mice fed control or Trypt-out diets for 4 weeks.

(N) Immunoblot for ApoE and ApoB in the livers of B6 mice fed control or Trypt-out diets for 3 weeks.

(O) Immunoblot for ApoE and ApoB in the serum of B6 mice fed control or Trypt-out diets for 3 weeks.

Fig. S6: High-Fat Tryp-out diet decreases body weight and protects fat liver accumulation in obese mice long-term DIO mice.

(A) Intraperitoneal glucose tolerance test (GTT) from male B6 mice fed either the HFD (n = 5) or HF Trypt-out (n = 5) diet. Data are presented as mean ± SD and were analyzed using an unpaired Welch's t-test.

(B) Serum hormone levels in male B6 mice fed either the HFD (n = 5) or the HF Trypt-out diet (n = 3-5). Data are presented as mean ± SD and were analyzed using an unpaired Welch's t-test.

(C) Daily Food consumption for 5 days by male B6 DIO mice fed either the HFD (n = 3) or HF Trypt-out Binge (n = 3) diet. Data are presented as mean ± SD and were analyzed using an unpaired Welch's t-test.

(D) Daily Food consumption for the 2 days in male B6 DIO mice fed either the HFD (n = 3) or HFD pair feeding (n = 3). Data are presented as mean ± SD and were analyzed using an unpaired Welch's t-test.

(E) Daily Food consumption for the 5 days in male B6 DIO mice fed either HFD (n = 3) or HF Trypt-out binge (n = 3) diet. Data are presented as mean ± SD and were analyzed using an unpaired Welch's t-test.

(F) Food consumption daily for the 2 days in male B6 DIO mice fed with the HFD (n = 3) or HFD ad libitum (n = 3). Data are presented as mean ± SD and were analyzed using an unpaired Welch's t-test.

(G) Food consumption normalized per body weight per day in male B6 DIO mice fed either the HFD (n = 3) or HF Trypt-out binge pair feeding (n = 3). Data are presented as mean ± SD and were analyzed using an unpaired Welch's t-test.

(H) Food consumption normalized per body weight per day in male B6 DIO mice fed either the HFD (n = 3) or HF Trypt-out-binge ad libitum (n = 3). Data are presented as mean ± SD and were analyzed using an unpaired Welch's t-test.

(I) Final body weight of male B6 DIO mice fed either the HFD (n = 3) or Binge (n = 3) diet at last week. Data are presented as mean ± SD and were analyzed using an unpaired Welch's t-test.

(J) Tissue weight (liver, inguinal and gonadal white adipose tissue) of B6 DIO mice fed either the HFD (n = 3) or Binge (n = 3) diet. Data are presented as mean ± SD and were analyzed using an unpaired Welch's t-test.

(K) Serum levels of aspartate aminotransferase (AST) in B6 DIO mice fed either the HFD (n = 3) or Binge (n = 3) diet. Data are presented as mean ± SD and were analyzed using an unpaired Welch's t-test.

Fig. S7: Trypt-out diet is a potent inhibitor of hepatic lipid and cholesterol biosynthesis in obese mice.

(A) Free fatty acids levels in the liver, iWAT and gWAT from male ob/ob mice fed either the control (n = 3) or Trypt-out (n = 3) diet for 4 weeks. Data are presented as mean ± SD and were analyzed using an unpaired Welch's t-test.

(B) Glycerol levels in the liver, iWAT and gWAT from male ob/ob mice fed either the control (n = 3) or Trypt-out (n = 3) diet for 4 weeks. Data are presented as mean ± SD and were analyzed using an unpaired Welch's t-test.

(C) LC-MS/MS metabolomics analysis of stool from male ob/ob mice fed either the control (n = 3) or Trypt-out (n = 3) diet for 4 weeks. Data are presented as mean ± SD and were analyzed using an unpaired Welch's t-test.

(D) Table of the urine profile of male ob/ob mice fed either the control (n = 4) or Trypt-out (n = 4) diet for 4 weeks. Data are presented as mean ± SD and were analyzed using an unpaired Welch's t-test.

(E) Total water consumed for 5 days while in a metabolic by male ob/ob mice fed either the control (n = 4) or Trypt-out (n = 4) diet. Data are presented as mean ± SD and were analyzed using an unpaired Welch's t-test.

(F) Total urine produced for 5 days while in urine metabolic cage by male ob/ob mice fed either the control (n = 4) or Trypt-out (n = 4) diet. Data are presented as mean ± SD and were analyzed using an unpaired Welch's t-test.

(G) TCA intermediates and total ketone in urine of male ob/ob (n = 3) mice fed either the control (n = 3) or Trypt-out (n = 3) diets. Data are presented as mean ± SD and were analyzed using an unpaired Welch's t-test.

(H) Liver bile acids produced by male B6 mice fed either the control (n = 4) or Trypt-out (n = 4) diets for 3 weeks. The ob/ob mice were fed either the control (n = 4) or Trypt-out (n = 4) diets for 4 weeks. The ob/ob mice were fed either the HFD (n = 3) or HF Trypt-out (n = 3) diets for 4 weeks. Data are presented as mean ± SD and were analyzed using an unpaired Welch's t-test.

(I) Schematic of the experimental design for Atorvastatin (ATO) treatment in ob/ob mice.

(J) Serum levels of alanine aminotransferase (ALT) in male ob/ob mice fed either the control (n = 3) with or without Atorvastatin (ATO) or Trypt-out with vehicle (n = 3) diet. Data are presented as mean ± SD and were analyzed using one-way ANOVA with Tukey multiple comparison test.

(K) Serum levels of aspartate aminotransferase (AST) in male ob/ob mice fed either the control (n = 3) with or without Atorvastatin (ATO) or Trypt-out with vehicle (n = 3) diet. Data are presented as mean ± SD and were analyzed using one-way ANOVA with Tukey multiple comparison test.

(L) Liver tissue weight of male ob/ob mice fed either the control (n = 3) with or without Atorvastatin (ATO) or Trypt-out with vehicle (n = 3) diet. Data are presented as mean ± SD and were analyzed using one-way ANOVA with Tukey multiple comparison test.

(M) Gonadal adipose tissue weight of male ob/ob mice fed either the control (n = 3) with or without Atorvastatin (ATO) or Trypt-out with vehicle (n = 3) diet. Data are presented as mean ± SD and were analyzed using one-way ANOVA with Tukey multiple comparison test.

REFERENCES

1 Xue, C. *et al.* Tryptophan metabolism in health and disease. *Cell Metab* **35**, 1304-1326 (2023). https://doi.org/10.1016/j.cmet.2023.06.004

2 Wu, Y. *et al.* Very-low-protein diets lead to reduced food intake and weight loss, linked to inhibition of hypothalamic mTOR signaling, in mice. *Cell Metab* **33**, 1264-1266 (2021). https://doi.org/10.1016/j.cmet.2021.04.016

3 Xiao, F. & Guo, F. Impacts of essential amino acids on energy balance. *Mol Metab* **57**, 101393 (2022). https://doi.org/10.1016/j.molmet.2021.101393

4 Varghese, A. *et al.* Unravelling cysteine-deficiency-associated rapid weight loss. *Nature* **643**, 776-784 (2025). https://doi.org/10.1038/s41586-025-08996-y

5 Tang, J., Krushelnycky, L., Shaqo, A. & Cho, C. E. A Comprehensive Review of Nutritional Influences on the Serotonergic System. *Adv Nutr* **16**, 100524 (2025). https://doi.org/10.1016/j.advnut.2025.100524

6 . (!!! INVALID CITATION !!!).

7 Perez-Castro, L., Garcia, R., Venkateswaran, N., Barnes, S. & Conacci-Sorrell, M. Tryptophan and its metabolites in normal physiology and cancer etiology. *FEBS J* **290**, 7-27 (2023). https://doi.org/10.1111/febs.16245

8 AbuSalim, J. E. *et al.* Host metabolism can produce many indoles and phenols independently of the microbiome. *Nat Metab* (2026). https://doi.org/10.1038/s42255-026-01550-8

9 Perez-Castro, L. *et al.* Tryptophan metabolite atlas uncovers organ, age, and sex-specific variations. *FEBS Open Bio* (2025). https://doi.org/10.1002/2211-5463.70123

10 Palego, L., Betti, L., Rossi, A. & Giannaccini, G. Tryptophan Biochemistry: Structural, Nutritional, Metabolic, and Medical Aspects in Humans. *J Amino Acids* **2016**, 8952520 (2016). https://doi.org/10.1155/2016/8952520

11 Venkateswaran, N. *et al.* Tryptophan fuels MYC-dependent liver tumorigenesis through indole 3-pyruvate synthesis. *Nat Commun* **15**, 4266 (2024). https://doi.org/10.1038/s41467-024-47868-3

12 Sadik, A. *et al.* IL4I1 Is a Metabolic Immune Checkpoint that Activates the AHR and Promotes Tumor Progression. *Cell* **182**, 1252-1270 e1234 (2020). https://doi.org/10.1016/j.cell.2020.07.038

13 Opitz, C. A. *et al.* An endogenous tumour-promoting ligand of the human aryl hydrocarbon receptor. *Nature* **478**, 197-203 (2011). https://doi.org/10.1038/nature10491

14 Lafita-Navarro, M. C. *et al.* The aryl hydrocarbon receptor regulates nucleolar activity and protein synthesis in MYC-expressing cells. *Genes Dev* **32**, 1303-1308 (2018). https://doi.org/10.1101/gad.313007.118

15 Lafita-Navarro, M. C. *et al.* Inhibition of the de novo pyrimidine biosynthesis pathway limits ribosomal RNA transcription causing nucleolar stress in glioblastoma cells. *PLoS Genet* **16**, e1009117 (2020). https://doi.org/10.1371/journal.pgen.1009117

16 Perez-Castro, L. *et al.* The AHR target gene Scinderin activates the WNT pathway by facilitating the nuclear translocation of beta-catenin. *J Cell Sci* (2022). https://doi.org/10.1242/jcs.260028

17 Feng, J. *et al.* The electrophilic metabolite of kynurenine, kynurenine-CKA, requires C151 in Keap1 to derepress Nrf2. *Redox Biol* **90**, 104009 (2026). https://doi.org/10.1016/j.redox.2026.104009

18 Stone, T. W. & Williams, R. O. Modulation of T cells by tryptophan metabolites in the kynurenine pathway. *Trends Pharmacol Sci* **44**, 442-456 (2023). https://doi.org/10.1016/j.tips.2023.04.006
19 Nicolaisen, T. S. *et al.* Dietary protein restriction elevates FGF21 levels and energy requirements to maintain body weight in lean men. *Nat Metab* **7**, 602-616 (2025). https://doi.org/10.1038/s42255-025-01236-7
20 Chaumontet, C. *et al.* Low-protein and methionine, high-starch diets increase energy intake and expenditure, increase FGF21, decrease IGF-1, and have little effect on adiposity in mice. *Am J Physiol Regul Integr Comp Physiol* **316**, R486-R501 (2019). https://doi.org/10.1152/ajpregu.00316.2018
21 Inagaki, T. *et al.* Inhibition of growth hormone signaling by the fasting-induced hormone FGF21. *Cell Metab* **8**, 77-83 (2008). https://doi.org/10.1016/j.cmet.2008.05.006
22 Markan, K. R. *et al.* Circulating FGF21 is liver derived and enhances glucose uptake during refeeding and overfeeding. *Diabetes* **63**, 4057-4063 (2014). https://doi.org/10.2337/db14-0595
23 Lafita-Navarro, M. C. *et al.* ZNF692 organizes a hub specialized in 40S ribosomal subunit maturation enhancing translation in rapidly proliferating cells. *Cell Rep* **42**, 113280 (2023). https://doi.org/10.1016/j.celrep.2023.113280
24 Forester, C. M. *et al.* Revealing nascent proteomics in signaling pathways and cell differentiation. *Proc Natl Acad Sci U S A* **115**, 2353-2358 (2018). https://doi.org/10.1073/pnas.1707514115
25 Dean, E. D. *et al.* The Response of Alpha-Aminoadipic Acid (2-AAA) to Short Term Lysine Ingestion in Healthy Individuals. *Endocrinol Diabetes Metab* **9**, e70168 (2026). https://doi.org/10.1002/edm2.70168
26 Gabela, A. M., Mthembu, N. & Hadebe, S. Tryptophan metabolism in health and disease-implications for non-communicable diseases. *Immunol Lett* **277**, 107093 (2025). https://doi.org/10.1016/j.imlet.2025.107093
27 Wang, X. *et al.* Adipocyte-derived ferroptotic signaling mitigates obesity. *Cell Metab* **37**, 673-691 e677 (2025). https://doi.org/10.1016/j.cmet.2024.11.010
28 Wang, X., Sato, R., Brown, M. S., Hua, X. & Goldstein, J. L. SREBP-1, a membrane-bound transcription factor released by sterol-regulated proteolysis. *Cell* **77**, 53-62 (1994). https://doi.org/10.1016/0092-8674(94)90234-8
29 Shreya, S., Grosset, C. F. & Jain, B. P. Unfolded Protein Response Signaling in Liver Disorders: A 2023 Updated Review. *Int J Mol Sci* **24** (2023). https://doi.org/10.3390/ijms241814066
30 Sozen, E. & Ozer, N. K. Impact of high cholesterol and endoplasmic reticulum stress on metabolic diseases: An updated mini-review. *Redox Biol* **12**, 456-461 (2017). https://doi.org/10.1016/j.redox.2017.02.025
31 Griffin, B. A., Mensink, R. P. & Lovegrove, J. A. Does variation in serum LDL-cholesterol response to dietary fatty acids help explain the controversy over fat quality and cardiovascular disease risk? *Atherosclerosis* **328**, 108-113 (2021). https://doi.org/10.1016/j.atherosclerosis.2021.03.024
32 Shore, D. & Albert, B. Ribosome biogenesis and the cellular energy economy. *Curr Biol* **32**, R611-R617 (2022). https://doi.org/10.1016/j.cub.2022.04.083
33 Warner, J. R. The economics of ribosome biosynthesis in yeast. *Trends Biochem Sci* **24**, 437-440 (1999). https://doi.org/10.1016/s0968-0004(99)01460-7

34 Christa Buechler , S. K., Kristina Eisinger. Adipose tissue fibrosis. *World J Diabetes* (2015). https://doi.org/DOI: 10.4239/wjd.v6.i4.548

35 Aileen H. Lee, L. O., Yun-Hee Youm , Rae Maeda, *et al*. Cysteine depletion triggers adipose tissue thermogenesis and weight loss. *Nature Metabolism* (2025). https://doi.org/https://doi.org/10.1038/s42255-025-01297-8

36 Dos Santos, I. L. *et al*. Targeting of neuroblastoma cells through Kynurenine-AHR pathway inhibition. *FEBS J* **291**, 2172-2190 (2024). https://doi.org/10.1111/febs.17109

37 Oelfah Patel , C. J. F. M., Elizabeth Joubert , Bernd Rosenkranz , Johan Louw , Charles Awortwe Therapeutic effects of an aspalathin-rich green rooibos extract, pioglitazone and atorvastatin combination therapy in diabetic db/db mice. *PlosOne* (2021). https://doi.org/DOI: 10.1371/journal.pone.0251069

38 Sharma, R. P. *et al*. Acute dietary tryptophan depletion: effects on schizophrenic positive and negative symptoms. *Neuropsychobiology* **35**, 5-10 (1997). https://doi.org/10.1159/000119323

39 Zebisch, K., Voigt, V., Wabitsch, M. & Brandsch, M. Protocol for effective differentiation of 3T3-L1 cells to adipocytes. *Anal Biochem* **425**, 88-90 (2012). https://doi.org/10.1016/j.ab.2012.03.005

40 Sieckmann, K. *et al*. AdipoQ-a simple, open-source software to quantify adipocyte morphology and function in tissues and in vitro. *Mol Biol Cell* **33**, br22 (2022). https://doi.org/10.1091/mbc.E21-11-0592

41 Perez-Castro, L. *et al*. Tryptophan metabolite atlas uncovers organ, age, and sex-specific variations. *FEBS Open Bio* **16**, 52-67 (2026). https://doi.org/10.1002/2211-5463.70123

42 Gliniak, C. M. *et al*. FGF21 promotes longevity in diet-induced obesity through metabolic benefits independent of growth suppression. *Cell Metab* **37**, 1547-1567 e1546 (2025). https://doi.org/10.1016/j.cmet.2025.05.011

Table S1: Reagents and resources in this study

REAGENT or RESOURCE	SOURCE	IDENTIFIER
Antibodies		
Rabbit monoclonal Acetyl-CoA carboxylase	Cell Signaling	3676
Rabbit monoclonal Adiponectin	Cell Signaling	2789
Rabbit FABP4	Cell Signaling	2120
Rabbit monoclonal Fatty acid synthase	Cell Signaling	3180
Rabbit monoclonal Perilipin-1	Cell Signaling	9349
PPARα	Invitrogen	PA1-822A
Rabbit monoclonal PPAR gamma	Cell Signaling	2435
Rabbit monoclonal BiP	Cell Signaling	3177
Mouse monoclonal CHOP	Cell Signaling	2895
Rabbit monoclonal PERK	Cell Signaling	5683
Rabbit monoclonal IRE1 alpha	Cell Signaling	3294
Rabbit Myc	Abcam	AB32072
Rabbit polyclonal MLXIP	Proteintech	13614-1-AP
Rabbit polyclonal PRDX3	Proteintech	10664-1-AP
Rabit ATP Citrate Lyase	Cell Signaling	4332
Rabbit monoclonal SCD-1	Cell signaling	2794S
Rabbit monoclonal HMGCS-1	Cell signaling	42201T
Rabbit monoclonal DHCR-7	Cell signaling	62115T
Rabbit polyclonal ACADS	Invitrogen	PA5-54580
Rabbit monoclonal ACADM	Abcam	ab92461
Rabbit polyclonal ACADL	Invitrogen	PA5-82450
Rabbit polyclonal CPT1A	Proteintech	15184-1-AP
Rabbit polyclonal CTP2	Proteintech	26555-1-AP
Rabbit monoclonal Hexokinase	Cell signaling	2024
Rabbit Aldolase A	Cell signaling	3188
Rabbit monoclonal ATF-4	Cell signaling	11815
Rabbit monoclonal ATF-6	Cell signaling	65880
Rabbit polyclonal MLXIPL	Proteintech	13256-1-AP
Rabbit monoclonal beta-Actin	Cell signaling	8457
Mouse monoclonal TUBA4A	Sigma	T6199
Rabbit monoclonal MLX	Cell signaling	85570T
Rabbit monoclonal xCT/SLC7a11	Cell signaling	12691S
Rabbit polyclonal hyperoxidized Peroxiredoxin-3	Cayman	39806
Rabbit monoclonal cleaved caspase-3	Cell signaling	9664
Rabbit polyclonal ApoB	Proteintech	20578-1-AP
Mouse monoclonal ApoE	Cell signaling	74417
Rabbit eIF2-alpha	Cell signaling	9722
Rabbit Phospho-eIF2-alpha	Cell signaling	9721
Rabbit monoclonal FGF21	Invitrogen	MA5-32652
Rabbit Histone H3	Cell signaling	9715S
Mouse monoclonal ACSL4	Santa Cruz	sc-271800
Rabbit GPX4	Cell signaling	52455
Rabbit polyclonal DDX21	Proteintech	10528-1-AP

Mouse Puromycin	Sigma	MABE343
Rabbit monoclonal MYCL	Cell signaling	76266
Sheep anti-Mouse IgG (HRP)	Abcam	ab6808
Donkey anti-Rabbit IgG (HRP)	Cytiva	NA934V

Chemicals, peptides, and recombinant proteins

Liproxstatin-1	Selleck Chem	S7699
RSL3	Selleck Chem	S8155
Ferrostatin-1	Sigma	SML0583
Fetal bovine serum (FBS)	Sigma	F2442-500ML
I3P	Sigma	I7017-5G
5-Hydroxy-L-Trp (L-5-HTP)	Sigma	399698
Kynurenine	Sigma	K8625-1G
DMEM, high glucose, GlutaMAX™	Fisher	016
Insulin from bovine pancreas	Sigma	I6634-100MG
DMEM F12, without Trp	US Biological	D9807-04
Denifanstat	MedChemExpress	HY-112829
Trans-ISRIB	Tocris	5284
Cycloheximide	Sigma	C4859
Sucrose	MP Biomedicals	S6942
MG132	Fisher	NC0022110
O-propargyl-puromycin (OPP)	BroadPharm	BP50103
Trypsin	Sigma	5643
Dialyzed FBS	Thermo	266-400-044
Penicillin-Streptomycin	Sigma	#P0781
Penicillin G potassium salt	Sigma	#P8721
Streptomycin sulfate	Thermo Fisher	#J61299.22
Dexamethasone	Sigma	D4902-25MG
Rosiglitazone	Sigma	R2408-10MG
Nitrocellulose membrane	Fisher	PI88018
L-Tryptophan	Sigma	T8941-25G
RPMI	Sigma	#5638
Atorvastatin	MedChemExpress	HY-B0589

Critical commercial assays

Bio-plex pro mouse diabetes	Bio Rad	171F7001M
NEFA	Millipore-Sigma	F6428, G7793

Diets

Histidine-free	Inotiv	TD.220729
Isoleucine-free	Inotiv	TD.220730
Leucine-free	Inotiv	TD.220731
Lysine-free	Inotiv	TD.220732
Methionine-free	Inotiv	TD.220733
Phenylalanine-free	Inotiv	TD.220734
Threonine-free	Inotiv	TD.220735
Valine-free	Inotiv	TD.220736

Lard amino acid (HFD)	Inotiv	TD.210437
Trp-deficient lard (HF Trypt-out)	Inotiv	TD.210438
Amino acid (control)	Inotiv	TD.99366
Tryptophan-free (Trypt-out)	Inotiv	TD.170394

Experimental models: Organisms/strains

C57BL6/J (B6)	The Jackson Lab	IMSR_JAX:000664
B6 ob/ob	The Jackson Lab	IMSR_JAX:000632
Fgf21 KO	The Jackson Lab	IMSR_JAX:033846
FVB	The Jackson Lab	IMSR_JAX:001800

Cell lines

H2.35 hepatocytes	ATCC	CRL 1995
3T3-L1	ATCC	CL-173

Software and algorithms

Prism	www.graphpad.com	Prism 11.0
MetaboAnalyst	www.metaboanalyst.ca	Metaboanalyst 6.0
NPDview2	www.hamamatsu.com	U12388-01
Incucyte	www.Sartorius.com	Incucyte ZOOM Live-Cell Analysis System
Biorender	https://www.biorender.com/	

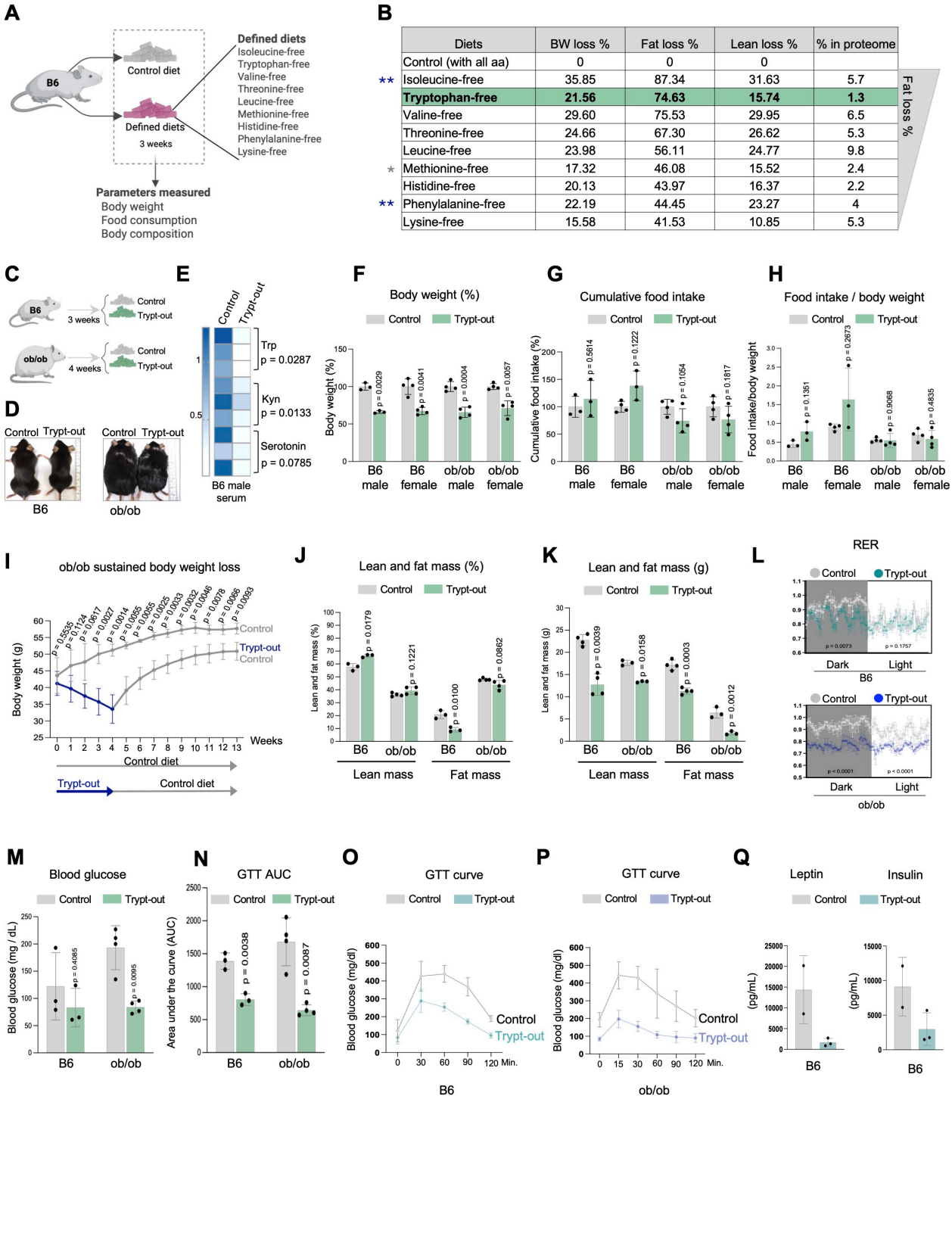

A
B6
Control diet
Defined diets
3 weeks
Defined diets
Isoleucine-free
Tryptophan-free
Valine-free
Threonine-free
Leucine-free
Methionine-free
Histidine-free
Phenylalanine-free
Lysine-free
Parameters measured
Body weight
Food consumption
Body composition
B
Diets | BW loss % | Fat loss % | Lean loss % | % in proteome
Control (with all aa) | 0 | 0 | 0 |
** Isoleucine-free | 35.85 | 87.34 | 31.63 | 5.7
Tryptophan-free | 21.56 | 74.63 | 15.74 | 1.3
Valine-free | 29.60 | 75.53 | 29.95 | 6.5
Threonine-free | 24.66 | 67.30 | 26.62 | 5.3
Leucine-free | 23.98 | 56.11 | 24.77 | 9.8
* Methionine-free | 17.32 | 46.08 | 15.52 | 2.4
Histidine-free | 20.13 | 43.97 | 16.37 | 2.2
** Phenylalanine-free | 22.19 | 44.45 | 23.27 | 4
Lysine-free | 15.58 | 41.53 | 10.85 | 5.3
Fat loss %
C
B6
3 weeks
Control
Trypt-out
ob/ob
4 weeks
Control
Trypt-out
D
Control Trypt-out
Control Trypt-out
B6
ob/ob
E
Control
Trypt-out
1
0.5
Trp
p = 0.0287
Kyn
p = 0.0133
Serotonin
p = 0.0785
B6 male serum
F
Body weight (%)
Control
Trypt-out
Body weight (%)
p = 0.0029
p = 0.0041
p = 0.0004
p = 0.0057
B6 male
B6 female
ob/ob male
ob/ob female
G
Cumulative food intake
Control
Trypt-out
Cumulative food intake (%)
p = 0.5614
p = 0.1222
p = 0.1054
p = 0.1817
B6 male
B6 female
ob/ob male
ob/ob female
H
Food intake / body weight
Control
Trypt-out
Food intake/body weight
p = 0.1351
p = 0.2673
p = 0.9068
p = 0.4835
B6 male
B6 female
ob/ob male
ob/ob female
I
ob/ob sustained body weight loss
Body weight (g)
p = 0.5535
p = 0.1124
p = 0.0617
p = 0.0027
p = 0.0014
p = 0.0055
p = 0.0025
p = 0.0033
p = 0.0032
p = 0.0046
p = 0.0078
p = 0.0066
p = 0.0093
Control
Trypt-out
Control
Weeks
Control diet
Trypt-out
Control diet
J
Lean and fat mass (%)
Control
Trypt-out
Lean and fat mass (%)
p = 0.0179
p = 0.1221
p = 0.0100
p = 0.0862
B6
ob/ob
B6
ob/ob
Lean mass
Fat mass
K
Lean and fat mass (g)
Control
Trypt-out
Lean and fat mass (g)
p = 0.0039
p = 0.0158
p = 0.0003
p = 0.0012
B6
ob/ob
B6
ob/ob
Lean mass
Fat mass
L
RER
Control
Trypt-out
p = 0.0073
p = 0.1757
Dark
Light
B6
Control
Trypt-out
p < 0.0001
p < 0.0001
Dark
Light
ob/ob
M
Blood glucose
Control
Trypt-out
Blood glucose (mg / dL)
p = 0.4085
p = 0.0095
B6
ob/ob
N
GTT AUC
Control
Trypt-out
Area under the curve (AUC)
p = 0.0038
p = 0.0087
B6
ob/ob
O
GTT curve
Control
Trypt-out
Blood glucose (mg/dl)
Control
Trypt-out
0 30 60 90 120 Min.
B6
P
GTT curve
Control
Trypt-out
Blood glucose (mg/dl)
Control
Trypt-out
0 15 30 60 90 120 Min.
ob/ob
Q
Leptin
Insulin
Control
Trypt-out
(pg/mL)
(pg/mL)
B6
B6

Figure 1

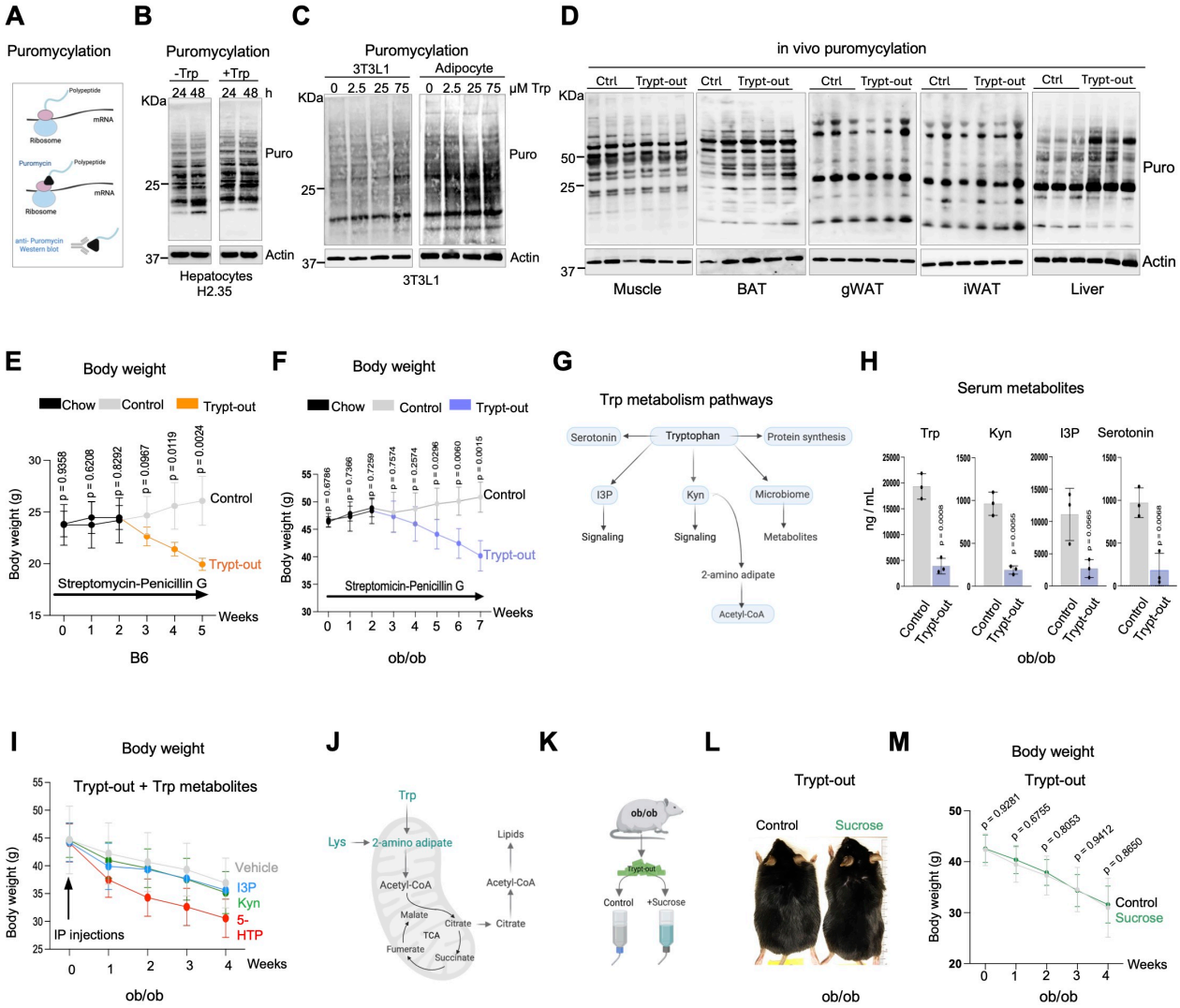

A
Puromycylation
Polypeptide
mRNA
Ribosome
Puromycin
anti- Puromycin Western blot
B
Puromycylation
-Trp
+Trp
24 48
24 48 h
KDa
Puro
25
37
Actin
Hepatocytes H2.35
C
Puromycylation
3T3L1
Adipocyte
0 2.5 25 75
0 2.5 25 75 µM Trp
KDa
Puro
25
37
Actin
3T3L1
D
in vivo puromycylation
Ctrl
Trypt-out
KDa
50
25
37
Puro
Actin
Muscle
BAT
gWAT
iWAT
Liver
E
Body weight
Chow
Control
Trypt-out
p = 0.9358
p = 0.6208
p = 0.8292
p = 0.0967
p = 0.0119
p = 0.0024
Body weight (g)
Control
Trypt-out
Streptomycin-Penicillin G
Weeks
B6
F
Body weight
Chow
Control
Trypt-out
p = 0.6786
p = 0.7366
p = 0.7259
p = 0.7574
p = 0.2574
p = 0.0296
p = 0.0060
p = 0.0015
Body weight (g)
Control
Trypt-out
Streptomicin-Penicillin G
Weeks
ob/ob
G
Trp metabolism pathways
Serotonin
Tryptophan
Protein synthesis
I3P
Kyn
Microbiome
Signaling
Signaling
Metabolites
2-amino adipate
Acetyl-CoA
H
Serum metabolites
Trp
Kyn
I3P
Serotonin
ng / mL
p = 0.0008
p = 0.0055
p = 0.0565
p = 0.0068
Control
Trypt-out
ob/ob
I
Body weight
Trypt-out + Trp metabolites
Body weight (g)
Vehicle
I3P
Kyn
5-HTP
IP injections
Weeks
ob/ob
J
Trp
Lys
2-amino adipate
Lipids
Acetyl-CoA
Acetyl-CoA
Malate
Citrate
Citrate
TCA
Fumerate
Succinate
K
ob/ob
Trypt-out
Control
+Sucrose
L
Trypt-out
Control
Sucrose
ob/ob
M
Body weight
Trypt-out
p = 0.9281
p = 0.6755
p = 0.8053
p = 0.9412
p = 0.8650
Body weight (g)
Control
Sucrose
Weeks
ob/ob

Figure 3

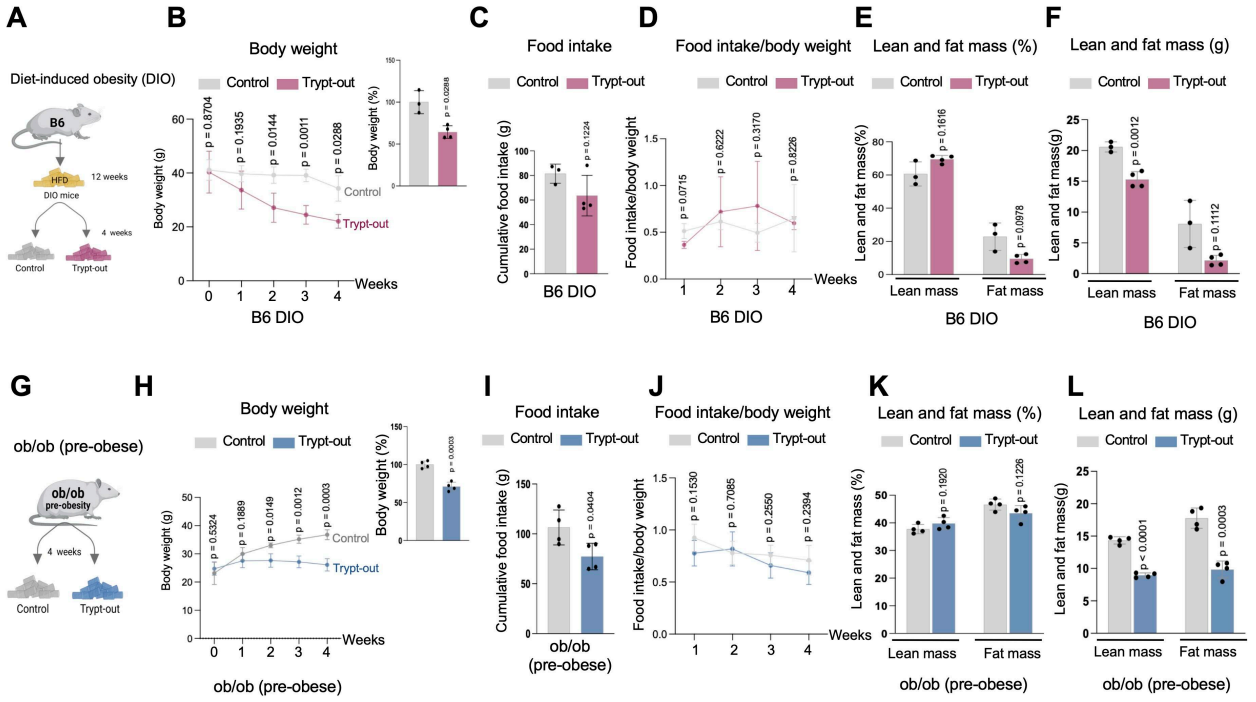

A
B
C
D
E
F
Diet-induced obesity (DIO)
B6
HFD
12 weeks
DIO mice
4 weeks
Control
Trypt-out
Body weight
Body weight (g)
Body weight (%)
Weeks
B6 DIO
Food intake
Cumulative food intake (g)
Food intake/body weight
Lean and fat mass (%)
Lean and fat mass (g)
Lean mass
Fat mass
G
H
I
J
K
L
ob/ob (pre-obese)
ob/ob
pre-obesity
ob/ob (pre-obese)
M
N
O
P
Q
R
B6 Liver
B6 Serum
ob/ob Liver
ob/ob Serum
KDa
FGF21
H3
Ponceau
Fgf21 KO
Fgf21 KO HFD
HFD
HF Trypt-out
HF-Trypt-out
Food intake (g)

Figure 2

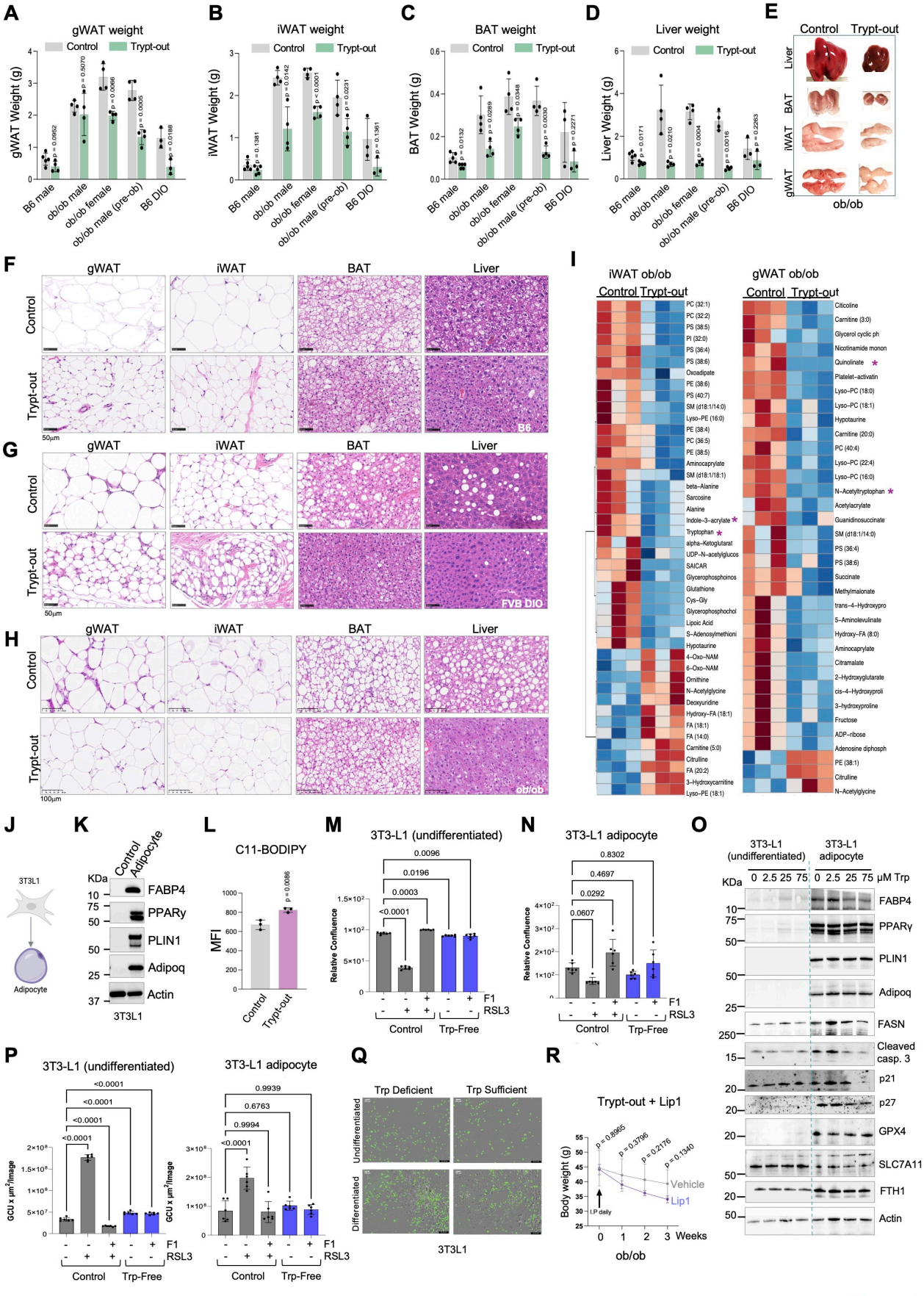
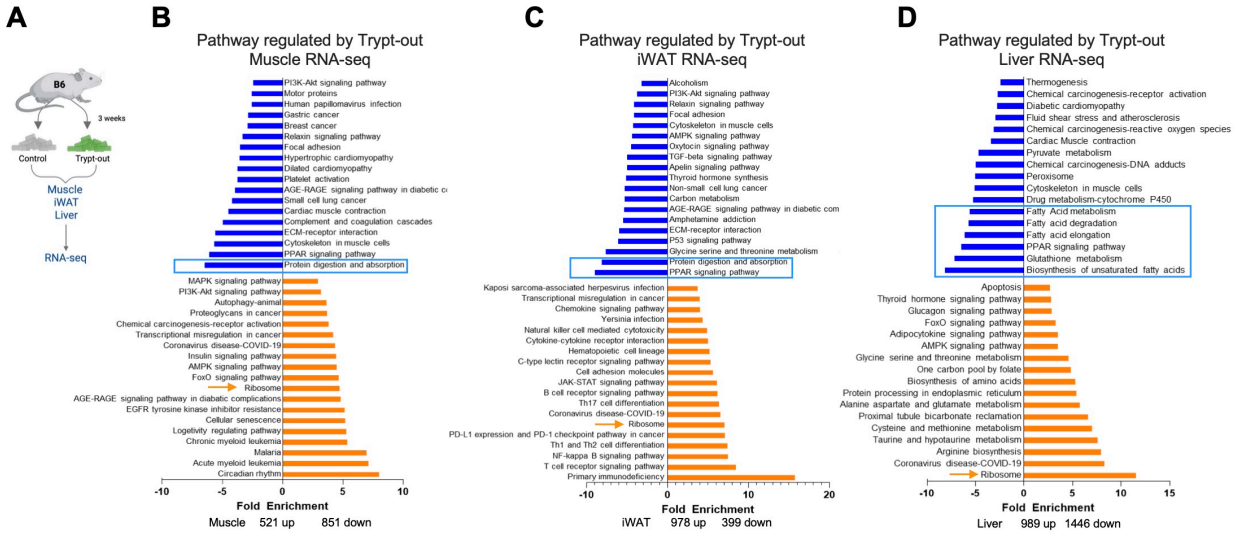

A
gWAT weight
Control
Trypt-out
gWAT Weight (g)
B6 male
ob/ob male
ob/ob female
ob/ob male (pre-ob)
B6 DIO
B
iWAT weight
iWAT Weight (g)
C
BAT weight
BAT Weight (g)
D
Liver weight
Liver Weight (g)
E
Control
Trypt-out
Liver
BAT
iWAT
gWAT
ob/ob
F
gWAT
iWAT
BAT
Liver
Control
Trypt-out
50μm
B6
G
FVB DIO
H
100μm
ob/ob
I
iWAT ob/ob
Control Trypt-out
gWAT ob/ob
Control Trypt-out
PC (32:1)
PC (32:2)
PS (38:5)
PI (32:0)
PS (36:4)
PS (38:6)
Oxoadipate
PE (38:6)
PS (40:7)
SM (d18:1/14:0)
Lyso-PE (16:0)
PE (38:4)
PC (36:5)
PE (38:5)
Aminocaprylate
SM (d18:1/18:1)
beta-Alanine
Sarcosine
Alanine
Indole-3-acrylate *
Tryptophan *
alpha-Ketoglutarat
UDP-N-acetylglucos
SAICAR
Glycerophosphoinos
Glutathione
Cys-Gly
Glycerophosphocho
Lipoic Acid
S-Adenosylmethioni
Hypotaurine
4-Oxo-NAM
6-Oxo-NAM
Ornithine
N-Acetylglycine
Deoxyuridine
Hydroxy-FA (18:1)
FA (18:1)
FA (14:0)
Carnitine (5:0)
Citrulline
FA (20:2)
3-Hydroxycarnitine
Lyso-PE (18:1)
Citicoline
Carnitine (3:0)
Glycerol cyclic ph
Nicotinamide monon
Quinolinate *
Platelet-activatin
Lyso-PC (18:0)
Lyso-PC (18:1)
Hypotaurine
Carnitine (20:0)
PC (40:4)
Lyso-PC (22:4)
Lyso-PC (16:0)
N-Acetyltryptophan *
Acetylacrylate
Guanidinosuccinate
SM (d18:1/14:0)
PS (36:4)
PS (38:6)
Succinate
Methylmalonate
trans-4-Hydroxypro
5-Aminolevulinate
Hydroxy-FA (8:0)
Aminocaprylate
Citramalate
2-Hydroxyglutarate
cis-4-Hydroxyproli
3-Hydroxyproline
Fructose
ADP-ribose
Adenosine diphosph
PE (38:1)
Citrulline
N-Acetylglycine
J
3T3L1
Adipocyte
K
Control
Adipocyte
KDa
FABP4
PPARγ
PLIN1
Adipoq
Actin
3T3L1
L
C11-BODIPY
MFI
p = 0.0086
Control
Trypt-out
M
3T3-L1 (undifferentiated)
Relative Confluence
F1
RSL3
Control
Trp-Free
N
3T3-L1 adipocyte
O
3T3-L1 (undifferentiated)
3T3-L1 adipocyte
0 2.5 25 75 0 2.5 25 75 μM Trp
FABP4
PPARγ
PLIN1
Adipoq
FASN
Cleaved casp. 3
p21
p27
GPX4
SLC7A11
FTH1
Actin
P
3T3-L1 (undifferentiated)
3T3-L1 adipocyte
GCU x μm²/Image
Q
Trp Deficient
Trp Sufficient
Undifferentiated
Differentiated
3T3L1
R
Trypt-out + Lip1
Body weight (g)
Vehicle
Lip1
I.P daily
Weeks
ob/ob

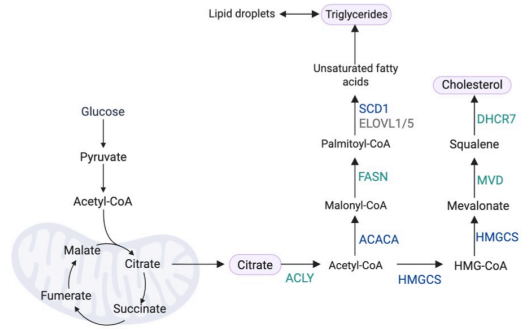
Figure 4

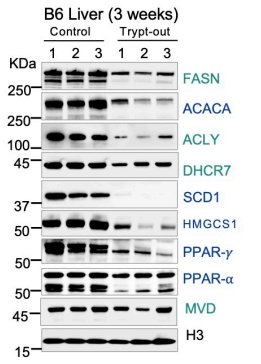


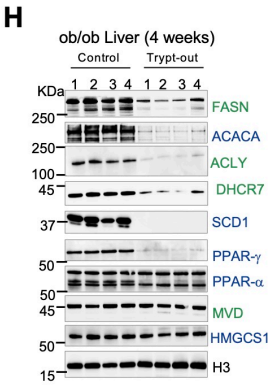
E

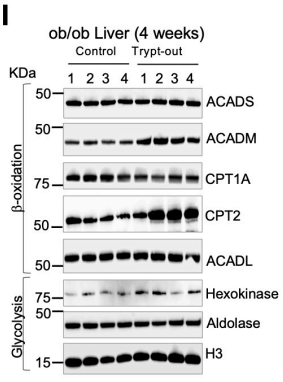
Proteomics liver Trypt-out/control

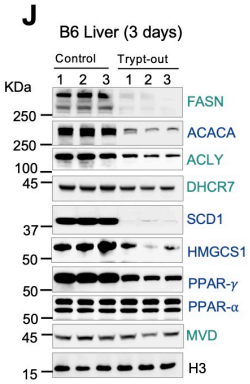
Gene	Trp # human/mouse	mRNA	Protein
SCD1	10/8	-79.3% *	-96%
HMGCS1	5/5	-66.5%*	-59%
PPAR-γ	1/1	ns	No
PPAR-α	0/0	ns	No
ACACA	27/27	-68.6% *	-96%
FASN	33/30	ns	-84%
DHCR7	20/21	ns	-81%
ACLY	11/11	ns	-63%
MVD	6/7	ns	-91%











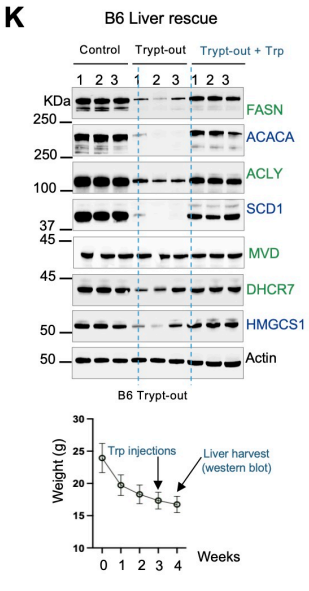


Figure 5

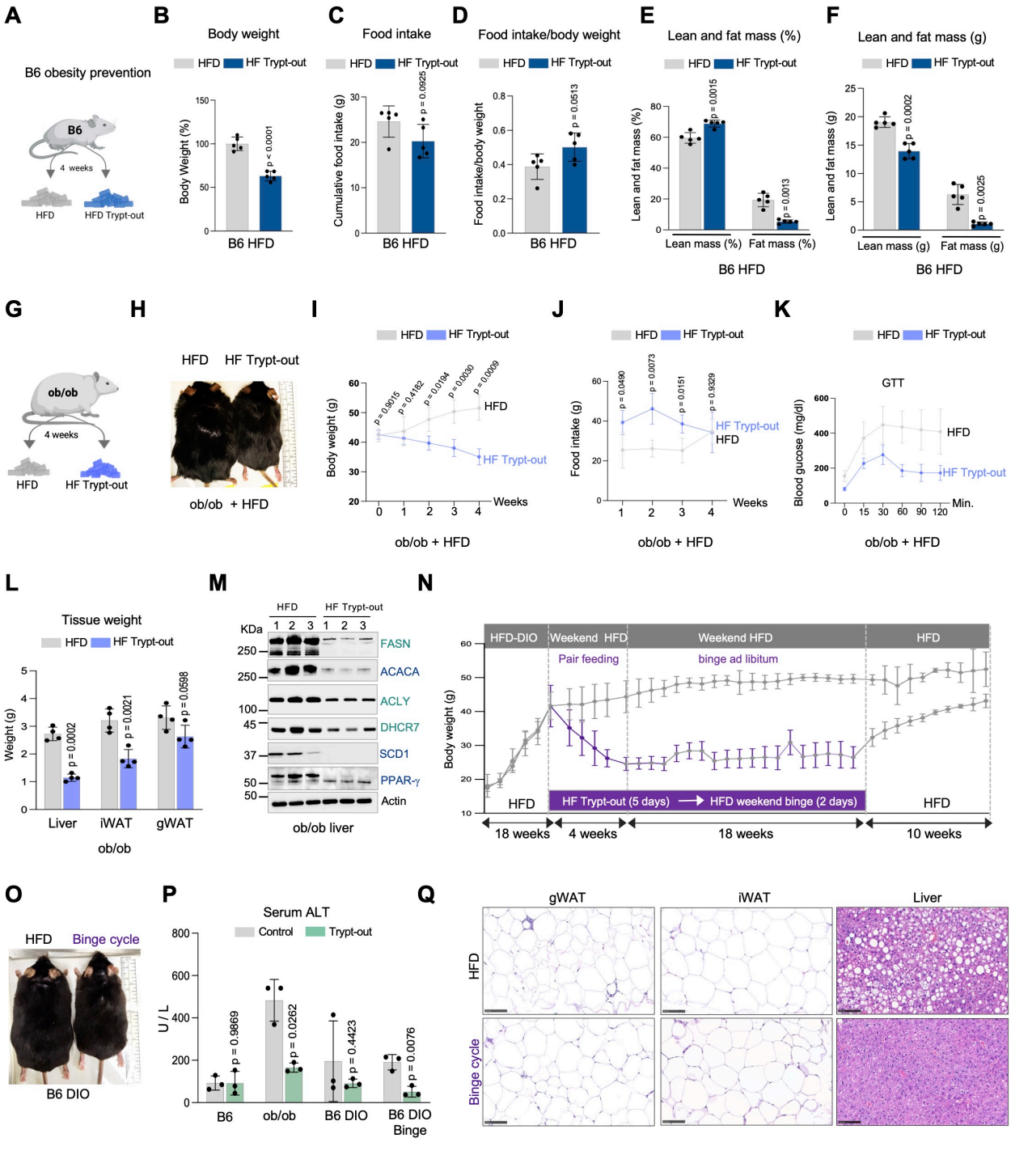

A
B6 obesity prevention
B6
4 weeks
HFD
HFD Trypt-out
B
Body weight
HFD
HF Trypt-out
Body Weight (%)
p < 0.0001
B6 HFD
C
Food intake
Cumulative food intake (g)
p = 0.0925
D
Food intake/body weight
Food intake/body weight
p = 0.0513
E
Lean and fat mass (%)
Lean and fat mass (%)
p = 0.0015
p = 0.0013
Lean mass (%)
Fat mass (%)
F
Lean and fat mass (g)
Lean and fat mass (g)
p = 0.0002
p = 0.0025
Lean mass (g)
Fat mass (g)
G
ob/ob
4 weeks
HFD
HF Trypt-out
H
HFD
HF Trypt-out
ob/ob + HFD
I
Body weight (g)
p = 0.9015
p = 0.4182
p = 0.0194
p = 0.0030
p = 0.0009
HFD
HF Trypt-out
Weeks
ob/ob + HFD
J
Food intake (g)
p = 0.0490
p = 0.0073
p = 0.0151
p = 0.9329
HF Trypt-out
HFD
Weeks
ob/ob + HFD
K
GTT
Blood gucose (mg/dl)
HFD
HF Trypt-out
Min.
ob/ob + HFD
L
Tissue weight
Weight (g)
p = 0.0002
p = 0.0021
p = 0.0598
Liver
iWAT
gWAT
ob/ob
M
HFD
HF Trypt-out
KDa
FASN
ACACA
ACLY
DHCR7
SCD1
PPAR-γ
Actin
ob/ob liver
N
HFD-DIO
Weekend HFD
Pair feeding
Weekend HFD
binge ad libitum
HFD
Body weight (g)
HF Trypt-out (5 days)
HFD weekend binge (2 days)
18 weeks
4 weeks
18 weeks
10 weeks
O
HFD
Binge cycle
B6 DIO
P
Serum ALT
Control
Trypt-out
U / L
p = 0.9869
p = 0.0262
p = 0.4423
p = 0.0076
B6
ob/ob
B6 DIO
B6 DIO Binge
Q
gWAT
iWAT
Liver
HFD
Binge cycle

Figure 6

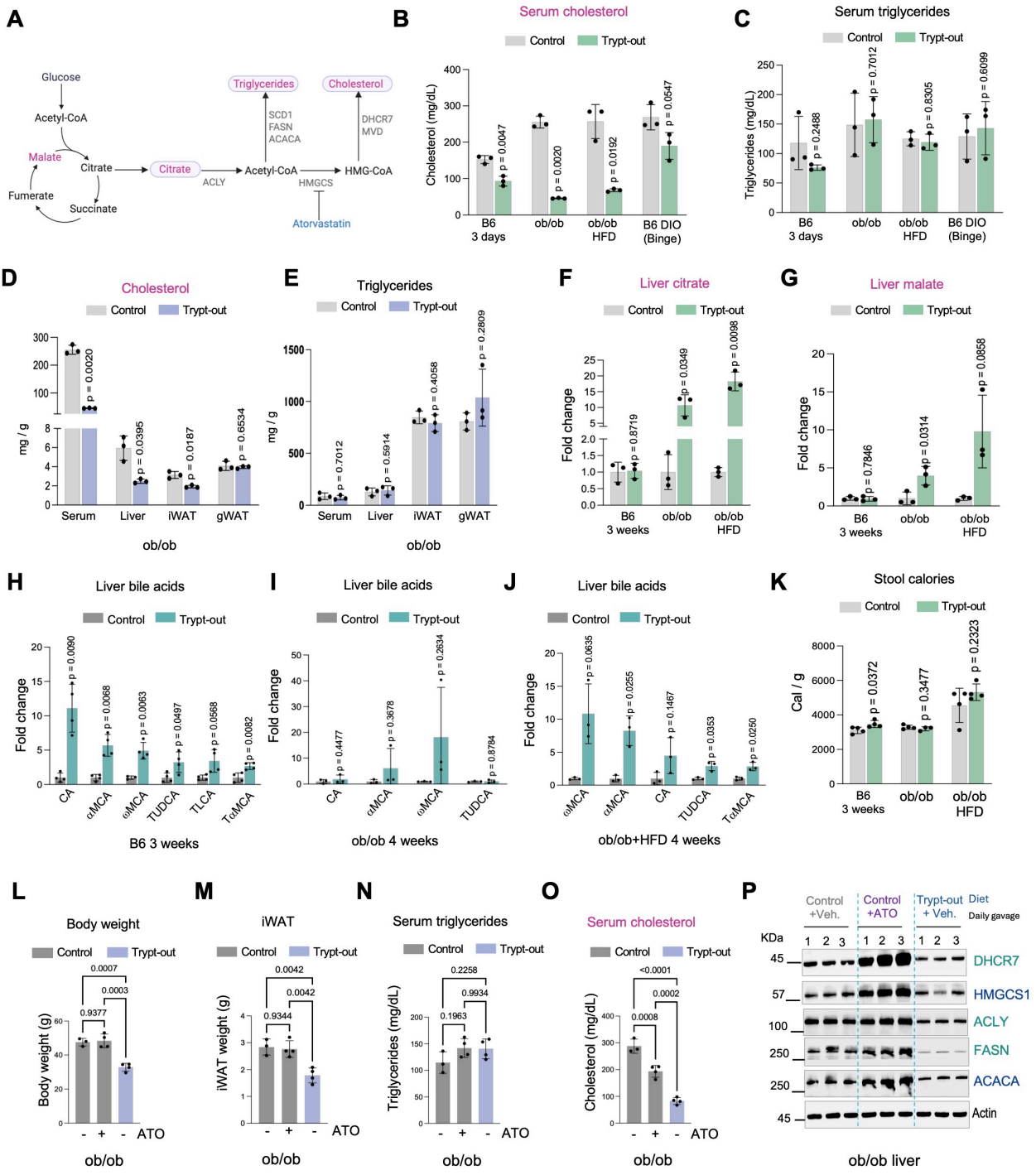

A
Glucose
Acetyl-CoA
Malate
Citrate
Citrate
Triglycerides
Cholesterol
SCD1
FASN
ACACA
DHCR7
MVD
ACLY
Acetyl-CoA
HMGCS
HMG-CoA
Fumerate
Succinate
Atorvastatin
B
Serum cholesterol
Control
Trypt-out
Cholesterol (mg/dL)
p = 0.0047
p = 0.0020
p = 0.0192
p = 0.0547
B6 3 days
ob/ob
ob/ob HFD
B6 DIO (Binge)
C
Serum triglycerides
Triglycerides (mg/dL)
p = 0.2488
p = 0.7012
p = 0.8305
p = 0.6099
D
Cholesterol
mg / g
p = 0.0020
p = 0.0395
p = 0.0187
p = 0.6534
Serum
Liver
iWAT
gWAT
ob/ob
E
Triglycerides
p = 0.7012
p = 0.5914
p = 0.4058
p = 0.2809
F
Liver citrate
Fold change
p = 0.8719
p = 0.0349
p = 0.0098
B6 3 weeks
G
Liver malate
p = 0.7846
p = 0.0314
p = 0.0858
H
Liver bile acids
p = 0.0090
p = 0.0068
p = 0.0063
p = 0.0497
p = 0.0568
p = 0.0082
CA
αMCA
ωMCA
TUDCA
TLCA
TαMCA
B6 3 weeks
I
Liver bile acids
p = 0.4477
p = 0.3678
p = 0.2634
p = 0.8784
ob/ob 4 weeks
J
Liver bile acids
p = 0.0635
p = 0.0255
p = 0.1467
p = 0.0353
p = 0.0250
ob/ob+HFD 4 weeks
K
Stool calories
Cal / g
p = 0.0372
p = 0.3477
p = 0.2323
L
Body weight
Body weight (g)
0.0007
0.0003
0.9377
ATO
M
iWAT
iWAT weight (g)
0.0042
0.0042
0.9344
N
Serum triglycerides
0.2258
0.9934
0.1963
O
Serum cholesterol
<0.0001
0.0002
0.0008
P
Control +Veh.
Control +ATO
Trypt-out + Veh.
Diet
Daily gavage
KDa
DHCR7
HMGCS1
ACLY
FASN
ACACA
Actin
ob/ob liver

Figure 7

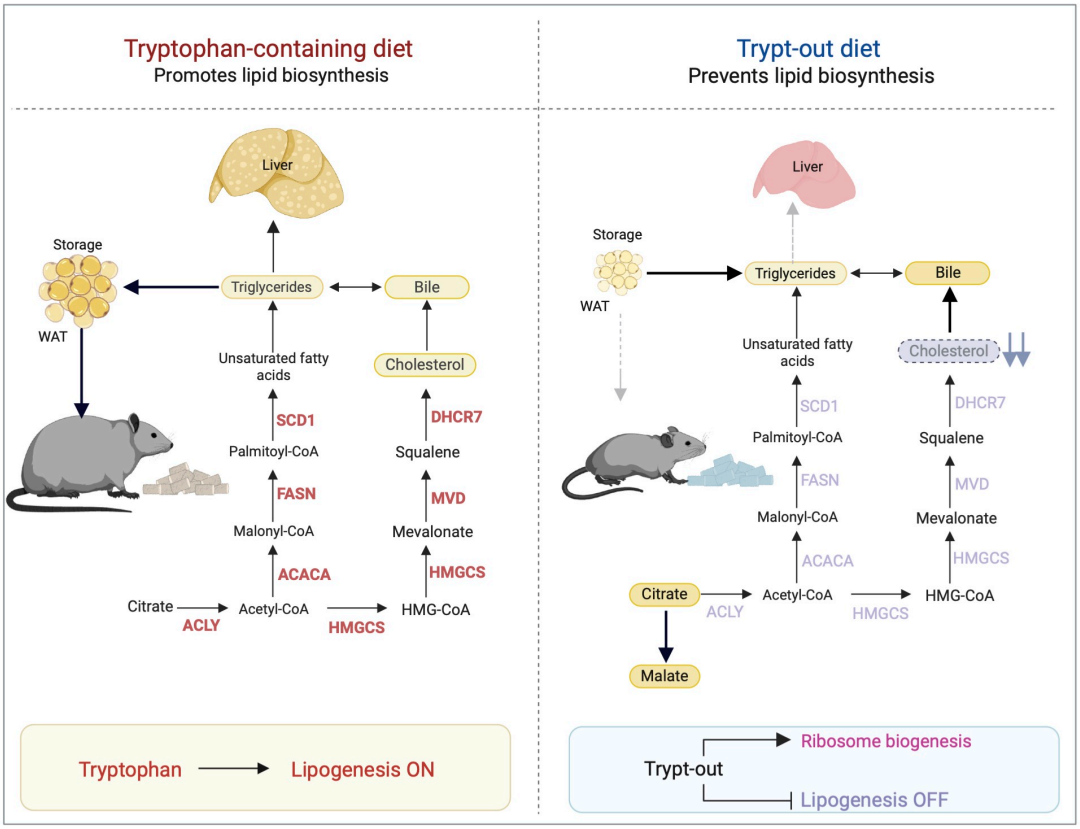
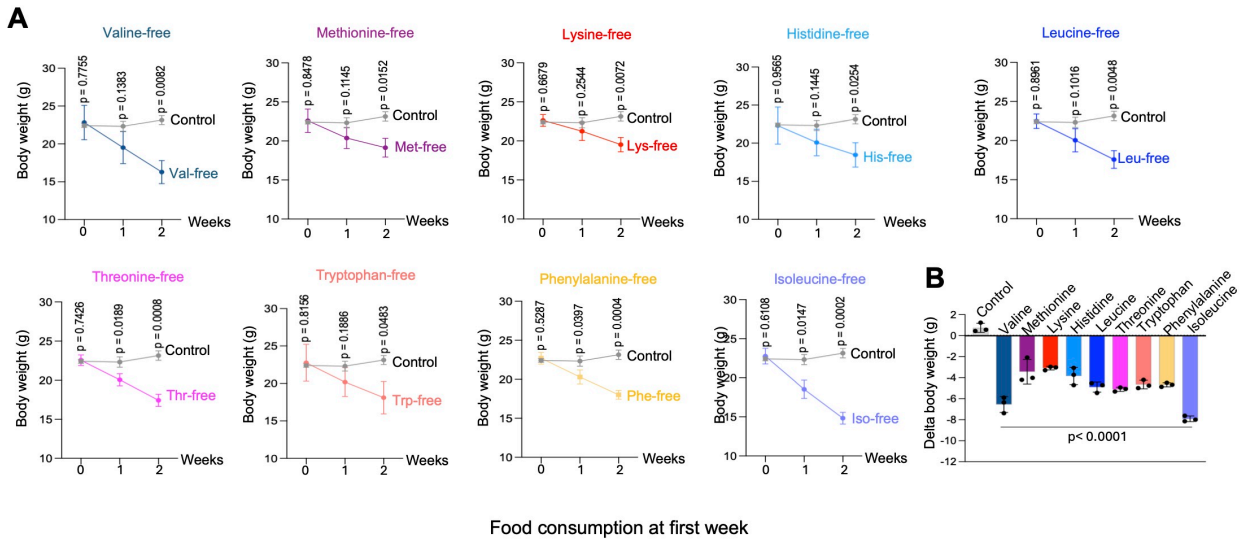
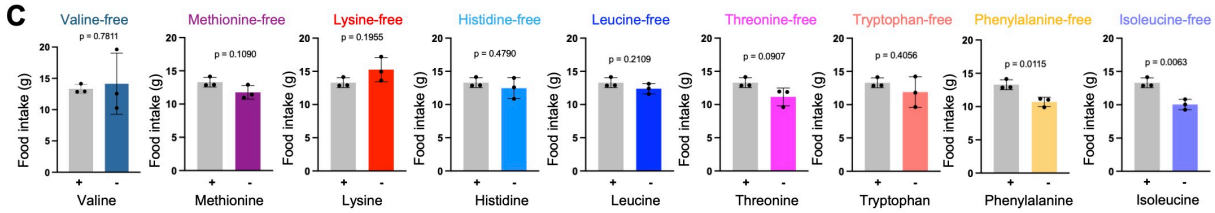
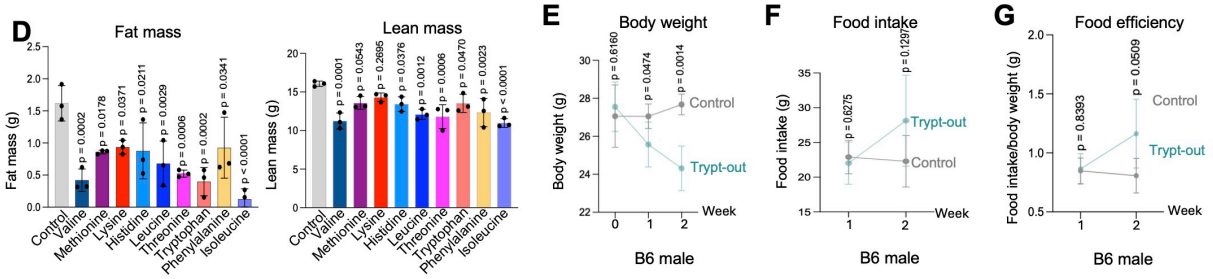

Tryptophan-containing diet
Promotes lipid biosynthesis
Liver
Storage
WAT
Triglycerides
Bile
Unsaturated fatty acids
Cholesterol
SCD1
DHCR7
Palmitoyl-CoA
Squalene
FASN
MVD
Malonyl-CoA
Mevalonate
ACACA
HMGCS
Citrate
ACLY
Acetyl-CoA
HMGCS
HMG-CoA
Tryptophan
Lipogenesis ON
Trypt-out diet
Prevents lipid biosynthesis
Liver
Storage
WAT
Triglycerides
Bile
Unsaturated fatty acids
Cholesterol
SCD1
DHCR7
Palmitoyl-CoA
Squalene
FASN
MVD
Malonyl-CoA
Mevalonate
ACACA
HMGCS
Citrate
ACLY
Acetyl-CoA
HMGCS
HMG-CoA
Malate
Trypt-out
Ribosome biogenesis
Lipogenesis OFF

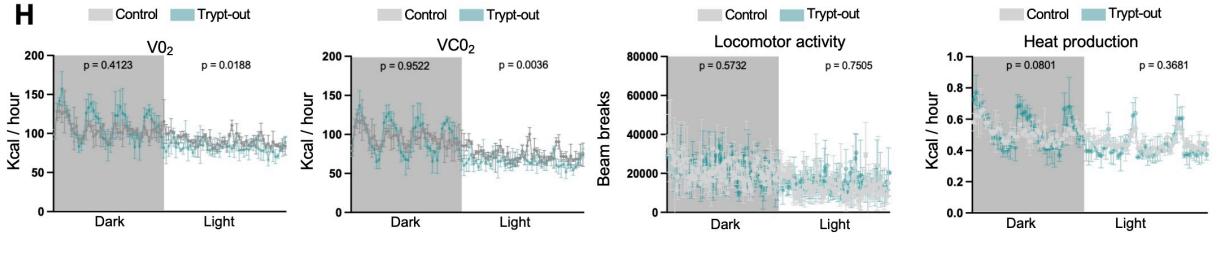
Figure 8



Food consumption at first week







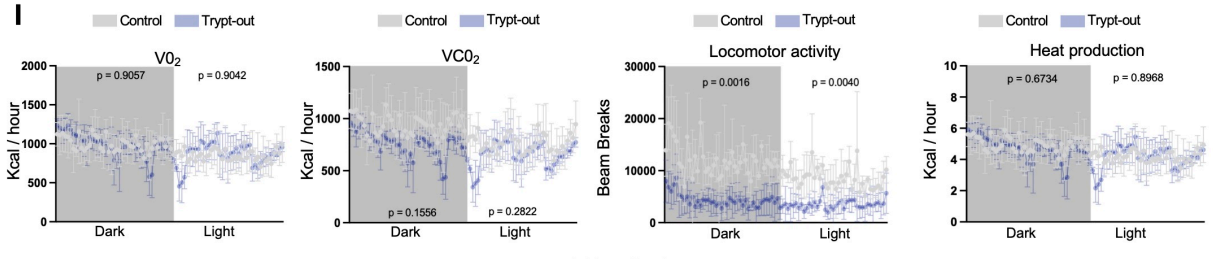


Figure S1

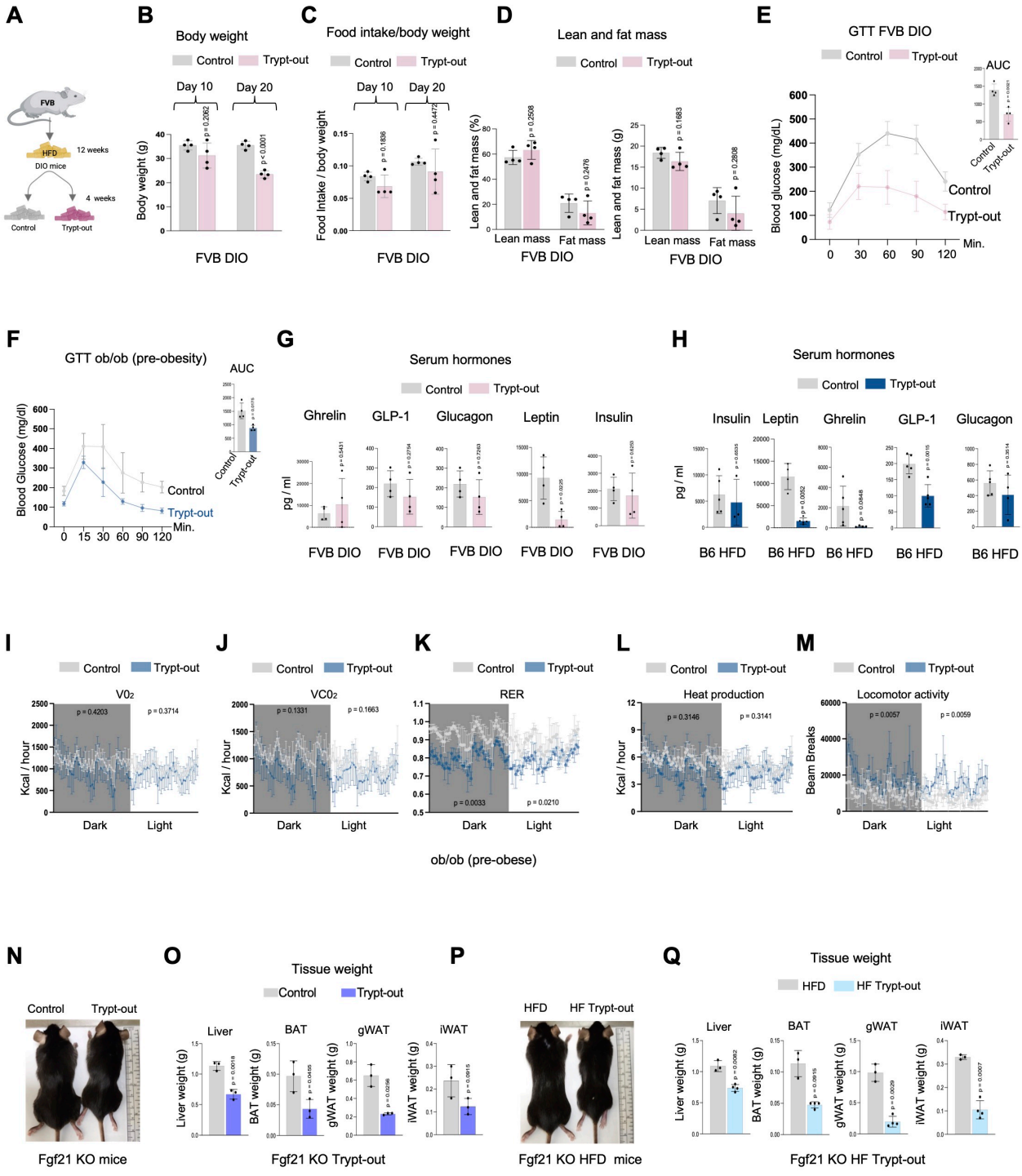
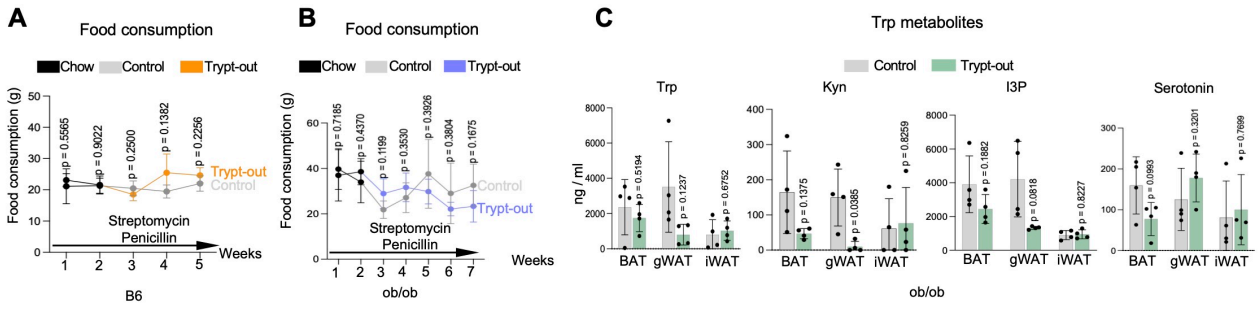
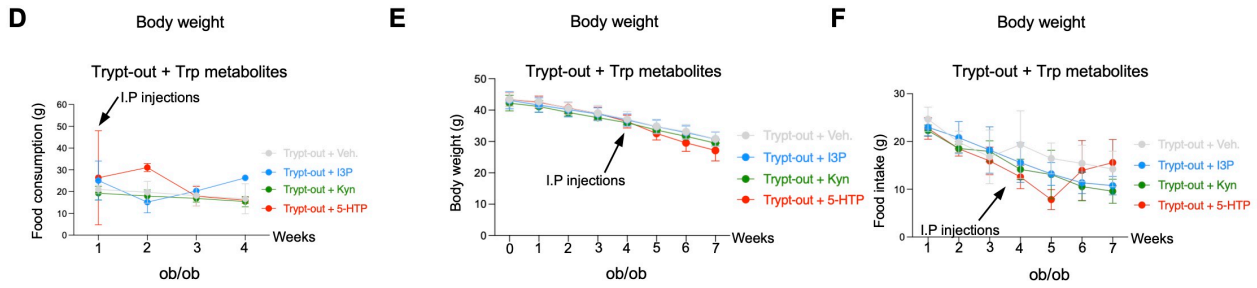
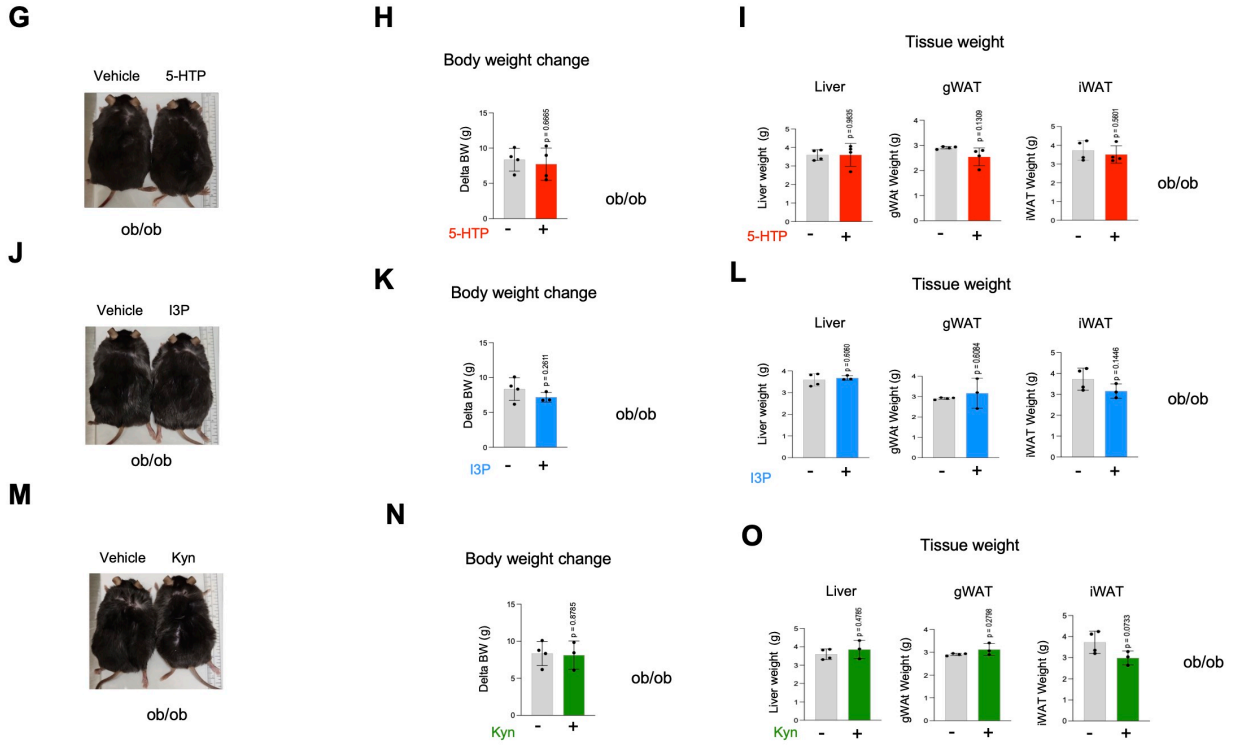

A
FVB
HFD
12 weeks
DIO mice
4 weeks
Control
Trypt-out
B
Body weight
Control
Trypt-out
Day 10
Day 20
Body weight (g)
p = 0.2062
p < 0.0001
FVB DIO
C
Food intake/body weight
Control
Trypt-out
Day 10
Day 20
Food Intake / body weight
p = 0.1836
p = 0.4472
FVB DIO
D
Lean and fat mass
Control
Trypt-out
Lean and fat mass (%)
p = 0.2508
p = 0.2476
Lean mass
Fat mass
FVB DIO
Lean and fat mass (g)
p = 0.1683
p = 0.2608
Lean mass
Fat mass
FVB DIO
E
GTT FVB DIO
Control
Trypt-out
Blood glucose (mg/dL)
Min.
AUC
Control
Trypt-out
F
GTT ob/ob (pre-obesity)
Blood Glucose (mg/dl)
Control
Trypt-out
Min.
AUC
Control
Trypt-out
G
Serum hormones
Control
Trypt-out
Ghrelin
GLP-1
Glucagon
Leptin
Insulin
pg / ml
FVB DIO
H
Serum hormones
Control
Trypt-out
Insulin
Leptin
Ghrelin
GLP-1
Glucagon
pg / ml
B6 HFD
I
Control
Trypt-out
V0₂
Kcal / hour
p = 0.4203
p = 0.3714
Dark
Light
J
Control
Trypt-out
VC0₂
Kcal / hour
p = 0.1331
p = 0.1663
Dark
Light
K
Control
Trypt-out
RER
p = 0.0033
p = 0.0210
Dark
Light
L
Control
Trypt-out
Heat production
Kcal / hour
p = 0.3146
p = 0.3141
Dark
Light
M
Control
Trypt-out
Locomotor activity
Beam Breaks
p = 0.0057
p = 0.0059
Dark
Light
ob/ob (pre-obese)
N
Control
Trypt-out
Fgf21 KO mice
O
Tissue weight
Control
Trypt-out
Liver
BAT
gWAT
iWAT
Liver weight (g)
BAT weight (g)
gWAT weight (g)
iWAT weight (g)
Fgf21 KO Trypt-out
P
HFD
HF Trypt-out
Fgf21 KO HFD mice
Q
Tissue weight
HFD
HF Trypt-out
Liver
BAT
gWAT
iWAT
Liver weight (g)
BAT weight (g)
gWAT weight (g)
iWAT weight (g)
Fgf21 KO HF Trypt-out

Figure S2


A
Food consumption
Chow
Control
Trypt-out
Food consumption (g)
p = 0.5565
p = 0.9022
p = 0.2500
p = 0.1382
p = 0.2256
Trypt-out
Control
Streptomycin
Penicillin
Weeks
B6
B
Food consumption
Chow
Control
Trypt-out
Food consumption (g)
p = 0.7185
p = 0.4370
p = 0.1199
p = 0.3530
p = 0.3926
p = 0.3804
p = 0.1675
Control
Trypt-out
Streptomycin
Penicillin
Weeks
ob/ob
C
Trp metabolites
Control
Trypt-out
Trp
Kyn
I3P
Serotonin
ng / ml
p = 0.5194
p = 0.1237
p = 0.6752
p = 0.1375
p = 0.0385
p = 0.8259
p = 0.1882
p = 0.0818
p = 0.8227
p = 0.0993
p = 0.3201
p = 0.7699
BAT
gWAT
iWAT
ob/ob


D
Body weight
Trypt-out + Trp metabolites
I.P injections
Food consumption (g)
Trypt-out + Veh.
Trypt-out + I3P
Trypt-out + Kyn
Trypt-out + 5-HTP
Weeks
ob/ob
E
Body weight
Trypt-out + Trp metabolites
Body weight (g)
I.P injections
Trypt-out + Veh.
Trypt-out + I3P
Trypt-out + Kyn
Trypt-out + 5-HTP
Weeks
ob/ob
F
Body weight
Trypt-out + Trp metabolites
Food intake (g)
I.P injections
Trypt-out + Veh.
Trypt-out + I3P
Trypt-out + Kyn
Trypt-out + 5-HTP
Weeks
ob/ob


G
Vehicle
5-HTP
ob/ob
H
Body weight change
Delta BW (g)
p = 0.6665
ob/ob
5-HTP
- +
I
Tissue weight
Liver
gWAT
iWAT
Liver weight (g)
p = 0.9835
gWAt Weight (g)
p = 0.1309
iWAT Weight (g)
p = 0.5801
ob/ob
5-HTP
- +
J
Vehicle
I3P
ob/ob
K
Body weight change
Delta BW (g)
p = 0.2611
ob/ob
I3P
- +
L
Tissue weight
Liver
gWAT
iWAT
Liver weight (g)
p = 0.6860
gWAt Weight (g)
p = 0.6084
iWAT Weight (g)
p = 0.1446
ob/ob
I3P
- +
M
Vehicle
Kyn
ob/ob
N
Body weight change
Delta BW (g)
p = 0.8765
ob/ob
Kyn
- +
O
Tissue weight
Liver
gWAT
iWAT
Liver weight (g)
p = 0.4785
gWAt Weight (g)
p = 0.2798
iWAT Weight (g)
p = 0.0733
ob/ob
Kyn
- +

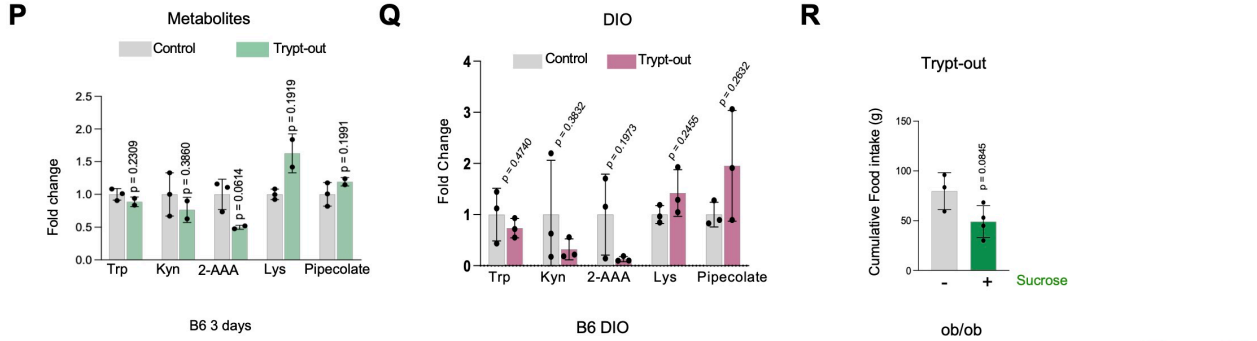
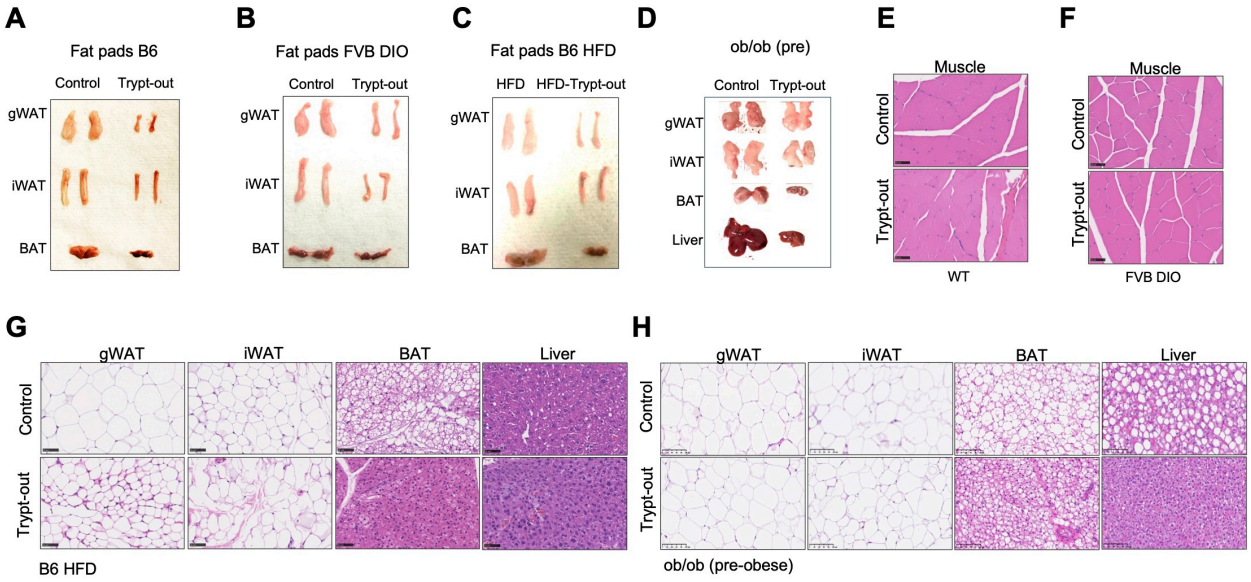
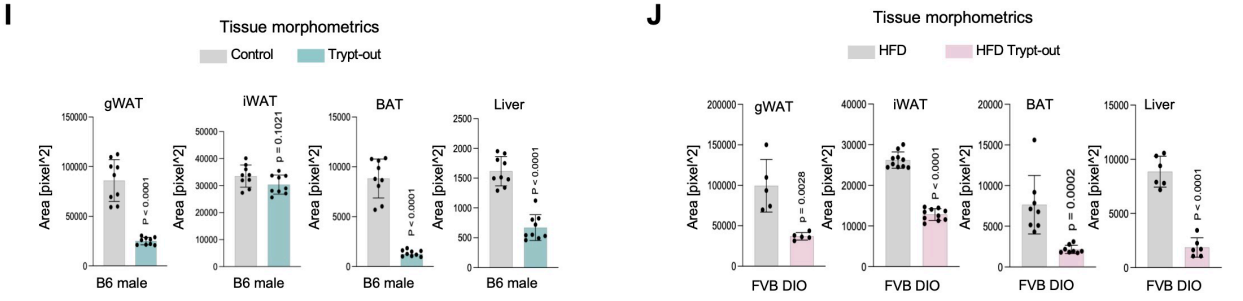
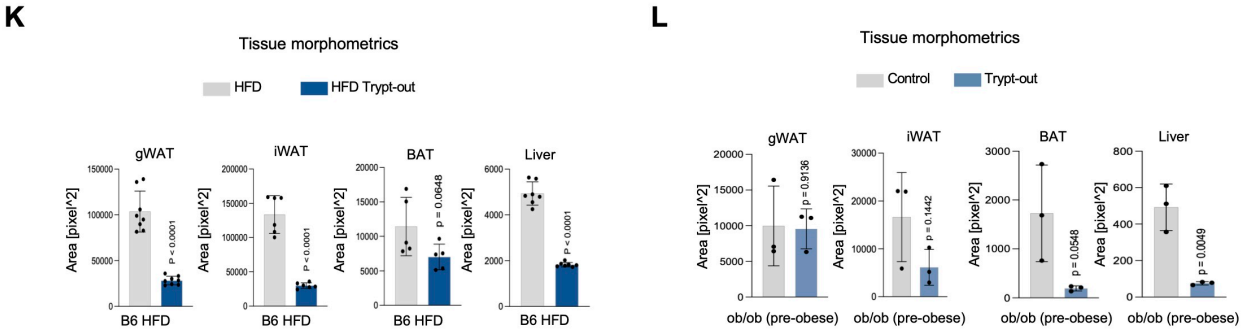

P
Metabolites
Control
Trypt-out
Fold change
p = 0.2209
p = 0.3860
p = 0.0614
p = 0.1919
p = 0.1991
Trp
Kyn
2-AAA
Lys
Pipecolate
B6 3 days
Q
DIO
Control
Trypt-out
Fold Change
p = 0.4740
p = 0.3832
p = 0.1973
p = 0.2455
p = 0.2632
Trp
Kyn
2-AAA
Lys
Pipecolate
B6 DIO
R
Trypt-out
Cumulative Food intake (g)
p = 0.0845
- +
Sucrose
ob/ob

Figure S3


A
Fat pads B6
Control
Trypt-out
gWAT
iWAT
BAT
B
Fat pads FVB DIO
Control
Trypt-out
gWAT
iWAT
BAT
C
Fat pads B6 HFD
HFD
HFD-Trypt-out
gWAT
iWAT
BAT
D
ob/ob (pre)
Control
Trypt-out
gWAT
iWAT
BAT
Liver
E
Muscle
Control
Trypt-out
WT
F
Muscle
Control
Trypt-out
FVB DIO
G
gWAT
iWAT
BAT
Liver
Control
Trypt-out
B6 HFD
H
gWAT
iWAT
BAT
Liver
Control
Trypt-out
ob/ob (pre-obese)


I
Tissue morphometrics
Control
Trypt-out
gWAT
iWAT
BAT
Liver
Area [pixel^2]
P < 0.0001
p = 0.1021
P < 0.0001
P < 0.0001
B6 male
J
Tissue morphometrics
HFD
HFD Trypt-out
gWAT
iWAT
BAT
Liver
Area [pixel^2]
p = 0.0028
P < 0.0001
p = 0.0002
P < 0.0001
FVB DIO


K
Tissue morphometrics
HFD
HFD Trypt-out
gWAT
iWAT
BAT
Liver
Area [pixel^2]
P < 0.0001
P < 0.0001
p = 0.0648
P < 0.0001
B6 HFD
L
Tissue morphometrics
Control
Trypt-out
gWAT
iWAT
BAT
Liver
Area [pixel^2]
p = 0.9136
p = 0.1442
p = 0.0548
p = 0.0049
ob/ob (pre-obese)

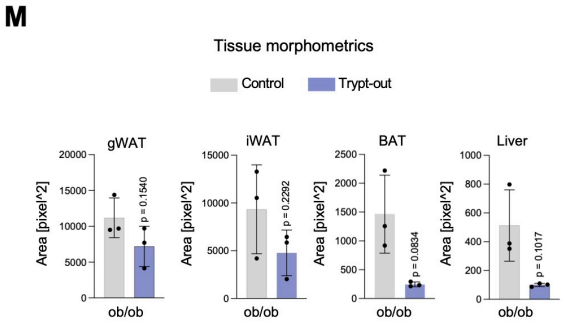

M
Tissue morphometrics
Control
Trypt-out
gWAT
iWAT
BAT
Liver
Area [pixel^2]
p = 0.1540
p = 0.2292
p = 0.0834
p = 0.1017
ob/ob

Figure S4

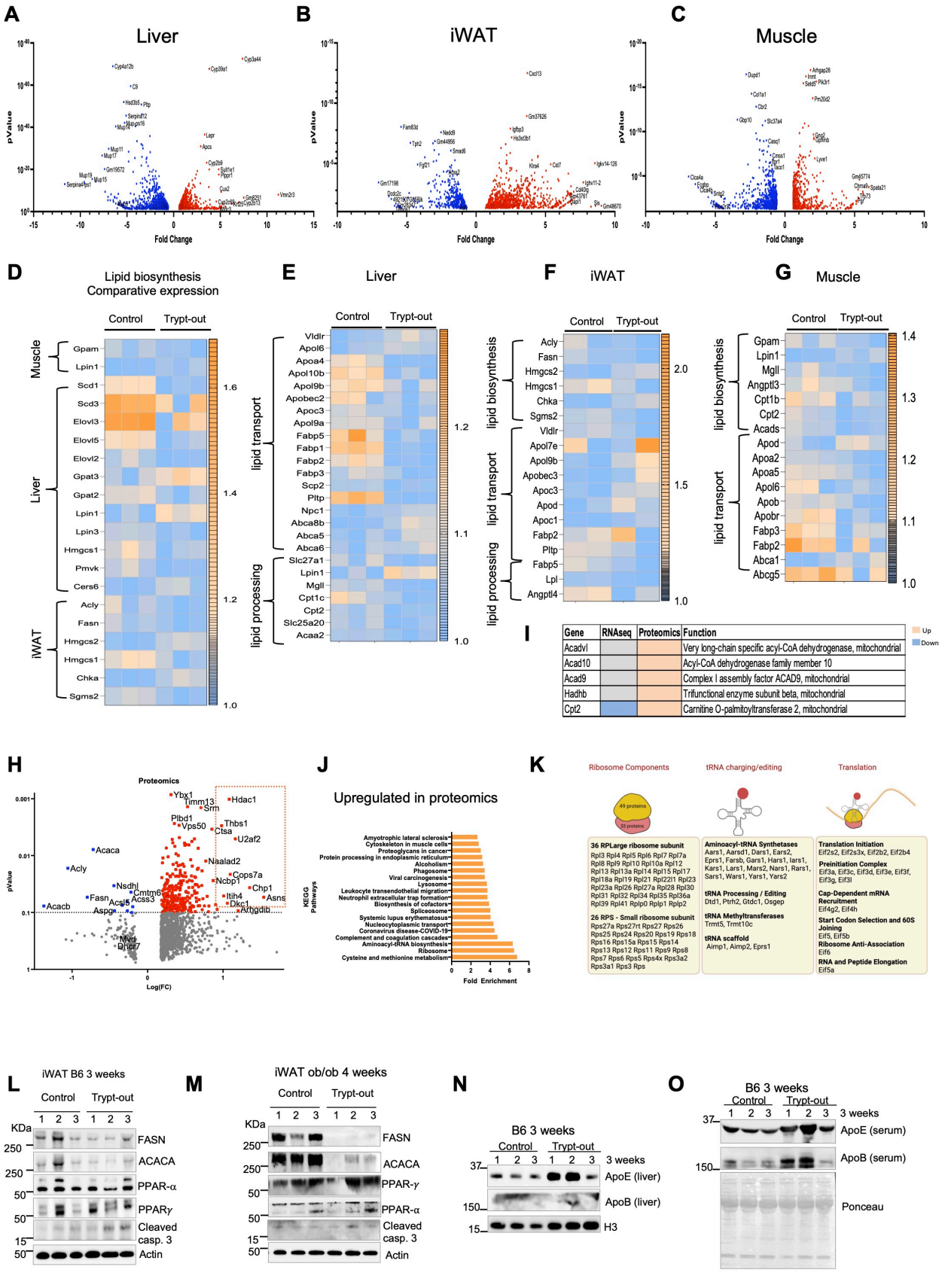

A
Liver
B
iWAT
C
Muscle
pValue
Fold Change
D
Lipid biosynthesis
Comparative expression
Control
Trypt-out
Muscle
Liver
iWAT
Gpam
Lpin1
Scd1
Scd3
Elovl3
Elovl5
Elovl2
Gpat3
Gpat2
Lpin1
Lpin3
Hmgcs1
Pmvk
Cers6
Acly
Fasn
Hmgcs2
Hmgcs1
Chka
Sgms2
E
Liver
lipid transport
lipid processing
Vldlr
Apol6
Apoa4
Apol10b
Apol9b
Apobec2
Apoc3
Apol9a
Fabp5
Fabp1
Fabp2
Fabp3
Scp2
Pltp
Npc1
Abca8b
Abca5
Abca6
Slc27a1
Lpin1
Mgll
Cpt1c
Cpt2
Slc25a20
Acaa2
F
iWAT
lipid biosynthesis
lipid transport
lipid processing
Acly
Fasn
Hmgcs2
Hmgcs1
Chka
Sgms2
Vldlr
Apol7e
Apol9b
Apobec3
Apoc3
Apod
Apoc1
Fabp2
Pltp
Fabp5
Lpl
Angptl4
G
Muscle
lipid biosynthesis
lipid transport
Gpam
Lpin1
Mgll
Angptl3
Cpt1b
Cpt2
Acads
Apod
Apoa2
Apoa5
Apol6
Apob
Apobr
Fabp3
Fabp2
Abca1
Abcg5
I
Gene | RNAseq | Proteomics | Function
Acadvl | | | Very long-chain specific acyl-CoA dehydrogenase, mitochondrial
Acad10 | | | Acyl-CoA dehydrogenase family member 10
Acad9 | | | Complex I assembly factor ACAD9, mitochondrial
Hadhb | | | Trifunctional enzyme subunit beta, mitochondrial
Cpt2 | | | Carnitine O-palmitoyltransferase 2, mitochondrial
Up
Down
H
Proteomics
Log(FC)
pValue
Ybx1
Timm13
Srm
Hdac1
Plbd1
Vps50
Thbs1
Ctsa
U2af2
Acaca
Naalad2
Acly
Cops7a
Ncbp1
Nsdhl
Cmtm6
Chp1
Fasn
Acsl3
Acsl1
Itih4
Asns
Acacb
Aspg
Dkc1
Mvd
Dhcr7
J
Upregulated in proteomics
KEGG Pathways
Amyotrophic lateral sclerosis
Cytoskeleton in muscle cells
Proteoglycans in cancer
Protein processing in endoplasmic reticulum
Alcoholism
Phagosome
Viral carcinogenesis
Lysosome
Leukocyte transendothelial migration
Neutrophil extracellular trap formation
Biosynthesis of cofactors
Spliceosome
Systemic lupus erythematosus
Nucleocytoplasmic transport
Coronavirus disease-COVID-19
Complement and coagulation cascades
Aminoacyl-tRNA biosynthesis
Ribosome
Cysteine and methionine metabolism
Fold Enrichment
K
Ribosome Components
tRNA charging/editing
Translation
49 proteins
33 proteins
36 RPLarge ribosome subunit
Rpl3 Rpl4 Rpl5 Rpl6 Rpl7 Rpl7a Rpl8 Rpl9 Rpl10 Rpl10a Rpl12 Rpl13 Rpl13a Rpl14 Rpl15 Rpl17 Rpl18a Rpl19 Rpl21 Rpl22l1 Rpl23 Rpl23a Rpl26 Rpl27a Rpl28 Rpl30 Rpl31 Rpl32 Rpl34 Rpl35 Rpl36a Rpl39 Rpl41 Rplp0 Rplp1 Rplp2
26 RPS - Small ribosome subunit
Rps27a Rps27rt Rps27 Rps26 Rps25 Rps24 Rps20 Rps19 Rps18 Rps16 Rps15a Rps15 Rps14 Rps13 Rps12 Rps11 Rps9 Rps8 Rps7 Rps6 Rps5 Rps4x Rps3a2 Rps3a1 Rps3 Rps
Aminoacyl-tRNA Synthetases
Aars1, Aarsd1, Dars1, Ears2, Eprs1, Farsb, Gars1, Hars1, Iars1, Kars1, Lars1, Mars2, Nars1, Rars1, Sars1, Wars1, Yars1, Yars2
tRNA Processing / Editing
Dtd1, Ptrh2, Gtdc1, Osgep
tRNA Methyltransferases
Trmt5, Trmt10c
tRNA scaffold
Aimp1, Aimp2, Eprs1
Translation Initiation
Eif2s2, Eif2s3x, Eif2b2, Eif2b4
Preinitiation Complex
Eif3a, Eif3c, Eif3d, Eif3e, Eif3f, Eif3g, Eif3l
Cap-Dependent mRNA Recruitment
Eif4g2, Eif4h
Start Codon Selection and 60S Joining
Eif5, Eif5b
Ribosome Anti-Association
Eif6
RNA and Peptide Elongation
Eif5a
L
iWAT B6 3 weeks
Control
Trypt-out
1 2 3 1 2 3
KDa
FASN
ACACA
PPAR-α
PPARγ
Cleaved casp. 3
Actin
M
iWAT ob/ob 4 weeks
Control
Trypt-out
1 2 3 1 2 3
KDa
FASN
ACACA
PPAR-γ
PPAR-α
Cleaved casp. 3
Actin
N
B6 3 weeks
Control
Trypt-out
1 2 3 1 2 3
3 weeks
ApoE (liver)
ApoB (liver)
H3
O
B6 3 weeks
Control
Trypt-out
1 2 3 1 2 3
3 weeks
ApoE (serum)
ApoB (serum)
Ponceau

Figure S5

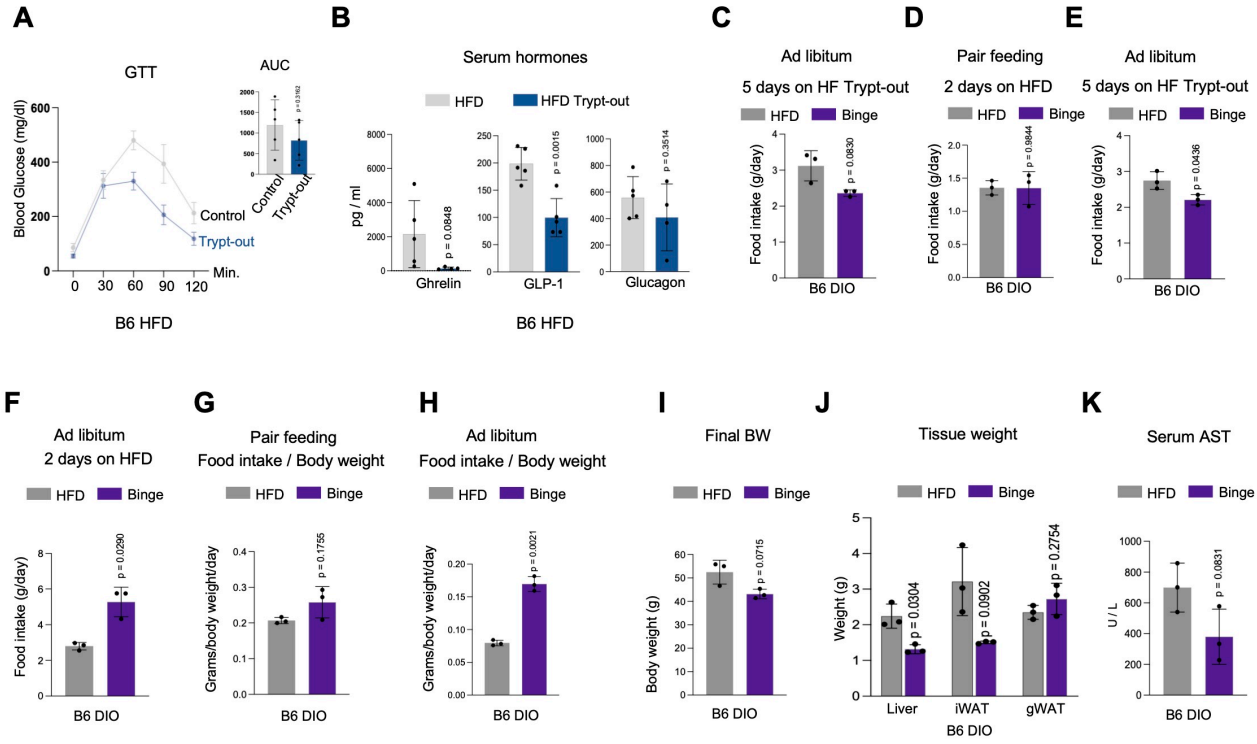
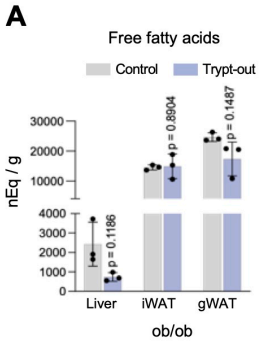
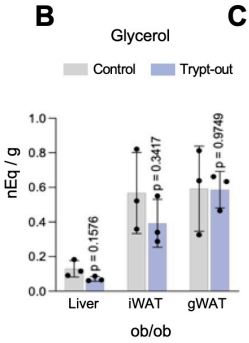
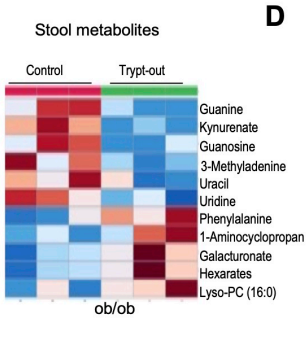

A
GTT
AUC
Blood Glucose (mg/dl)
Control
Trypt-out
Min.
B6 HFD
B
Serum hormones
HFD
HFD Trypt-out
pg / ml
Ghrelin
GLP-1
Glucagon
B6 HFD
C
Ad libitum
5 days on HF Trypt-out
HFD
Binge
Food intake (g/day)
B6 DIO
D
Pair feeding
2 days on HFD
E
Ad libitum
5 days on HF Trypt-out
F
Ad libitum
2 days on HFD
G
Pair feeding
Food intake / Body weight
H
Ad libitum
Food intake / Body weight
I
Final BW
Body weight (g)
J
Tissue weight
Weight (g)
Liver
iWAT
gWAT
K
Serum AST
U / L

Figure S6



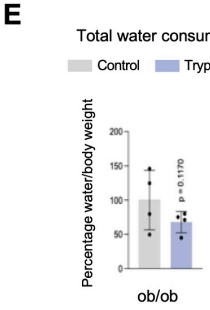


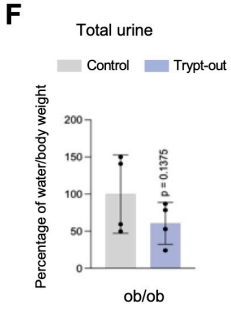


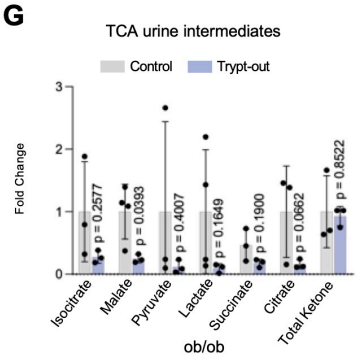
D

Urine products of ob/ob male mice

Product	Control	Trypt-out	p value
Amylase	383.5	141.75	0.0305
Blood urea nitrogen	1186.175	1628.7	0.6411
Calcium	4.055	8.2125	0.271
Chloride	120.025	174.15	0.6027
Creatinine	4.1825	6.525	0.3467
Glucose	28.66666667	25.5	0.7474
Potassium	57.2175	63.4125	0.8592
Magnesium	6.595	11.395	0.5776
Sodium	33.475	51.95	0.5633
Phosphorus	69.5	72.495	0.9397
Urine protein	8.85	7.075	0.2444
Uric acid	5.5	6.8725	0.391



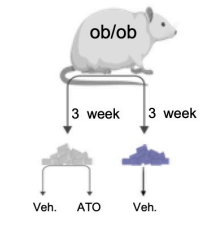


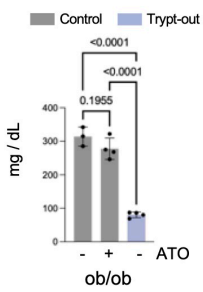


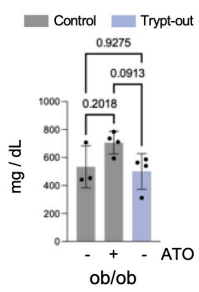
H

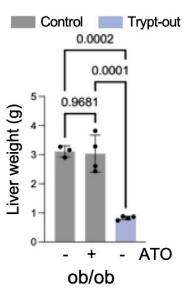
Liver bile acids of B6, ob/ob and ob/ob + HFD male mice

Product	Full name	B6 3 weeks (p value)	ob/ob 4 weeks (p value)	ob/ob + HFD 4 weeks (p value)
TomegaMCA	Tauro-omega-muricholic acid	0.1452	0.1605	0.0948
TaMCA	Tauro-alpha-muricholic acid	0.0082	0.9685	0.0250
TbMCA	Tauro-beta-muricholic acid	0.3142	0.0104	0.0384
TUDCA	Tauroursodeoxycholic acid	0.0497	0.8784	0.0353
THCDA	Chenodeoxycholic acid	0.4764	0.8928	0.0055
oMCA	Omega-muricholic acid	0.0063	0.2634	0.0635
aMCA	Alpha-muricholic acid	0.0068	0.3678	0.0255
TCA	Taurocholic acid	0.6226	0.1093	0.0113
bMCA	Beta-muricholic acid	0.5501	0.3837	0.0036
GCA	Glycocholic acid	0.3510	0.1552	0.1465
CA	Cholic acid	0.0090	0.4477	0.1467
TCDCA	Taurochenodeoxycholic acid	0.1452	0.1605	0.0948
TDCA	Taurodeoxycholic acid	0.1167	0.2170	0.0612
CDCA	Chenodeoxycholic acid	0.0129	0.4729	0.2015
DCA	Deoxycholic acid	0.5550	0.8954	0.8320
GLCA	Glycolithocholic acid	0.9722	0.4647	0.3614
LCA	Lithocholic acid	0.0265	0.0653	0.7137
TLCA	Taurolithocholic acid	0.0568	0.1540	0.0056









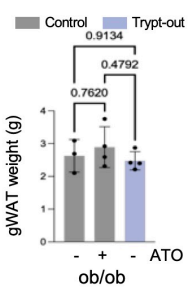


Figure S7

Supplementary Files

This is a list of supplementary files associated with this preprint. Click to download.

- WBraw2.pdf